U.PORTO

FEUP FACULDADE DE ENGENHARIA UNIVERSIDADE DO PORTO

IMPACT OF MIXED ADHESIVE JOINTS FOR THE AUTOMOTIVE INDUSTRY

MÁRIO RUI GONÇALVES SILVA

A dissertation submitted in partial fulfilment of the requirements for the degree of

MASTER IN MECHANICAL ENGINEERING – MANUFACTURING, PRODUCT DEVELOPMENT AND AUTOMOTIVE ENGINEERING

Supervisor: Professor Lucas Filipe Martins da Silva (FEUP – DEMec)

Co-supervisor: Eduardo André de Sousa Marques (INEGI)

JULY 2015

Abstract

As the transport industry is concerned with fuel consumption, lightweight materials should be implemented to reduce the weight of the vehicles and the pollution emissions. However, this implementation brings difficulty in assembling and bonding, sometimes impossible using traditional methods. Adhesive bonding can successfully bond different materials and complex structures, providing the basic vehicle parameters such as mechanical strength and security for the passengers, while keeping the costs of production at a low value. However, when this technique is used in the automotive industry, impact loadings have an important role. The joint must offer enough strength to transmit the load to other materials without fracturing to ensure the integrity of the car's components. Flexible and ductile adhesives are more suitable for impact behaviour, however, to achieve structure stiffness and static strength, rigid and strong adhesives are necessary. A possible solution combining both of the requirements is the mixed adhesive technique, applying two different adhesives on the same overlap, thus improving joint strength.

This work introduces and studies different configurations for static and impact tests of mixed adhesive joints with Momentive RTV106, Nagase Chemtex XNR6852E-2, Araldite AV138 and 3M DP-8005 in different combinations. Using a drop-weight impact test machine, the impact strength, durability and mechanical behaviour of the joints are studied, all of which are key issues for the automotive industry.

The main objective of the experimental tests is the achievement of a strong adhesive joint with the provided materials and development of an equivalent numerical model using finite elements with cohesive properties in order to validate the results.

The results were discussed and analysed by comparing the P-Delta curves of static tests and the load-time history of the impact tests to evaluate the best adhesives combination and configuration of the overlap for different applications. It is concluded that the use of the mixed adhesive technique improves both static and impact strength by introducing flexibility to the joint and allowing for more energy absorption.

Resumo

Uma vez que a indústria dos transportes está preocupada com o consumo de combustíveis, deverão ser adotados materiais leves de forma a reduzir o peso e a emissão de poluentes. No entanto, esta implementação traz dificuldades na fase de montagem e ligação, por vezes impossível recorrendo aos métodos tradicionais. As ligações adesivas permitem a ligação de diferentes materiais e estruturas complexas com sucesso, oferecendo requisitos básicos tais como boas propriedades mecânicas e segurança para os ocupantes, enquanto mantêm os custos de produção a níveis baixos. Quando a técnica é usada em automóveis, as condições de impacto são um fator importante. As juntas deverão oferecer resistência suficiente para transmitir forças a outros materiais sem quebrarem, assegurando a integridade da estrutura do veículo. Adesivos flexíveis são os mais indicados para condições de impacto mas para conseguir estruturas rígidas, serão necessários adesivos consistentes. Uma possível solução combinando ambos os requisitos é a técnica de juntas adesivas mistas, aplicando dois adesivos diferentes na mesma sobreposição, melhorando a resistência das juntas.

Este trabalho estuda diferentes configurações para ensaios estáticos e de impacto de juntas adesivas mistas com os adesivos Momentive RTV106, Nagase Chemtex XNR6852E-2, Araldite AV138 e 3M DP-8005 em diferentes combinações. Usando uma máquina de teste de impacto do tipo *Drop-weight*, estudou-se a resistência ao impacto e o comportamento mecânico das juntas, questões chave para a indústria automóvel.

O objetivo principal dos testes experimentais é a obtenção de uma junta forte com os materiais fornecidos e o consequente desenvolvimento de um modelo numérico equivalente usando elementos finitos com propriedades coesivas de forma a validar os resultados.

Os resultados foram discutidos e analisados comparando as curvas P-Delta dos testes estáticos e dos testes de impacto, de forma a avaliar a melhor combinação de adesivos e configurações de sobreposição para diferentes aplicações. Conclui-se que o uso da técnica de juntas adesivas mistas melhora a resistência tanto para condições estáticas como para impacto, oferecendo flexibilidade às juntas e possibilitando maiores absorções de energia.

Acknowledgements

I would like to express my sincere gratefulness to my co-supervisor Eduardo Marques for the attention and patience that he gave me to accomplish this work. Special thanks go to him for the assistance provided since the first day. Also, I am very thankful to Rodrigo Mata for his tips and advices, always helping me in difficult phases.

I also want to acknowledge Guilherme Viana, Filipe Chaves, Marcelo Costa and Ricardo Carbas for the advice and experience shared.

Last but not least, special thanks goes to my supervisor professor Lucas da Silva for his support and consideration.

Contents

List of Figures

List of Tables

List of acronyms

DCB	Double Cantilever Beam
SLJ	Single Lap Joint
FEA	Finite Element Analysis
ASTM	American Society for Testing and Materials
TAST	Thick Adherend Shear Test
ENF	End Notched Flexure test
EN	European Standards Organization
ISO	International Organization for Standardization
CBBM	Compliance-Based Beam Method
CCZM	Continuum Cohesive Zone Method
DCZM	Discrete Cohesive Zone Method
HTA	High-temperature Adhesive
LTA	Low-temperature Adhesive
MAJ	Mixed Adhesive Joint
SHPB	Split Hopkinson Pressure Bar
DIN	Deutsches Institut für Normung
SDEG	Scalar Stiffness Degradation

List of symbols

τ	Shear stress
σ	Tensile stress
M	Bending moment
b	Joint width
t	Thickness
P	Applied load
k	Bending moment factor
l	Overlap length
T_g	Glass transition temperature
G	Shear modulus
G_I	Fracture toughness in mode I
G_{IC}	Critical fracture toughness in mode I
G_{II}	Fracture toughness in mode II
G_{IIC}	Critical fracture toughness in mode II
a	Crack length
a_0	Initial crack length
a_{eq}	Equivalent crack length
E	Young's modulus
δ	Displacement
t_n	Tensile strength
t_s	Shear strength

1. Introduction

1.1 Background and motivation

Nowadays, complex structures in aeronautical, automotive and aerospace industries are being developed, requiring in most of the applications adhesive bonding. As the technique is being used more often in many applications, a lot of research it is still necessary in terms of durability.

One of the applications of adhesive bonding in the automotive industry is the bonding of complex composite and lightweight structures such as carbon fibre, to produce lighter and efficient vehicles. As the technology combines various materials with their unique characteristics to get a superior combination when pushed together, composite materials have gained popularity in high-performance products, providing reduced weights and still strong and consistent structures, and thus, helping in the matter of fuel consumption and world pollution levels and limitations of energy resources.

In Figure 1, the prediction for the next 15 years shows an even more critical situation than the current one, being the pollution levels almost three times higher than the actual ones, sufficient reason for immediate acting.

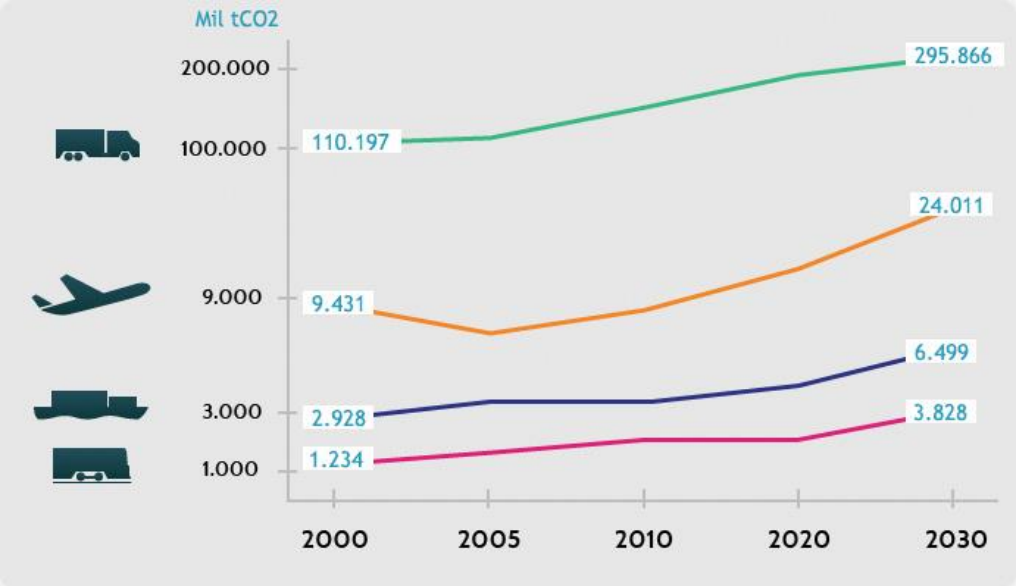

Figure 1. CO2 emissions volume prediction for the next 15 years [1].

To solve this problem, adhesive bonding can be used and researched, enabling the possibility to join the desired complex and lightweight materials in car body and structures and developing more efficient, clean and safe vehicles, while keeping strength and safety at low cost. Another advantage is the efficiency compared with mechanical joints, because they can distribute loads over a much broader area and absorb more energy without failing, mainly due to their flexibility and ductility. In addition, bonded joints do not require intrusive processes such as drilling holes and fastening, which creates local stress concentrations and therefore bearing damage and delamination through the thickness of the adherends.

The adhesives more suitable for working under impact behaviour (and consequently more entitled for automotive industry) are the flexible and ductile ones. However, to achieve structure stiffness and static strength, strong and rigid adhesives are needed. It is generally not possible to have both extremes simultaneously using only one type of adhesive, and thus bringing a problem on this matter. A possible solution for these problems are the mixed adhesive joints, as many of these combine materials with different elastic modulus to increase the joint strength, compared with a single adhesive application. The main objective of the mixed adhesive joint concept is to provide stiffness and strength with one component and flexibility and impact strength with the other. In order to properly design this type of joint, the behaviour of the used adhesives needs to be fully characterized, so experimental and numerical simulation tests should be performed in order to optimize the joint strength and durability.

1.2 Problem definition

There is significant importance in studying the impact behaviour of adhesively bonded joints in the automotive industry. It is important to understand the behaviour of the adhesives under high strength rates and compare the results with static conditions to comprehend the differences that can occur and thus, implement optimization methods to achieve the best operating conditions for the right applications. The technique of mixed adhesive joints has been proposed to improve joint strength of joints under static conditions but only a few impact situations were investigated within this concept and therefore its use in this applications is analysed during the course of this work.

1.3 Objectives

The objective of the present thesis research is to design and investigate the impact behaviour of mixed adhesive joints with two adhesives along the overlap. The main concern is the production of high strength joints with simple configurations and geometries with reduced weights and manufacturing costs. This type of joints opens the possibility of bonding different materials in complex configurations and demanding conditions, especially in automotive industry.

The specific objectives are listed below:

- Manufacture and test the required adhesive joint configurations;
- Built a finite element model including boundary conditions and proper mechanical properties;
- Analyse and optimize the results of the different joint configurations.

1.4 Research Methodology

The methodology defined to achieve the formerly explained main purpose is described in this section. The proposed plan to achieve the required results for this research work consisted in various tasks and steps such as:

- Study of previous work in the area. Improved previously performed work trying to increase joint strength with mixed adhesive joints research;
- Assess the adhesive and adherend properties;
- Specimens manufacture applying two adhesives along the overlap of a single lap joint for different combinations of adhesives and overlaps;
- Testing under static and impact conditions the specimens manufactured and study the influence of the mixed adhesive technique on the strength of the joints. Load-displacement curves are recorded and the failure modes are investigated;
- Numerical model construction for each type of configuration joint and testing conditions.
- Analyse and compare the results between the different configurations and different applications.

1.5 Thesis overview

The structure of the thesis is divided in the following chapters:

Chapter 2: A summarized review of the adhesive bonding technique is presented, starting by describing the general concepts and requirements for automotive industry. A detailed description of cohesive elements is also included. It is followed by an approach to the mixed adhesive concept and its characteristics. Lastly, a revision of relevant impact results for adhesive joints is presented.

Chapter 3: Specimens geometry and configuration are described. Static and impact test procedures of single lap joints are detailed and analysed and the testing settings are defined. The manufacturing process of the specimens is explained and the problems encountered are discussed.

Chapter 4: A numerical simulation with finite element models and cohesive zone elements is performed for static and dynamic analysis. A linear traction-separation cohesive law is developed from the failure behaviour. Boundary conditions are applied to simulate the experimental tests.

Chapter 5: Results for static and impact tests are shown and discussed. Best configurations for the mixed adhesive joints technique are analysed for both static and impact conditions. Simulation tests are evaluated with the experimental results for validation.

Chapter 6: The conclusions obtained within this work are drawn, describing the differences in behaviour of the adhesives under static and impact loadings. The influence of the mixed adhesive technique under impact conditions is evaluated.

Chapter 7: Suggestions to improve and continue the research of mixed adhesive joints under impact conditions of single lap joints are mentioned.

2. Literature review

2.1 Adhesive joints overview

Due to the requirements of bonding complex new concepts and lightweight structures, the automotive industry is becoming the most active industry in adhesive application. Recently, in this industry there is a trend to employ difficulty geometries and manufacturing configurations that are becoming impossible to be assembled using traditional methods, which results in a new demand for adhesively bonded joints. This is also in part due to the increasing use of composite parts. This technique simplifies their introduction with ease and versatility, suitable to almost every material while bringing the possibility of joining complex structures without the need of screws, holes or rivets, as well as reducing material deformation created by welding. In addition, this carries the possibility of joining thin plates, allowing the construction of very light but strong structures [2]. The scheme from Figure 2 demonstrates the advantage of adhesive bonding in improving stress distribution.

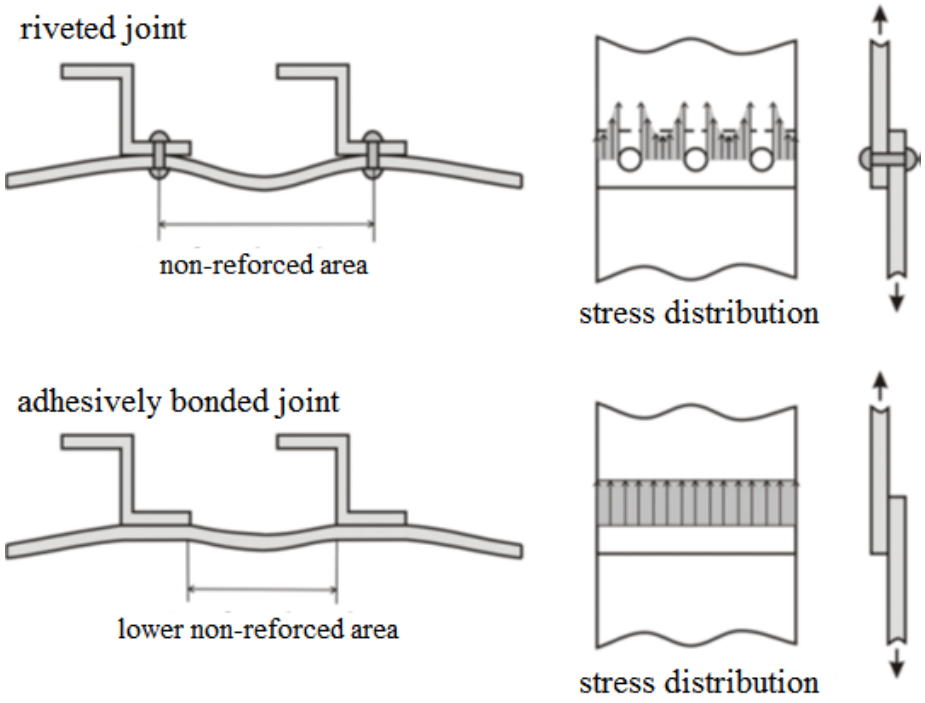

Figure 2. Comparison of two stress distributions caused by tension on a sheet part with a traditional riveted assembly and an adhesive bonded assembly [2].

Adhesively bonded joints have advantages relating to the stress distribution and vibration absorbing. If composite materials with high strength and multi-material applications are considered, the technique provides also the construction of lightweight structures with different expansion coefficients, all of this with low costs in comparison to the traditional methods. The process can also be automated providing cost and manufacturing time reductions.

In relation to the automotive industry, the vehicle requires mainly strength, stiffness, low cost and security for passengers, as well as high resistance to impact load conditions as it can be an occurrence with high probability in this area. It is important however to take in consideration that in most cases, adhesives are weak to peel and cleavage loadings, sensible to environment conditions such as humidity and temperature and can require high temperatures for the curing process which can cause high thermal stresses in the adhesive layer and the substrates. Due to all this factors, the resistance of adhesives in extreme conditions can be compromised.

Furthermore, the first step to properly project an adhesively bonded joint shall consist in a preliminary design, defining the joint configurations, the dimensions and the necessary materials. This is followed by an analysis of the stress distribution of the imposed configuration in order to avoid, as possible as can be, the concentration of peeling forces, cleavage and impact and obtain the maximum bond surface area on a continuous, uniform and thin bond line [2].

2.2 Joint geometry

Although the ideal situation for joint properties characterization relies on testing, sometimes the use of this method for complete structures can result in significant costs and impracticable situations. As a result, the use of computational simulation can be a solution to obtain behaviour predictions of joints for real situations. However, the properties of the materials are not usually fully provided by the manufacturers on the respective datasheets. Thus, the stress-strain curves of the adhesives shall be studied and applied, allowing for the determination of the Young's modulus, tensile strength and strength at failure, as well as the specific stress distribution and adequate failure criteria.

To determine the intrinsic properties of the adhesives, the most commonly performed tests are the shear, tensile and compressive tests. This can also be divided into two main categories: tests on a bulk specimen and tests in a joint. Although the bulk tests are simpler to be performed and follow the plastic material standard, the tests in a joint are more representative of real conditions, however, due to variable characteristic factors of the adhesive joints such as the curing process, layer thickness and surface preparation of the adherends, the stress distribution along the overlap may not be perfectly uniform and, consequently, result in a failure that differs from what is expected in real situations [3].

The most common and simple geometric configuration of adhesively bonded structures is the single lap joint (SLJ), which has been widely used as a standard test to evaluate some adhesive properties and to study the behaviour of the substrates and adhesives at different types of solicitations. It can be manufactured with various variables and characteristics, such as the adhesive thickness, joint overlap, width, length and thickness of the substrates, and different types and methods of adhesive application such as fillets and chamfers [3].

Figure 3 shows a typical adhesively bonded single lap joint under tensile load. As the load increases, the inner rectangles represented starts to deform in result of the shear stress created, τ, by transferring load from one adherend to the other. In real situations, this load-transfer creates a rotation force reaction of the substrates due to the eccentricity of the applied load and generates a concentration of peeling stresses, σ, on the edges of the overlap which are the main points of failure as it results in peeling off the adhesive from the adherend.

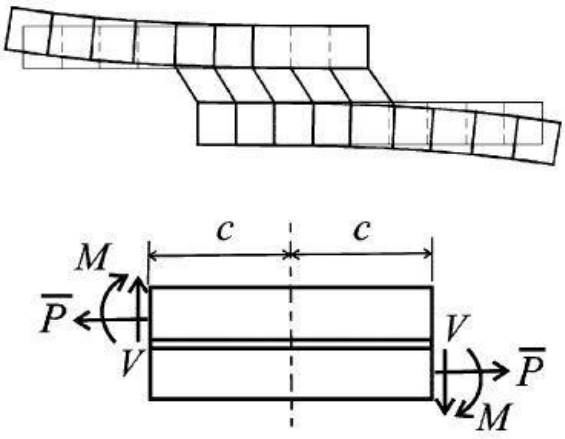

Figure 3. Deformed single lap joint specimen at the top and loading type's subject at the bottom [3].

Figure 4 shows the typical shear and peel stress distributions of the adhesives under tensile load, and it can be seen that that the major stresses are concentrated at the edges of the bondline.

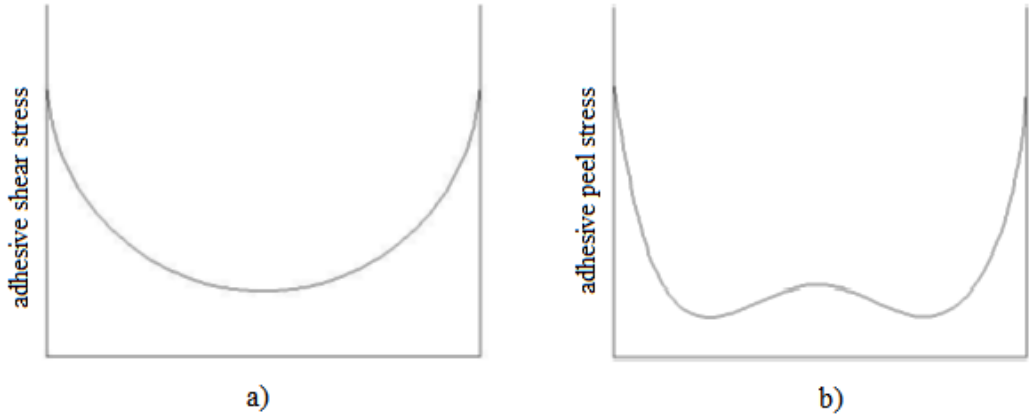

Figure 4. Typical stress distribution along the overlap of an adhesive single lap joint. a) shear stress, b) peel stress

2.2.1 Effect of overlap length on joint strength

For overlap length criteria, Adams et al. [4] found that, for the same adhesives and supposing that both adhesive and substrate can deform plastically, generally the substrates start failing at a certain failure load, giving a constant value of maximum resistance independent of the overlap. In those cases, the maximum resistance of the joint is determined with the maximum tensile strength of the substrates and, consequentially, the design of the joint is not optimized to full capacity, as the adhesive is more resistant than the substrates. For lower overlap lengths (< 30 mm), the maximum strength of the joint is governed by the adhesive rather than the substrates and generally increases with an increase of the overlap length. However, this result occurs when the yield strength of the substrates is not too high. For hard steel substrates (1810 MPa yield strength), overlap length becomes important even at high failure loads, which keeps increasing with longer overlaps. At a certain point, the joint starts to fail in result of a failure of the substrate, in case the maximum resistance of the adhesive is greater than the substrates, or a failure of the adhesive, in case of the opposite. At this point, the resulting failure load will remain constant with the variation of the overlap, which is the same result of the behaviour of lower yield strength substrates [2, 3].

Figure 5 shows a comparison of the failure load in function of the overlap length of a single lap joint. The same adhesive was used with different adherends and overlaps.

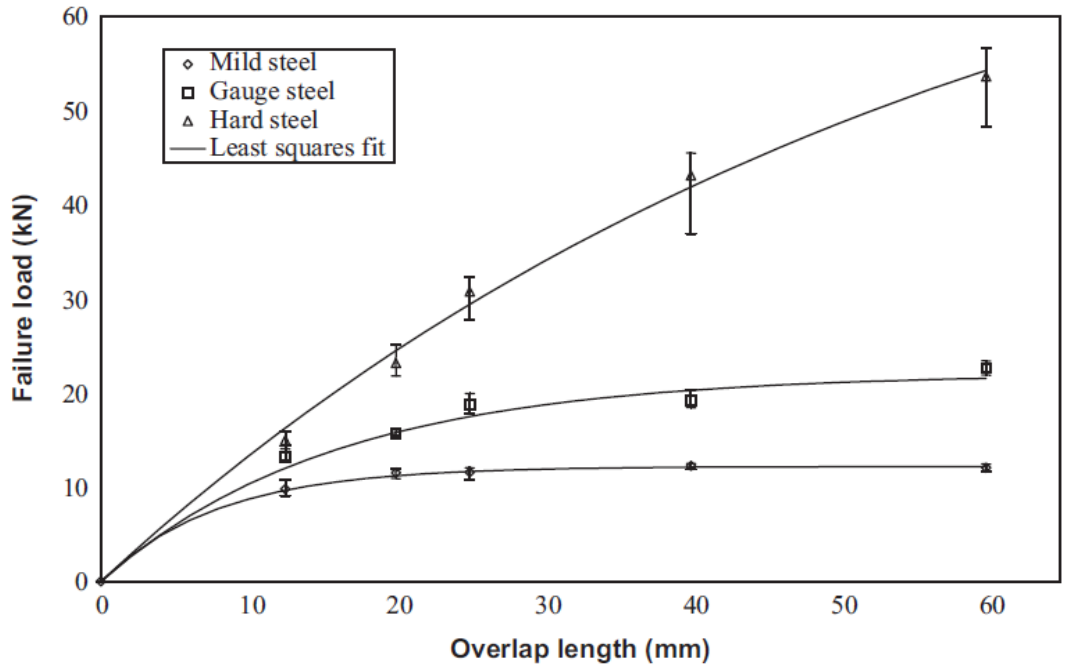

Figure 5. Failure load prediction in function with the overlap length for different adherends under the same adhesive [5].

Trying to optimize the joint resistance and overcome the problem of a substrate failure, a simple prediction method for single lap joints was developed by Adams to analyse the maximum overlap of a joint, with a specific adhesive, without the failure of the substrates or prematurely failure of the joint due to high plastic deformation.

For this analysis, it is supposed that both adhesive and substrate can deform plastically, which can be a very important detail in maximum strength of the joints with ductile substrates. The failure of the substrates normally creates an additional deformation on the adhesives, which can be critical and contribute for an early failure of the joints [6].

The maximum beam flection stress considering elastic deformation according to the beam theory can be:

$$\sigma_f = \frac{6M_f}{b \cdot t^2} \quad (1)$$

By the analytical model of Goland and Reissner, the flection moment on the edge of the overlap is given by:

$$M_f = \frac{k \cdot P_t}{2} \tag{2}$$

where *k* is a factor of joint rotation effect concerning the load applied, *P*, and the flection moment created. The values for *k* are encountered between 0 and 1. The maximum flection stress is:

$$\sigma_f = \frac{3k \cdot P}{b \cdot t} \tag{3}$$

Moreover, once there is a normal traction stress in the substrates due to the applied load, then:

$$\sigma_t = \frac{P}{b \cdot t} \tag{4}$$

which results a maximum normal stress of:

$$\sigma_n = \frac{P(1+3k)}{b \cdot t} \tag{5}$$

The maximum stress that a substrate can resist before suffering plastic deformation can be obtained by:

$$P_{max} = \frac{\sigma_y \cdot b \cdot t}{(1+3k)} \tag{6}$$

For low applied loads and small overlap lengths, the factor *k* can be approximated to 1, resulting in:

$$P_{max} = \frac{\sigma_y \cdot b \cdot t}{4} \tag{7}$$

otherwise, the *k* factor should be decreased as the overlap length rises. The lower value for the factor is 0, which corresponds to a relation where the overlap is 20 times higher than the thickness of the joint, $^{l}/_{t} \geq 20$. The Equation 6 can then be written as:

$$P_{max} = \sigma_y \cdot b \cdot t \tag{8}$$

meaning that a full plasticization of the substrates is considered.

On Figure 6 is exemplified the prediction of the failure load as a function of the overlap length, representing the behaviour of the adhesive and the substrate, according to the method demonstrated by Adams before discussed.

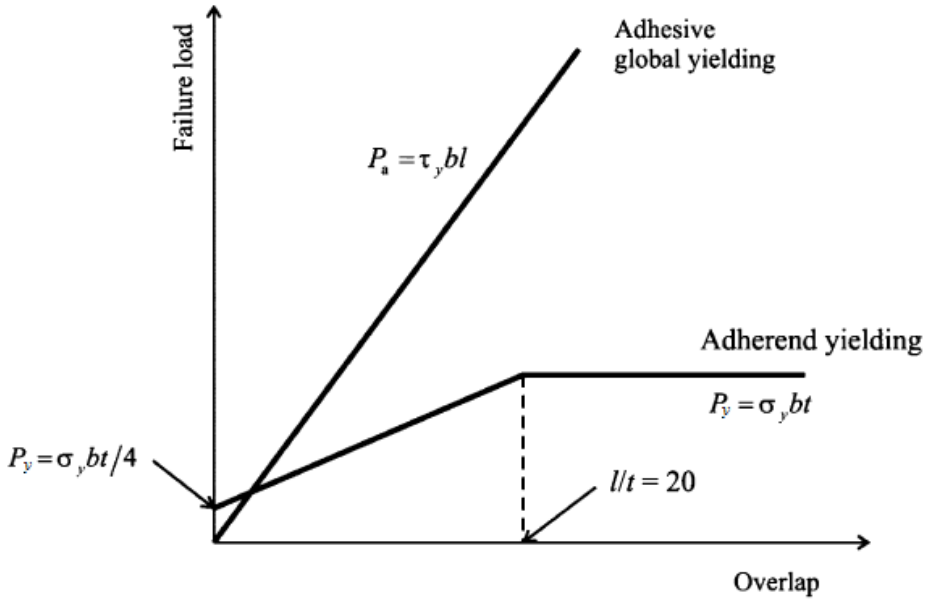

Figure 6. Joint strength prediction model by Adams et al. [7].

2.3 Mixed adhesive joints

2.3.1 Concept

The mixed adhesive concept is one that has the potential to be widely useful in a variety of applications, such as the automotive, aerospace and aeronautical industries.

As the stress distributions on a single lap joints aren't always equally distributed along the overlap, an ideal adhesive joint should be one that includes a variation of the flexibility and strength properties of the adhesive to accommodate and equalize the forces created, solutions usually referenced as functionally graded adhesive joints. The best way to do this is by putting a ductile and flexible adhesive at the overlap ends to absorb and reduce the stress concentrations that happens normally in a single lap joint, while a stiff and less-ductile adhesive should be used in the middle. As the metal dissipates the energy through plastic deformation, which is found more often in impact situations, the best suitable adhesives are the flexible and ductile ones. On the other hand, to increase structure

stiffness and static strength, rigid and strong adhesives should be used [8]. To combine these two necessities and enlarge the application possibilities, different approaches have been proposed: softening of rigid adhesives through rubber particles, stiffening of flexible adhesives by means of glass-spheres, combination of different adhesives, among others [9].

Mixed modulus joints have been proposed in the past by many researchers [10-13] with the objective of improving the distribution of stresses and increasing the strength of the joints with high-modulus adhesives. This type of joints was introduced decades ago but only recently this approach was experimentally tested, where the authors achieved improvements in joint strength. The use of dual adhesive joints was first proposed by Raphael [10] as a possible solution, with a technique that enables the possibility to reduce the stress concentrations at the ends of the overlap, typical for single lap joints, by applying a ductile adhesive to reduce premature joint failure. The concept entails the introduction of a more flexible adhesive at the ends of the overlap, while a stiff adhesive is used in the central section of the joint, less subjected to deformation during loading. In 1973, Hart-Smith [11] recognized that the use of mixed adhesive joints could yield improvements in mechanical strength for joints subjected to large temperature gradients. Later, Fitton and Broughton [12] and da Silva and Adams [13] achieved strength improvements with the use of composite adherends and an epoxy mixed adhesive on a single lap joint. In the case of a single adhesive application with high stiffness, the capacity of the composite joints was limited by the low through-thickness strength of the adherends, resulting in delamination of the composites, normally at the ends of the overlap where the stress concentrations is higher. On the other hand, when a mixed adhesive joint was made with the same adherends, this resulted in the same strength capacity but with a cohesive failure within the bondline, which is a better result [8].

Compared to a normal adhesive application on a single lap joint, it is possible to gain strength by transferring the load uniformly along the overlap and reducing the load concentrations on the edges of the joint where the forces are normally higher and tend to create peeling, which are the main cause of failure in structural bonded joints. Mixed adhesive joints can comprise a better combination of ductility and strength by using low and high modulus adhesive in the same joint, providing best results than with the same stiff adhesive in a standalone application. That can be observed in Figure 7, representing the stress distribution along the overlap of a mixed adhesive joint, where it can be seen

by the area above the curve that the global shear strength of a mixed joint can be better distributed along the overlap rather than in a joint with only a stiff adhesive of the same kind.

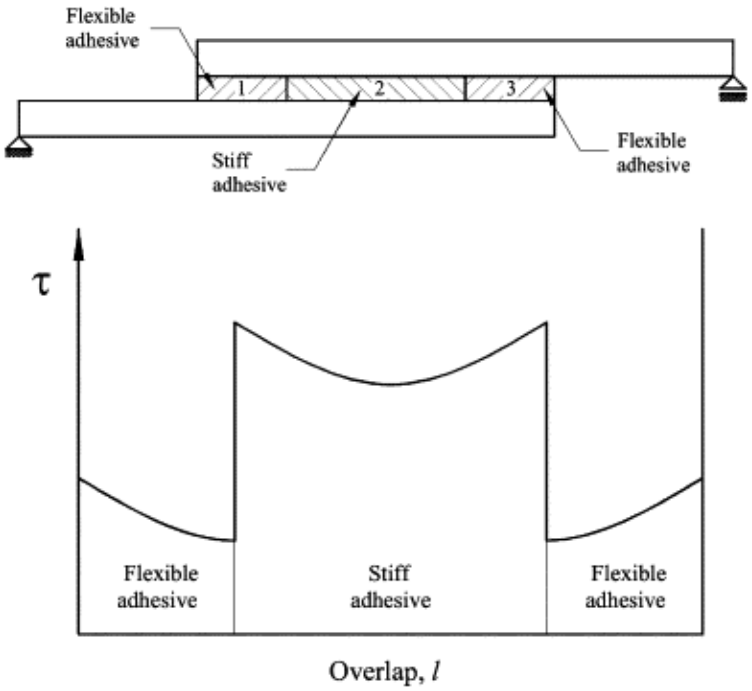

Figure 7. Mixed-modulus bondline of a Mixed adhesive joint concept for improved joint strength (τ is the shear stress) [8].

Figure 8 is a schematic representation of the shear stress distribution at failure of a mixed adhesive joint with the adhesives AV138 and DP-8005 investigated by da Silva and Lopes [14] where they found that the average shear strength of the mixed adhesive joint was higher than both adhesives when used alone. The lower strength for the brittle adhesive was a result of load concentration at the ends of the overlap which reduced the load carried by the central part of the overlap. On the other hand, the combination of a ductile and brittle adhesives leads to a better contribution of the overlap length, making this types of joints stronger than a joint with brittle adhesives alone in the majority of the cases. Yet, for this conclusion to be true, it is important to verify that the load carried by the brittle adhesive is higher than the load carried by the ductile adhesive taking in consideration the ratio of the adhesive modulus variation, otherwise the overall joint strength could be compromised. The following condition shall be satisfied:

$$\tau_y < \tau_r \frac{2l_{brittle} \cdot \sinh \lambda l_{brittle}}{\lambda(l - l_{brittle}) \cdot l_{brittle} \cdot [1 + \cosh \lambda l_{brittle}]} \quad (9)$$

Where τ_y is the global yielding strength of the ductile adhesive, τ_r is the maximum shear stress of the brittle adhesive and l is the overlap length. λ can be calculated with the following equation:

$$\lambda^2 = \frac{G}{t_a} \cdot \left(\frac{2}{E \cdot t_s}\right) \quad (10)$$

where G and E are the shear and elastic modulus of the substrates, respectively, t_a is the bondline thickness and t_s is the thickness of the adherends.

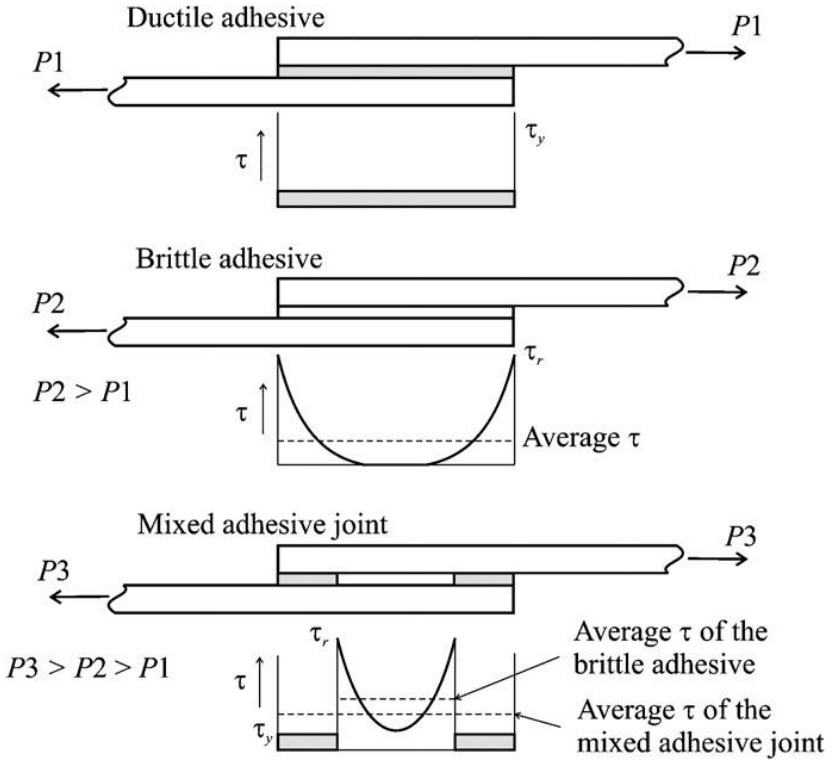

Figure 8. Schematic shear stress distribution at failure in mixed adhesive joints with AV138 + DP8005 [14].

2.3.2 Applications with temperature

The mixed adhesive joints can also be advantageous in applications that are subjected to extreme temperature conditions, enlarging the range of possibilities. As generally most of the adhesives do not behave the same way with high and lower temperatures, where they can be too brittle or suffer degradation, a mixed adhesive joint can solve this problem and tolerate the temperature differences more adequately. Thus, a mixed adhesive joint should have good strength within a great range of temperatures, as demonstrated in Figure 9.

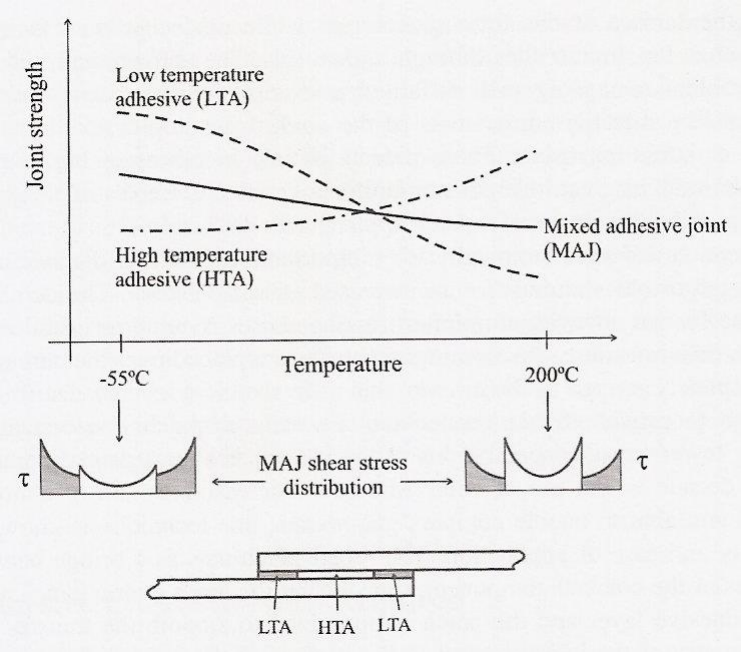

Figure 9. Mixed adhesive joint concept for low and high temperatures [8].

The glass transition temperature (T_g) is an important aspect of an adhesive and its mechanical properties are determined by the operation temperature. Below the glass transition temperature, a reduction of the temperature, the ductility of the adhesives decreases with an increase of the modulus and strength. At T_g there is a rapid reduction in the modulus and strength as the temperature increases, weakening the adhesive and rendering it unable to carry any substantial load.

This approach has been studied by da Silva and Adams [13], where a high-temperature adhesive (HTA) in the middle of the joint retains the strength and transfers the total load at high temperatures while a low-temperature adhesive (LTA) acts to reduce the stress of the high-temperature adhesive at low temperatures, absorbing the majority of the loads.

This technique was proven to work with good results when dissimilar adherends were used [8].

An optimal joint for low and high temperatures can be obtained as long as the adhesive is loaded in the temperature range for which it has been designed.

2.3.3 Adhesives combination

The most important task in designing a mixed adhesive joint is the selection of adhesives, which needs to be reasonable to achieve strength improvements. Ideally, it would be desirable to have both of the adhesives with high strength and strain at failure but Fitton [15] proved in his works that a combination like that is most likely to be impossible. That way, a rational and coherent selection of the adhesives will necessarily consider at least compatible working characteristics, curing regimes, resistance to environmental exposure and surface pre-treatments of the adherends. Both base adhesives must [9]:

- Be chemically compatible;
- Have sufficiently different mechanical properties;
- Be able to be polymerized with a common curing cycle.

Also, the most appropriate mechanical properties of the candidate adhesives should be determined. A better indicator for improving joint performance should be the stiffness of a bulk adhesive and not the shear strength data because the service life condition of the joint and the material of the adherends that often limits its capacity, could affect the selection [8].

Another important step is to know the interaction between the stiffness and strength of the adhesives and adherends in order to evaluate the magnitude and location of concentrated stresses generated in the bond line due to the combination of materials. Even in a well-designed balanced joint, significant peel stresses are still generated, so it's important to analyse the design of the joint and the adherends used, especially when composites or dissimilar adherends makes part of the structure. It was been proven experimentally by Gordon and Fakley [16] that the joint strength of various adhesives can be correlated with the adherends elastic modulus and, when using stiff adherends, the

stresses of the bondline are reduced as the adherends deform less in tension, reducing differential shear, and there is less joint rotation, which reduces peel stresses.

2.3.4 Adhesive ratio selection

As has been said over along this section of mixed adhesive joints, an important characteristic is the ratio of the two adhesives on the overlap, which needs optimization to maintain a high joint strength. Srinivas [17] has concluded in his numerical analysis with finite elements (FEA) that optimum lengths of stiff and flexible bonds could be chosen to assure the lowest possible stresses in the bondline. Even though, the suggestion from Raphael [10] of matching the stress distribution to adhesive strengths seemed to be a more rational methodology as the strengths of flexible and stiff adhesives can vary greatly. Later on, Fitton [15] made a numerical analysis, by studying the effect of different adhesive modulus combinations and different configurations, offered a conception of the variation in shear and peel stresses according to the adhesive stiffness. Moreover, he also focused on understanding the optimal amount the lower modulus adhesive should spread along the overlap. At this point, Fitton studies became essential in determining the effectiveness of the mixed adhesive placement in the joint along with the ratio of adhesive stiffness (E_{LM}/E_{HM}). This way, the lower modulus adhesive is the determinant on the peak peel stresses, considering it's extended as far enough into the overlap.

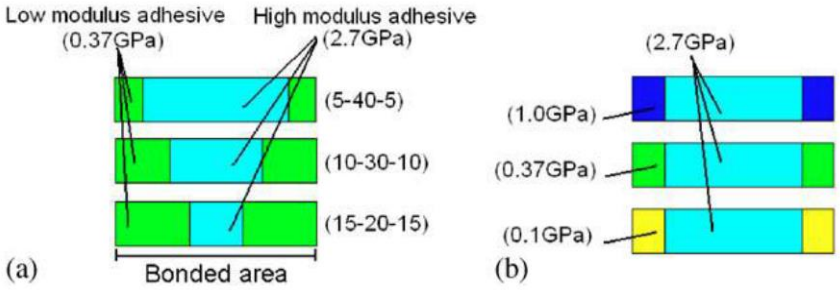

Figure 10. Adhesive placement in FE models. (a) – Modulus transition point variation and (b) – Different modulus of the adhesive at the ends of the overlap [12].

Figure 10 represents a simple scheme of the finite elements studies by Fitton, to analyse the influence of the modulus transition local on shear stress distributions. Figure 10.a)

shows a modelling where there were studied the stress distributions with a combination of two adhesives in variable ratios of stiffness along the overlap. The respective stress distribution curves is reproduced in Figure 11.

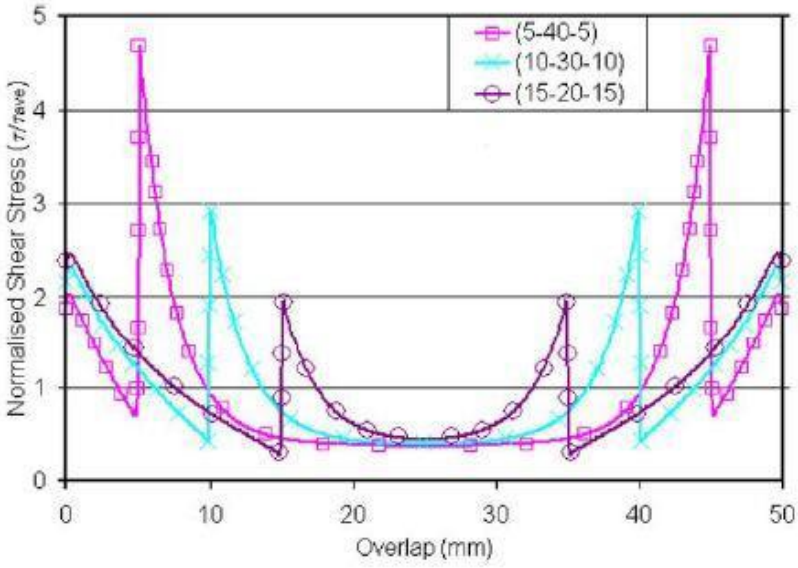

Figure 11. Effect of varying modulus transition point on shear stresses [12].

Figure 10.b) represents a study with the same objectives but using the same high modulus adhesive and ratios of stiffness, varying the low modulus adhesive. The stress distribution curve for the second study (Figure 12) shows that as the modulus is increased at the ends of the joint the more shear stress is carried by that adhesive and less is carried by the high modulus adhesive in the middle of the joint.

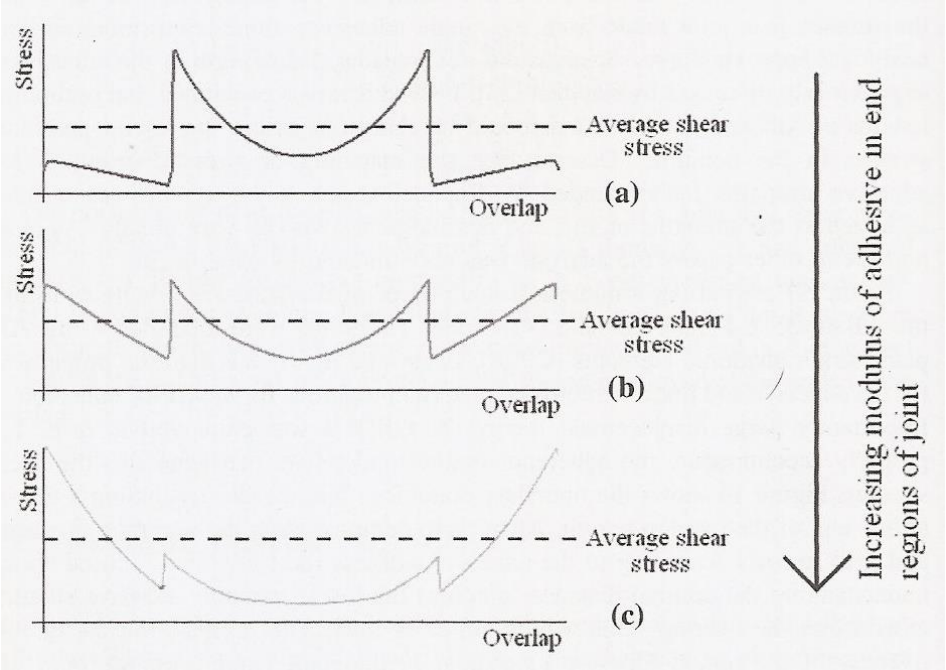

Figure 12. Effect of adhesive modulus on shear stress distributions [8].

It can also be noticed that lower shear stresses are obtained when the peak shear stress is equal in both of the adhesives, which was a previous suggestion made by Raphael [10]. This concept is not the optimum for achieving strength improvement, but it's well-designed for obtaining lower shear stress distributions. Figure 13 shows the results of the numerical simulation tests for the shear stress distribution curve in function with the modulus of the overlap end adhesive. da Silva and Lopes [14] have recently studied experimentally mixed adhesive single-lap joints with the same technique as Fitton in his numerical tests of using the same brittle adhesive in the middle of the overlap and varying the edge adhesive using three different ductile adhesives. They found better results in terms of strength capacity in all cases using mixed adhesive joints compared to a brittle adhesive in a normal single application.

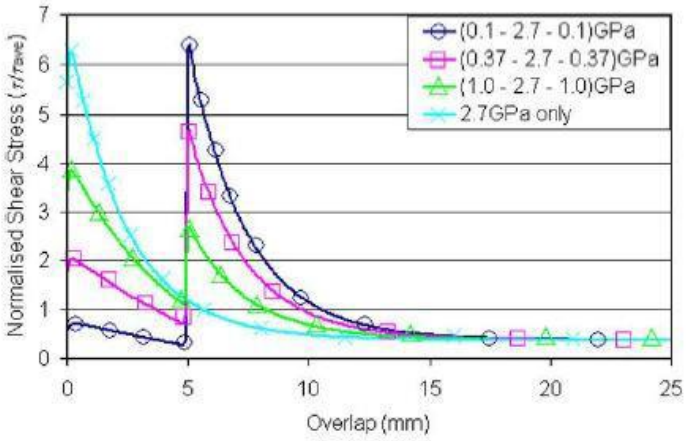

Figure 13. Effect of changing adhesive modulus at the end of the overlap shear stresses (half of overlap) [12].

In addition, Chiminelli et al. [9] approached the mixed adhesive technique with aluminium/composite joints under shear loads by an optimization procedure based on finite element calculations and considering continuous variations of properties within the adhesive layer, to determine the optimum grading of properties in a bondline to maximize the ultimate loading capacity of a single lap joint. They prepared and tested single lap joints with 50 mm overlap with bi-adhesive configurations with a strategy based on mixtures of two structural adhesives, a relatively rigid one and other more flexible. With adjusted layer lengths through FEA calculations, they compared the results with the mono-adhesive solution specimens and found a primary conclusion showing a global improvement of about 57%, evidencing the potential of the technique, with less stress concentration in all the adhesive thickness and also in the adhesive-substrate interface. For the simulations, a model considering "banded" or discrete approaches was analysed to optimize the displacement of the adhesives and try to fit the optimum continuum distributions. The objective was to obtain the most effective distribution in adhesive bands given an optimum continuum grading. Three solutions to achieve this objective were proposed, as seen in Figure 14: one where the adhesive bondline was divided into bands of the same length, with an interpolation variable, ρ, calculated as the average of the function in each band domain; other where the length of the band extremes required to be equal; and another where all parameters were left free to change within the operational range.

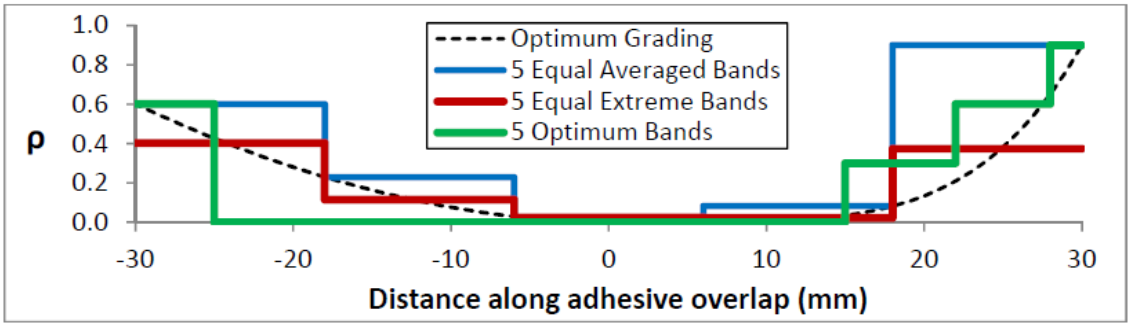

Figure 14. Interpolation variable along the adhesive bondline for three different solutions [9].

Figure 15 shows the results of Chiminelli's numerical analysis for the three discretization proposals above discussed, for the evolution of the maximum load with the number of bands used.

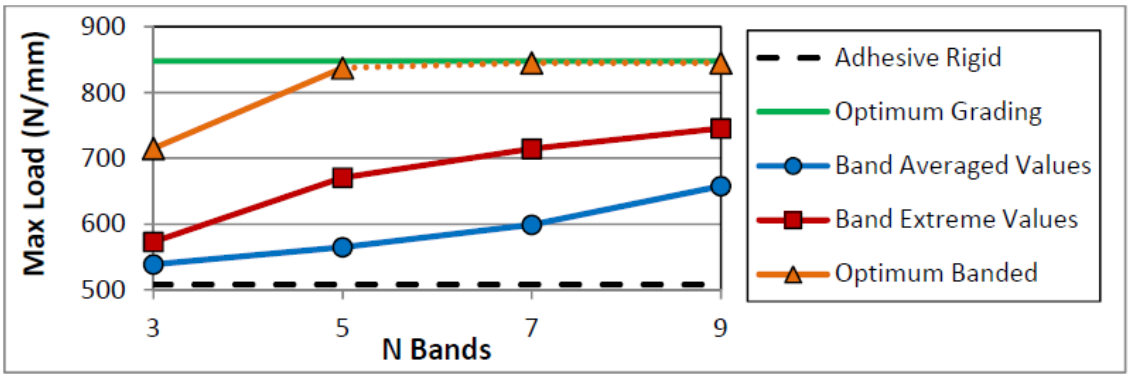

Figure 15. Evolution of the maximum load with the number of adhesive bands for the different solution schemes [9].

From this results, the authors concluded that for the joint analysed and considering a cohesive failure mode, the ultimate load can be improved by around a 70%. Also, they found that the way on which the best continuum grading is approximated by means of bands, strongly affects the level of improvement finally reached [9].

The optimal stress distribution should comprehend a spreading load accordingly to the modulus of each adhesive and taken in consideration the working load conditions, where the higher stresses should be delivered to the stiffer adhesives and the lower loads to the flexible ones. An excessively large proportion of the low modulus adhesive could limit the joint capacity in result of the characteristic low shear strength delivered by these types of adhesives. Thus, according to this results, an optimal distribution of shear stresses shall be one that aims a simultaneous failure of both adhesives and not one that results in the

lowest distribution of stress. Therefore, a balanced optimization of a mixed joint should approach a compromising of shear stresses equilibrium and strength of the joint, which could be a difficult task as the non-linear behaving of the adhesives and substrates can be an important fact due to the changing in stress distributions with the yielding of the adhesives and thus, a determinant of improvement.

Furthermore, a non-optimally designed mixed joint could compromise the global performance, leading to a reduction in the overall shear capacity of the joint. It is important to select a proper combination of adhesives and respective adherends for the various types of applications.

2.3.5 Manufacturing process

The manufacture of a mixed adhesive joint isn't easy as it requires the application of two or more adhesives on the same overlap and avoid adhesive mixing, being it one of the problems associated with the mixed adhesive technique. To assure a proper separation and mixing free problems when the pressure is applied, a physical separation is important. In previous works, Pires et al. [18] had controlling and consequent mixing problems in adhesive overlap length under application of pressure because of not using adhesive separation. Later, it was found that the best way to control the process is by using film adhesives, which can be implemented in production lines, although it is difficult to find compatible ones in the film form [8].

Already experimented from previous works, the adhesives separation can be done by a wire or a silicone spacer. Even though a small portion of the load-bearing area is reduced, silicone spacer seems to be the best solution, as it already has been explored by da Silva and Lopes with good results [8, 14], but this method should only be used in long overlaps as the area occupied with the silicone stripes, which is a non-working area, will cause reductions in joint performance. For short overlaps and thin bond-lines, Marques and da Silva [19] tried the use of a nylon line with the same thickness of the adhesive layer glued to the adherends with a small amount of a general-purpose cyanoacrylate with good separation when manufacturing double strap joints with and without tapers. They found that the method can be a reliable and good substitute, providing good dimensional control without significant consequences to the overlap.

Also, the mixed adhesive technique is more sensible to curing temperatures and time as normally the curing procedures vary from adhesive to adhesive. A previous analysis in the design stage of the adhesives combination and curing processes shall be taken in consideration to study and search to verify if a match is possible, as it can be very hard or impossible to cure a mixed joint with an adhesive that cures with temperature and another one that degrades at the requiring temperature of the first. An intermediate temperature between the curing temperatures of the adhesives selected for a specific joint can be a simple solution for the curing process but that can compromise a proper curing procedure between the two adhesives and lead to bad results.

2.4 Impact test and behaviour

The impact conditions are an important characteristic for some applications like the automotive industry, where the impact situations have an enhanced probability of occurrence. The impact behaviour shall then be taken in consideration if structural bonded adhesive joints are the chosen technique to bond the structures, as safety regulations and manufacturer quality standards exists. Ordinary car structures comprised of steel panels and have been mainly joined by spot welding. Now, as the aim is to reduce the weight of the cars, the adhesives have become an interesting approach generally consisting in a combination of adhesive bonding plus spot welding, which increases the torsional stiffness, fatigue life and damping of the body.

2.4.1 Adhesive and joint behaviour

When designing an adhesive joint for automotive industry it is necessary to define the performance parameters at high strain rates in order to investigate how different from static conditions can the mechanical properties be and how this changes the performance of a joint. Under this type of conditions, the adhesives normally tends to deform with higher stress and lesser ductility, causing higher resisting loads but lower absorbed energy. Such a response of viscoelastic materials in the region of the glass transition

temperatures is related to their molecular movements because these materials under applied stresses relax with time due to their molecular rearrangement and the relaxation mechanisms are affected directly by the strain rate. If the test time is long enough, molecular rearrangement takes place, leading to relaxation in the polymer chains and resulting in high elongation. On the other hand, if the test time is too short to start relaxation due to the molecular rearrangement, then the response of the viscoelastic material resembles that of stiff materials, as experienced under the impact test.

Under impact load it is crucial to transfer the load to the steel without fracturing the joint thus assuring the integrity of the car under a crash situation and absorb the maximum energy possible to keep the passengers safety. The major difference between impact and static cases is the consideration of stress wave propagations in stress analysis, the dependency of stress-strain relations and the strength of materials. The first requires complicated experimental setups to assess material properties under high rate loading and the second involves difficult analysis to determine the stress distribution and its variation with respect to time. Given that, it is hard to accurately predict failure for impact loads. To solve this obstacles, FEA simulations have become a good research tool, especially for components with complex shape.

In many cases, it is necessary to predict the mechanical properties of adhesives for a larger range of strain rates, such as the high velocities that are normally applied under impact conditions, and this sometimes can be difficult to achieve. A solution to this problem can be the use of an extrapolation criteria applied to the experimental lower values of strain rate. However, the adhesives normally exhibit a non-linear relationship between stress and strain, which does not allow for a modelling using only the Young's modulus and Poisson's ratio [20].

Also, the mechanical strength of the materials must not be oversimplified. In impact situations, the need for a strong joint can be subjective as in this case a strong joint does not necessarily mean a high bond strength, which normally carries a very low strain to failure value for single lap shear specimens and could be an important determinant for a low strength failure under impact loading. While peak failure load value may be very high, the joint may well be very brittle and perform bad under impact. Given that, when selecting the adhesives for impact condition joints, it is important to select one with great values of strain to failure, so that the energy absorption capacity is enhanced and the resistance to damage is increased. Standard epoxy adhesives used to increase stiffness

have insufficient energy-absorption properties which also mean reduced shear strength and peel resistance under impact, being impossible to create a joint that is able to keep the bonded components together in a crash situation. By introducing rubber particles that were finely dispensed in an epoxy matrix, in the 1990s a new generation of toughened epoxy adhesives called crash-resistant adhesives, came onto the market with good high strength at high velocities and a high energy absorption [21].

Results for single lap joints under drop impact load tests were found [22] with a high elongation epoxy adhesive and mild steel playing the role of the ductile adherends. The results showed that the failure mode of the high strain-rate test was nearly the same as that in quasi-static tests. The main differences consisted in the behaviour of the substrates due to the sensitivity to the high strain-rate, which exhibited less deformation that in quasi-static tests, thus absorbing less energy. As for the adhesive, it experienced similar damage as in the quasi-static tests despite of the increased failure load, as it can be seen in Figure 16 where it represented a comparison of the adhesive behaviour between impact and quasi-static test results.

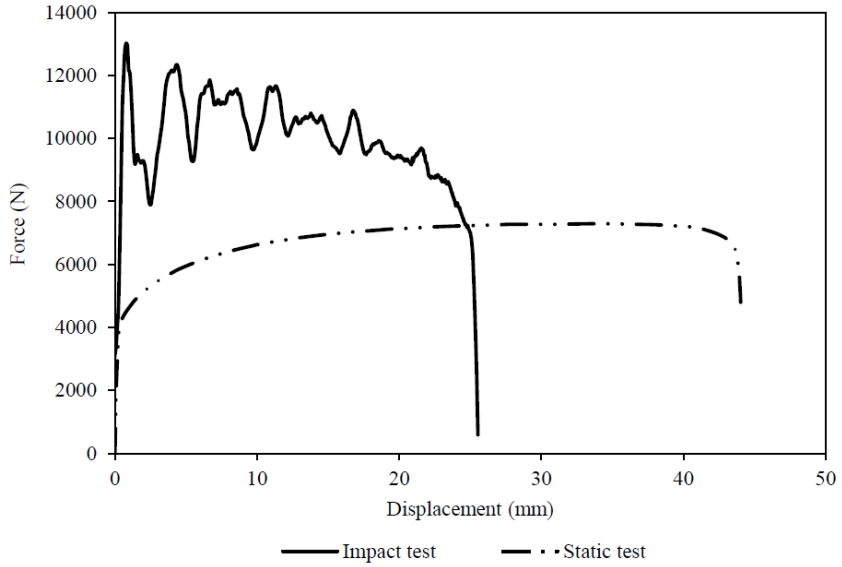

Figure 16. Comparison of different strain-rates for a single lap joint with mild steel adherends (1 mm/min for static and 4.47 m/s for impact) [22].

In addition, Adams and Harris [23] have investigated the impact behaviour of single lap joints with aluminium alloy specimens and concluded from a pendulum type impact machine that, for a range of adhesives, the joint strength is not significantly affected by high rates of loading. They found an interaction between the joint strength and energy

absorption with an inverse proportionality, concluding that the energy absorption came mainly from the deformation of the adherends, thus, the highest energy absorption was found with the use of ductile aluminium alloys adherends due to the low yield strength, while the use of high yield strength aluminium alloys resulted in low energy absorption. They claimed also that by applying a correct failure criterion to the finite element results, the effects of impact loading could be predicted with reasonable values. Goglio and Rossetto [24], investigated the mechanical behaviour of lap joints under impact loading focusing in the thickness of the adhesive layer, and concluded that higher joint strengths could be obtained under impact loading compared to static conditions and that relatively thin adhesive layers were advantageous compared to thick layers, also exhibiting higher failure loads.

Kadioglu and Adams [25] investigated the behaviour of a flexible adhesive under impact loading using the single lap joint configuration with high strength steel adherends, tested with a pendulum impact machine. They found results that showed that the lap joint strength increases considerably under impact loading compared with those under quasi-static loading and that there is a relationship between the joint performance and the loading speeds. The adhesive showed a high strain to failure with good strength, which improves structural crashworthiness. The response of the adhesive under impact loading approaches the behaviour of structural adhesives, giving an increase in the maximum stress with relatively small strains to failure [25].

A reasonable selection of adhesives and adherends shall be taken in consideration and the type and area of application could be determinant. While a high peak failure load could be good for aerospace applications, the toughened system is much more likely to be the choice for an automotive structure.

2.4.2 Impact testing

Although the use of adhesives in recent years has increased due to its many advantages over conventional joining techniques, there's not yet a full assurance to the performance offered at extreme conditions such as an impact situation. Not much research on impact situations of adhesively bonded joints has been performed so far because the conditions are hard to replicate and expensive as setups requires high-performance sensors and data

logging systems. Although, thanks to the progress of electronics, this obstacle is recently being removed, but the real testing aspect is always important as it provides real results that in some cases can be unpredictable and unexpected.

At first glance, the adhesive bonding can comprehend applications with two types of impact conditions: the first corresponds to the situations where impact loads are a normal condition and the mechanisms are designed mainly to undergo discontinuous loading; the second case relates to the structures where an impact loading corresponds to an impulsive situation strange to the normal service conditions such as an accident. This second instance is where the automotive industry is related, in which the crashes are very important. The expectations depends on the case and can be different. If the impact loadings are a normal service condition, mechanisms must designed to sustain repeatedly loadings without damage, while in the other hand, if the impact is an occasional situation, the system must be designed to minimize its consequences and a certain level of damage must be accepted and inevitable. From this, the behaviour of an adhesive subjected to impact could bring two typical issues: turning a non-brittle adhesive under static or quasi-static conditions into a brittle behaviour when an abrupt loading is applied and, consequently, affecting the capability of absorbing energy; assessing the influence of the loading rate on the adhesives response and thus its sensitivity to the strain rate [8].

The impact tests can be performed as a part of the process of design or to check the properties of an adhesive as a quality control [2]. To analyse the behaviour of an adhesive joint under impact conditions there is already a range of different tests, such as for example, the Wedge-peel test, Drop-weight, Block impact test, Split Hopkinson Bar, to evaluate the adhesive properties and aim at measuring the energy to break the bound of the joints, in order to achieve the best results. Three main types of them are used to analyse the impact effects and methodologies depend on the type of loading rate [21]:

1. Low velocity - Experiments with pendulum impact testers with impact rates below 5 m/s.
2. Medium velocity - Drop-weight tests, with rates up to 10 m/s.
3. High velocity - A split Hopkinson pressure bar (SHPB) testing technique for rates up to 100 m/s.

where in the low velocity range the problems are treated as a vibrating system, in medium velocity the stress and strain propagates as waves in materials and in high velocity a body

collides with another faster than their sound velocity, which increases up to the impact velocity.

Bezemer et al. [26] developed a rod-ring specimen to load the adhesive in pure shear on impact. The authors tested the specimens with three different materials: a tough adhesive, a brittle adhesive and a sealant, at five layer thicknesses and three test speeds. They concluded from a drop-weight tower and an air gun testing results that the specimen used was suitable for impact tests and for comparing impact tests with static tests. In most cases, increasing the load rate caused an increase in energy absorption, which was the case of the tough adhesive, exhibiting a greater energy absorption than the brittle adhesive. Also, they found an optimum adhesive thickness at different test speeds, in result of the constant failure displacement [26].

So far, results of studies of adhesives under impact loading have been controversial as some researchers report similar results for impact and quasi-static conditions. The increase in demand from the industry and the progress of computer technologies made the finite element analysis into a very good method to predict the response of adhesive joints under impact loading, as the adhesives generally exhibit strain rate-dependent material properties under impact conditions. The explicit finite element solvers can easily solve large deformation problems and dynamic events where inertia of the structure is of significant importance. One of the rising and promising research areas is impact problems of composite materials bonded adhesively, where this analysis will be more important [21].

2.4.3 Mixed adhesive joints under impact conditions

It is already proven that the technique of mixed adhesive joints can improve the strength of a joint by using adhesives with different modulus, especially when the technique is applied to a stiff and very brittle adhesive. At the moment, the majority of experimental and numerical test have been investigated with static conditions and there is a few information related to the behaviour of the adhesives under extreme conditions such as impact. The concept of mixed adhesives has not yet been truly explored, so there is a need to confirm if the technique fits the automotive industry and if the results can be as good as in static conditions [27].

Although the more suitable adhesives for impact conditions are the ductile ones, for structure stiffness and static strength the rigid and strong adhesives must be used. This way, an adhesively bonded complex structure like a car chassis for example, shall comprehend a balanced and optimized adhesive type application, ensuring the best equilibrium between strength and flexibility in the majority of the situations. To solve this problem, the mixed adhesive conception can again be an appreciated solution, using one adhesive to absorb the energy and another that provides stiffness and strength. Given that, the dual adhesive system might be more appropriate when a compromise of strength and ductility are wanted as the flexible and ductile adhesive at the ends of the overlap gives a higher capacity to deform and is less sensitive to defects [8].

2.5 Cohesive elements

The advantage of cohesive damage modelling is the introduction of a combination of both continuum and fracture mechanics in an mixed-mode damage model, based on the interface element formulation with the help of finite element analysis (FEA), opening the possibility to predict the crack propagation as a result of a simulated degradation of the material, including both the strength and the energy parameters of the debonding process [28].

The cohesive element methodology can be explained on the simple scheme view of the crack tip of the Figure 17. It exists a process zone acting as a transition between traction free and linear elastic of the bulk material regions. The existing cohesive forces are represented by a set of springs, which results in a unique traction profile at the crack edge [29], which can be considered as a continuum of cohesive forces in *Continuum Cohesive Zone Method* (CCZM) or be discretely taken into account in *Discrete Cohesive Zone Method* (DCZM) [30].

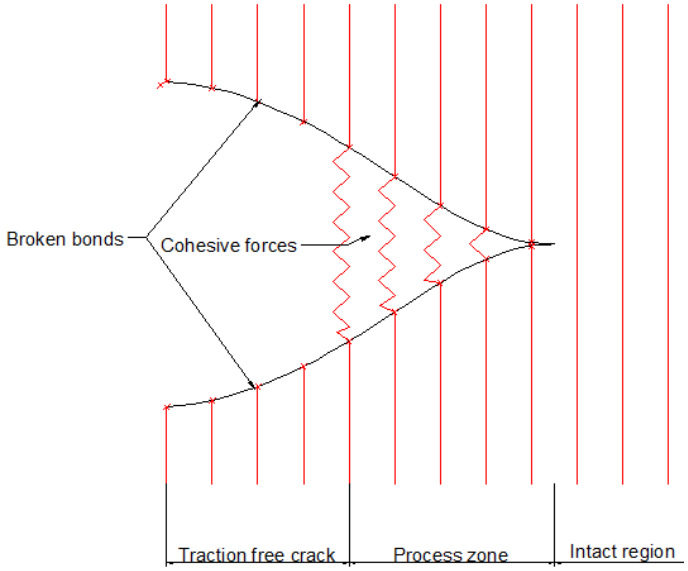

Figure 17. Cohesive forces of the bonds on a debonding process zone [31].

The cohesive zone modelling can be defined in terms of pure modes, which can be mode I - opening, mode II - in-plane shear and mode III - out-of-plane shear (see Figure 18), and mixed mode which is a combination of the pure modes and a closer encounter with real application conditions.

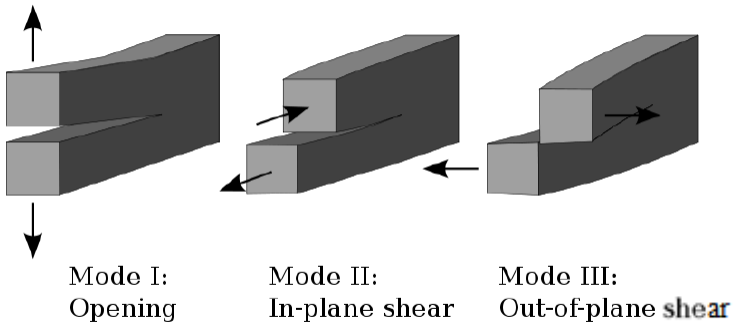

Figure 18. Failure modes resulted by the three modes of loading [32].

At this moment, there are different cohesive laws relating the adhesive properties, as it's represented in Figure 19. For very ductile adhesives, it is suggested the use of a trapezoidal law as it takes into account the remaining constant adhesive strength before the failure of the joint is initialized, which is common with ductile adhesives. For very brittle adhesives, both triangular and exponential laws are well applied [28].

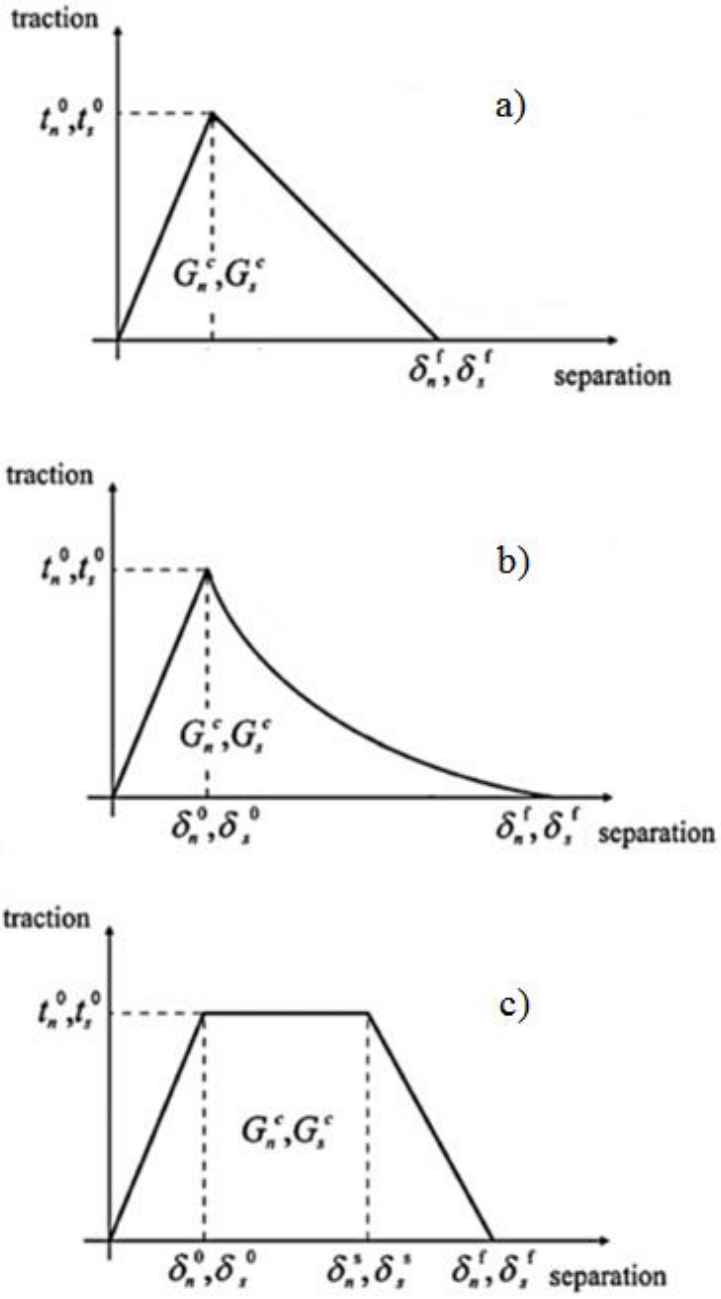

Figure 19. Different types of cohesive zone damage model, (a) triangular, (b) exponential, (c) trapezoidal [28].

The constitutive equation for pure mode I can be defined in two different methods (Figure 20) between the stresses (σ) and the relative displacement (δ_r) between homologous points.

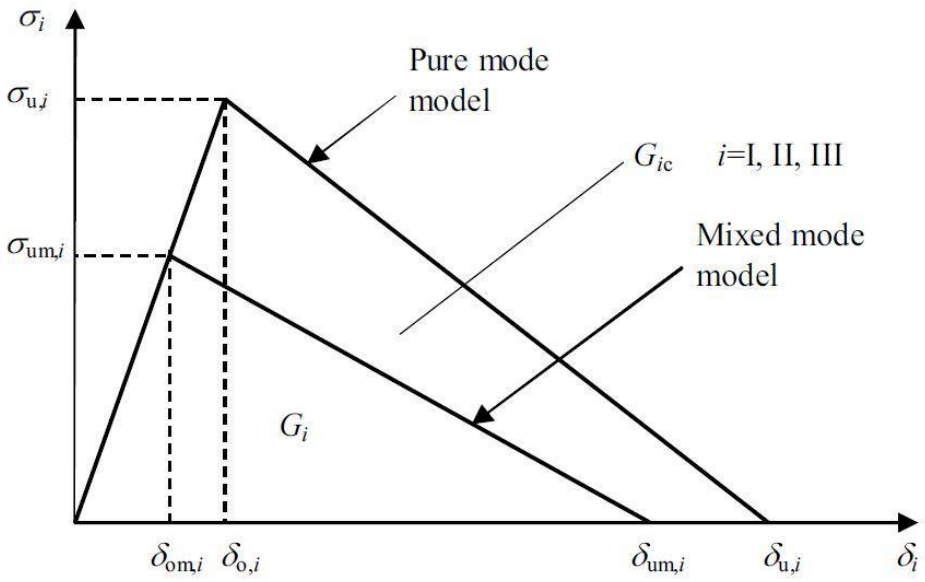

Figure 20. Triangular law for pure mode and mixed-mode [33].

The stresses before damaging starts to grow can be determined by:

$$\sigma = D \cdot \delta_r \tag{11}$$

where D is a diagonal matrix containing the pure mode (d_i, i = I, II, III) penalty parameters. The material starts suffering damage and relaxes linearly between the points of maximum local strength ($\sigma_{u,i}$) up to failure, where this strength is zero. The area under the line of adhesive softening behaviour simulates the energy released in a cohesive zone, corresponding to a damage parameter implemented numerically varying from zero to unit, being the zero for an undamaged zone and one for a complete loss of stiffness zone. The constitutive relationship is:

$$\sigma = (I - E) \cdot D \cdot \delta_r \tag{12}$$

where I represents the identity matrix and E is a diagonal matrix containing the damage parameters, e_i, which can be calculated with the following equation:

$$e_i = \frac{\delta_{u,i} \cdot (\delta_i - \delta_{o,i})}{\delta_i \cdot (\delta_{u,i} - \delta_{o,i})} \tag{13}$$

where $\delta_{0,I}$ is the displacement corresponding to the onset of damage and δ_i the current relative displacement. The area below the softening curve, corresponding to the value of

G_{IC} can be calculated with maximum local strength ($\sigma_{u,i}$) and maximum relative displacement ($\delta_{u,i}$) values with the following relation:

$$G_{IC} = \frac{1}{2} \cdot \sigma_{u,i} \cdot \delta_{u,i} \tag{14}$$

It is also possible to characterize the cohesive zone parameters experimentally using DCB and ENF tests to incorporate it in a numerical analysis with good behaviour prediction accuracy of the joints.

3. Experimental procedure

As the most effective method to obtain the strength of an adhesive joint and its behaviour under different conditions is a test by itself, a wide range of specimens were made and tested under static and impact conditions. The designed joints had different overlap lengths, different adhesive combinations and different manufacturing techniques, leading to a combination of two adhesives along the overlap with optimized geometry, in order to achieve strength improvements over the standard single lap joints with a single adhesive application. The manufacture process of the specimens was also an important stage of the experimental work due to many critical aspects of the mixed-joint concept such as the separation of the two adhesives, controlling of adhesive layer thickness, curing schedules and surface treatments of the adherends. Static and dynamic tests were performed in order to analyse by comparison the relationship of the results between the two types of tests in terms of joint strength, durability and energy absorption and to investigate the behaving between different adhesives in different combinations on the same overlap.

3.1 Materials

For the experimental component, four adhesives were selected: two very ductile and flexible adhesives and two other stiffer and brittle. The selections of ductile adhesives includes a silicone rubber acetoxy type adhesive Momentive RTV106 (Albany, NY) used in high temperature applications and a two-component structural acrylic adhesive type DP-8005 from 3M Scotch-weld (St. Paul, MN, USA). The stiffer adhesives consist of a very stiff and brittle epoxy adhesive, Araldite AV138/HV998 from Huntsman (Salt Lake City, UT) and an hybrid epoxy one-part system crash resistant adhesive of the XNR6852 type, a third formula version prototype supplied by Nagase Chemtex, (Osaka, Japan). This last adhesive is particularly relevant to the automotive industry due to its improved resistance to impact, deforming significantly without breaking by absorbing enough energy to keep the bonded components together. This type of adhesive combines the high toughness of polyurethane and the high strength of an epoxy.

The RTV106 silicone properties were determined by Banea [34], the 3M DP-8005 properties were determined by da Silva et al. [35] and Pinto et al. [36] and the Araldite AV138/HV998 properties were obtained by da Silva et al. [37]. The XNR6852E-2 is a new version of the adhesive formula and a successor of the XNR6852E-1 so its properties were determined during the course of this work by characterization tests. The Young's modulus – E – and the tensile strength – t_n^0 – were determined in a bulk test of the adhesive, the shear modulus – G – and the shear strength – t_s^0 – were measured by a TAST, mode I fracture energy – G_I – was determined with a DCB test and the mode II fracture energy – G_{II} – was obtained with an ENF test. The properties are shown in Table 1.

Table 1. Adhesive properties.

Adhesives	Test	RTV106	DP-8005	AV138	XNR6852E-2
Young's modulus E [MPa]	Failure strength test	1.6	590	4890	1742
Shear modulus G [MPa]	Thick adherend shear test (TAST)	0.86	159	1560	645.2
Tensile strength t_n [MPa]	Failure strength test	2.3	6.3	41.0	42.9
Shear strength t_s [MPa]	Thick adherend shear test (TAST)	1.97	8.4	30.2	28.7
Mode I fracture energy G_I [N/mm^2]	Double cantilever beam test (DCB)	2.73	1.1	0.35	N/A
Mode II fracture energy G_{II} [N/mm^2]	End notched flexure test (ENF)	5	6	4.91	18

The value for the mode I fracture energy was determined with a DCB test and the results are shown in Section 3.2.1.

Table 2 shows the curing requirements for the adhesives used, according to the datasheet provided by the manufacturers. For all of them, applied pressure during the curing process is always essential, in order to avoid voids in the bondline and ensure the specimens thickness.

Table 2. Curing requirements for the adhesives used.

Adhesive	Temperature	Time
RTV106	Room temperature	3 days
AV138	100 ºC	10 minutes
DP-8005	Room temperature	8-24 hours
XNR6852E-2	150 ºC	3 hours

To avoid plastic deformation of the adherends, the substrates were made of DIN 55 Si7, heat treated steel. Also, mild steel DIN 17100 ST33 was used for joint behaving reference purpose, as it has a strong presence in the automotive industry for car body shells. Table 3 shows the properties of the adherends used.

Table 3. Adherend properties.

Adherends	Mild steel	High strength steel
Young's modulus E [GPa]	210	210
Tensile yield strength σ_y [MPa]	175	1078
Tensile strength σ_r [MPa]	270	1600
Tensile failure strain ε_f [%]	17.6	6

3.2 Adhesive properties characterization

The characterization of the new version of the hybrid epoxy XNR6852 was undertaken during the course of this work. These properties were obtained with a series of tests performed by some of the elements of the adhesives group at FEUP and the test that was previously intended to be associated to this work was the DCB test for the determination of the mode I fracture energy, G_{IC}.

Also, bulk tests were performed for the adhesives AV138 and DP-8005 to obtain properties at different strain rates in order to investigate the strain rate dependency of these adhesives. The results were properly operated in order to create a cohesive law for a finite element numerical simulation with dynamic settings to simulate the impact testing. The properties at high strain rate for the XNR6852E-2 adhesive were experimentally obtained during the course of this work.

3.2.1 Mode I fracture energy – Double Cantilever Beam (DCB) test

3.2.1.1 *Manufacturing process*

To determine the critical strain energy release rate in mode I, G_{IC}, of the new version of the adhesive XNR6852 (E-2) from Nagase Chemtex, a DCB test was performed on 4 specimens with the D 3433-99 ASTM standard geometry of the Figure 21.

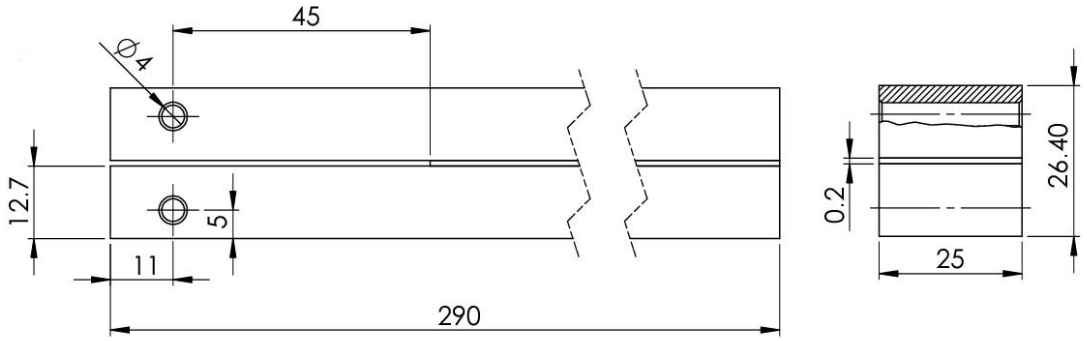

Figure 21. Geometry of the DCB specimen used for the test (dimensions in mm) [38].

The specimen configuration and material of the adherends was chosen to avoid plastic deformation. The properties for the adherends are shown in Table 4.

Table 4. DCB specimen material properties.

DIN 40 CrMnMo 8-6-4 [PM 300 Impax Supreme]			
Young's modulus [GPA]	**Yield strength [MPa]**	**Tensile strength [MPa]**	**Strain (%)**
205	895.5 ± 34.5	1034 ± 34	15.5 ± 1.5

Figure 22 shows the final result of the manufactured specimens. Five of them were manufactured but due to the consistency of the results, only four were tested and the last one was stored for future testing if needed.

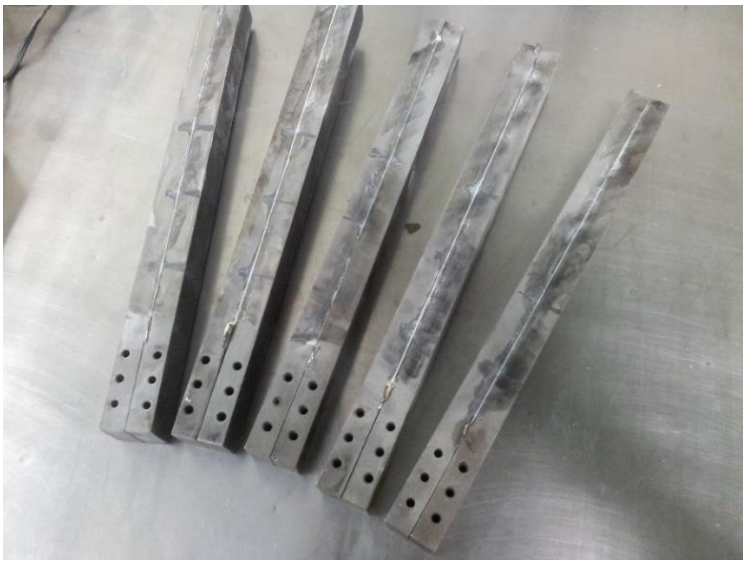

Figure 22. DCB specimens made for testing.

The preparation of the specimens consisted firstly in the surface preparation of the adherends that were sandblasted prior to the application of the adhesive. Then, to guarantee the adhesive bondline thickness, calibrated tape was used as a spacer and inserted between the adherends on both ends. To introduce a pre-crack to ensure a cohesive crack propagation from the beginning of the test, two steel plates were glued to

a razor blade of 0.05 mm thickness positioned in between and placed in the A_0 position of the specimen. On the other end, a steel tape of 0.2 mm was used to make sure the proper bondline thickness. With the support from the mould of the single-lap joints (Figure 23), previously cleaned with acetone and surface covered with the mould release agent FREKOTE 770-NC by Loctite®, adhesive was applied in both adherends and then assembled in position on the mould for correct alignment. The mould was then placed inside an hydraulic hot plate press for 4 hours at 150 ºC and a pressure of 2 MPa. An extra curing hour was given to ensure a complete cure of the adhesive.

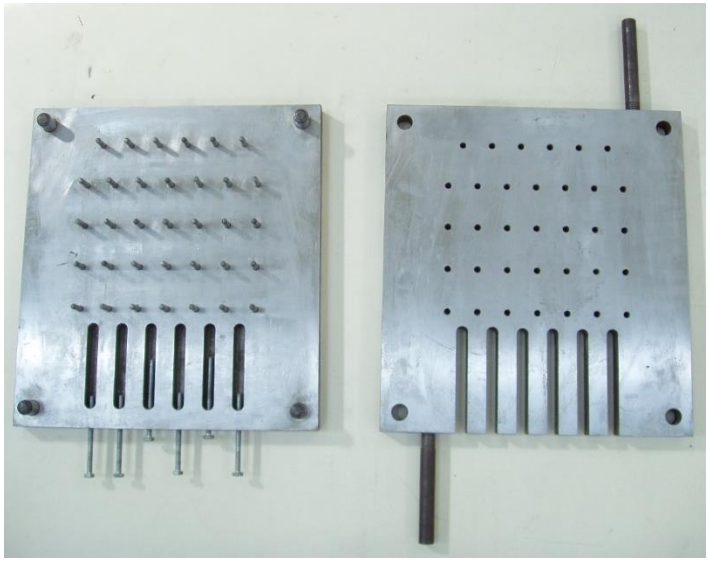

Figure 23. Mould used to manufacture the specimens.

Once the curing was complete, the specimens were removed from the mould and any excess of adhesive from the specimen sides was removed. A thin layer of white typewriter correction fluid was painted on the specimens to facilitate the measurement of crack growth and a scalar tape was placed bellow the bondline to aid the crack length measurement.

The specimens were then tested according to standard ASTM D3433 in an INSTRON® universal test machine (Norwood, Massachusetts, USA), equipped with a load cell with a capacity of 30 kN. The test consists of a vertical loading that is applied to the specimen inducing a mode I fracture in the adhesive layer of a specimen as shown in the Figure 24. The tests were made at room temperature and at a constant displacement rate of 0.2 mm/min. Crack length growth during was recorded during the test using a digital camera taking high resolution pictures with 5 seconds intervals.

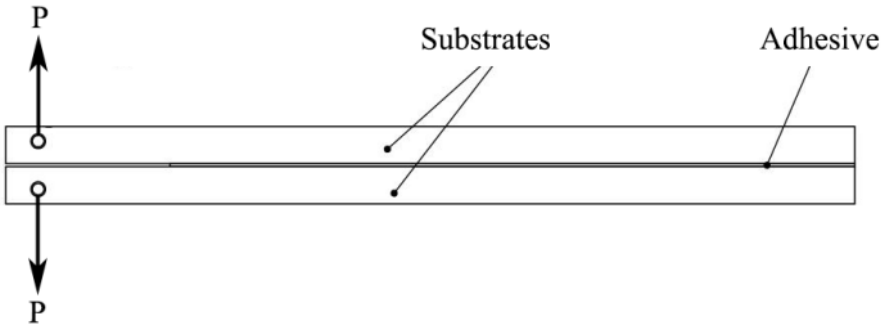

Figure 24. Loading application in mode I fracture energy test [38].

3.2.1.2 *Experimental results*

A typical P-Delta curve obtained from the tests is presented in Figure 25.

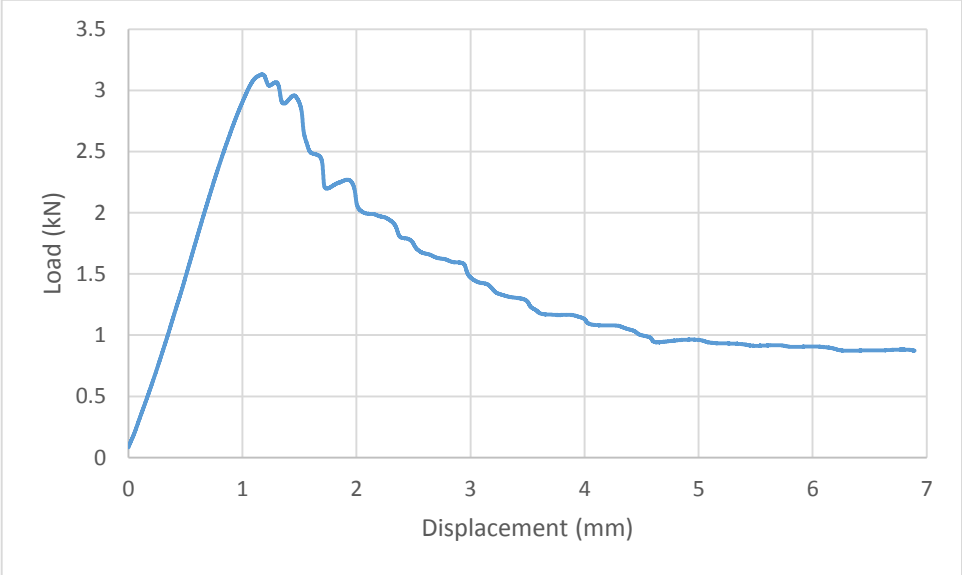

Figure 25. Typical P-Delta curve obtained, specimen 1.

The average peak load measured during the tests was 3.21 kN with a standard deviation of 0.75 kN.

Also, for each specimen, in order to find a suitable value for the mode I fracture energy, an R-curve was outlined by the Compliance-Based Beam Method (CBBM), which is a method that consists on an approach of specimen's compliance and a crack equivalent concept, thus not requiring the measure of the crack length. Figure 26 shows a typical R-curve of one specimen obtained by this method.

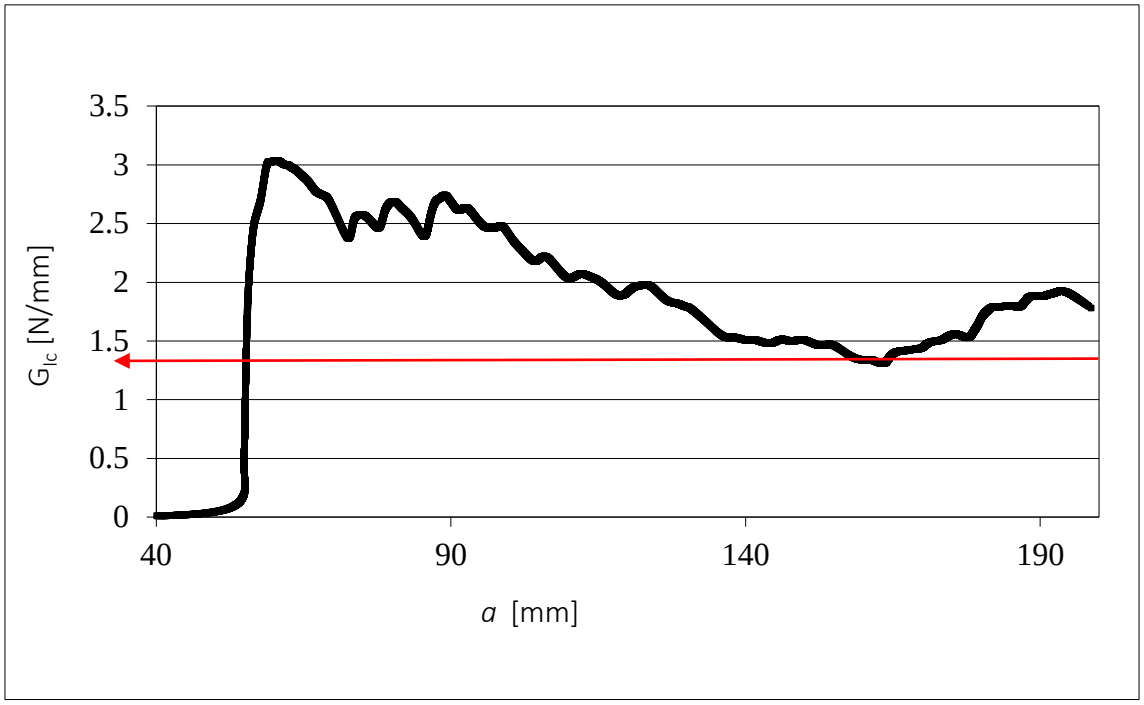

Figure 26. Typical R-curve obtained, specimen 1.

Values for the G_{IC} obtained from the R-curves were found to be between 1.4 and 2.0 N/mm, so by an average of the four test results, a final value of 1.68 N/mm was determined, with a standard deviation of 0.3 N/mm.

Furthermore, the failure mode was cohesive in the adhesive for all four specimens and no deformation of the substrates was found.

3.2.2 Bulk tensile test

3.2.2.1 *Manufacturing process*

The main objective of bulk testing was to determine the stress-strain curves at high strain rates with the measuring of the load and the displacement during the test, for the AV138 and DP-8005 adhesives as to be able to properly perform numerical simulations with dynamic impact conditions. The technique consists in loading the specimen in a longitudinal direction until failure, generally at a rate of 1 mm/min for the determination of the Young's modulus. The dimensions and geometry of the dog-bone shape specimens

according for tensile testing are defined in the scheme of the Figure 27, in accordance to the standard EN ISO 527-2. For rigid adhesives like the epoxies where the displacements are small, the long dimensions specimens should be used (Figure 27.a), while for flexible adhesives, short specimens are well-suited (Figure 27.b).

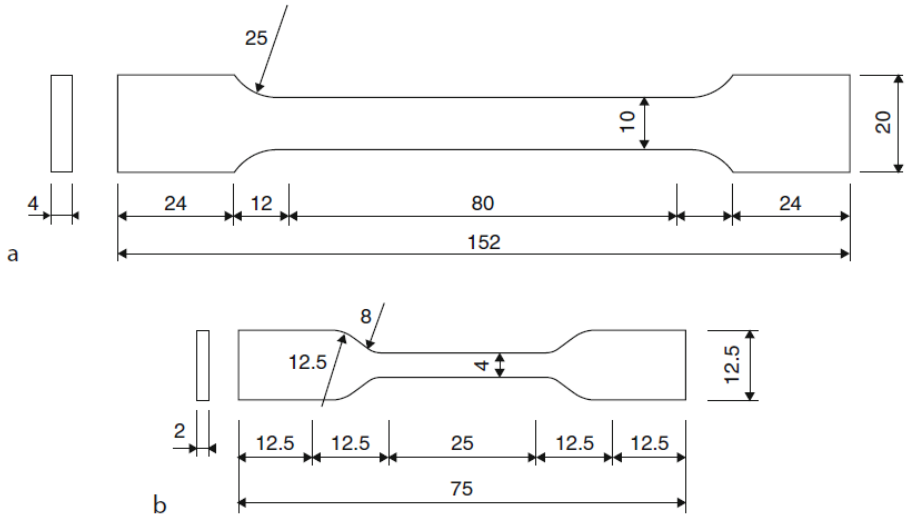

Figure 27. Geometry of the specimens according to EN ISO 527-2 (dimensions in mm): (a) long specimen and (b) short specimen [39].

Within this, as the AV138 is a very brittle epoxy adhesive, long specimens were manufactured from two bulk plates, while for the ductile and very flexible adhesive DP-8005, short type specimens were manufactured from one single bulk plate.

The bulk plates were produced by curing the adhesive between steel plates of a mould as shown in Figure 28, using a silicone rubber frame according to the French standard NF T 76-142 to avoid the adhesive from flowing out. The adhesive was placed in the centre part of the mould in a quantity slightly greater (5% in volume) than the volume corresponding to the internal part of the silicone rubber frame.

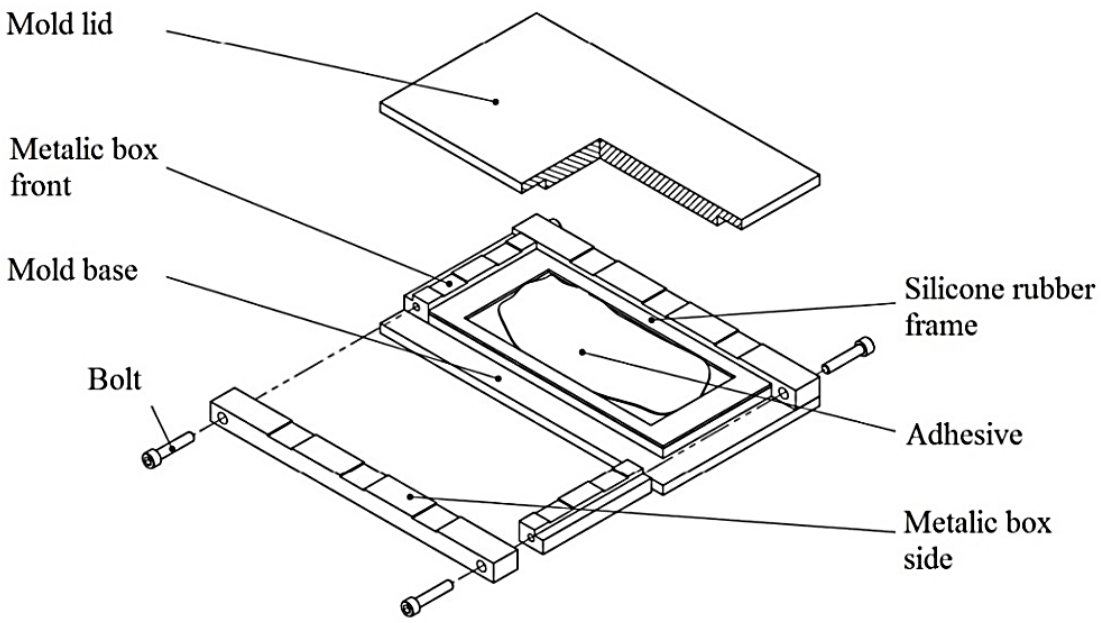

Figure 28. Scheme of the used mould to produce plate specimens under high pressure. Exploded view [38].

After spreading the adhesive onto the mould, the whole set was placed in the hot press for 1 hour at 100 ºC and with a pressure of 2 MPa. After the adhesive cure, the mould was left for a slow cooling till room temperature in order to guarantee a uniform temperature in the mould and avoid residual stresses. Also, the plate was not removed until the mould has reached room temperature to avoid residual stresses that could deform the plate permanently. After that, the specimens were then removed from the mould and went to manufacturing stage. Figure 29 shows the final result of 2 manufacturing bulk plates of the adhesive AV138 prior to machining. With the two bulk plates it was possible to manufacture 6 long dog-bone specimens, as seen in Figure 30.

Figure 29. Final result of bulk sheet plates of adhesive AV138

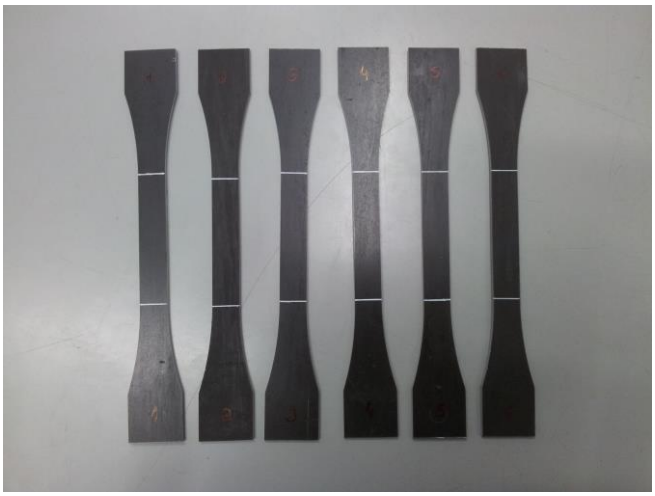

Figure 30. AV138 bulk specimens manufactured.

For the manufacturing process of the DP-8005 bulk plate, the same method was used but due to the short working time of this adhesive and its high flexibility and rubbery behaviour, the manufacturing was a bit hard and required a lot of patience. At first try, the mould was pressed in the hot press with 2 MPa at room temperature just for a few minutes, and then left curing outside the hot press for 6 days at room temperature. The attempt of opening the mould was a total failure and consequently the bulk sheet was damaged as seen in Figure 31. Although mould release agent was extensively used on the mould, the adhesive still adhered to the mould on both sides, making impossible to remove it without creating damage. Also, a large amount of voids were found in the sheet plate, perhaps due to the limited working time of the adhesive and bad mixing of the two composed parts.

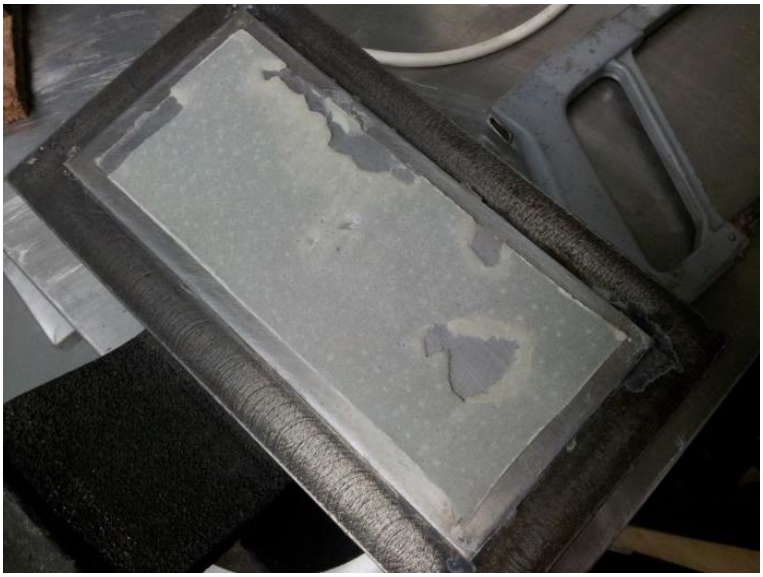

Figure 31. Damage found in the bulk plate after the opening of the mould

After a proper cleaning of the mould, a second attempt was made but this time using a thin sheet of wax paper on both sides between the plates of the mould and the adhesive. This way, the adhesive does not had contact with the metal and thus no problems were found at the unmoulding point. The wax paper sheets were also easy to remove from the bulk plate and from the silicone frame. The mould was inside the hot press for 24 hours with 2 MPa pressure applied and room temperature conditions to avoid the appearance of voids inside the bulk plate. Only one bulk plate was manufactured that was then removed from the mould and went to manufacturing stage. 8 short type dog-bone specimens were produced from the bulk plate, as seen in Figure 32.

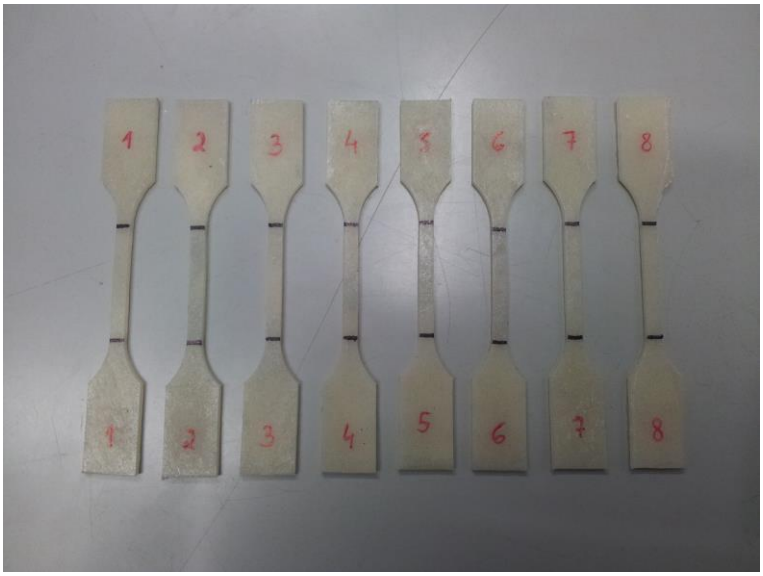

Figure 32. DP-8005 bulk specimens manufactured.

The manufactured specimens were then tested in an INSTRON® model 3367 universal test machine with a capacity of 30 kN (Norwood, Massachusetts, USA), at room temperature and constant displacement rate of 100 mm/min. An extensometer to record the displacement was used. Loads and displacements were recorded up to failure.

3.2.2.2 *Experimental results*

Figure 33 shows the experimental curves for the AV138 bulk specimens tested. Due to the consistency of the results, only 4 of 6 specimens were necessary to obtain the required adhesive properties.

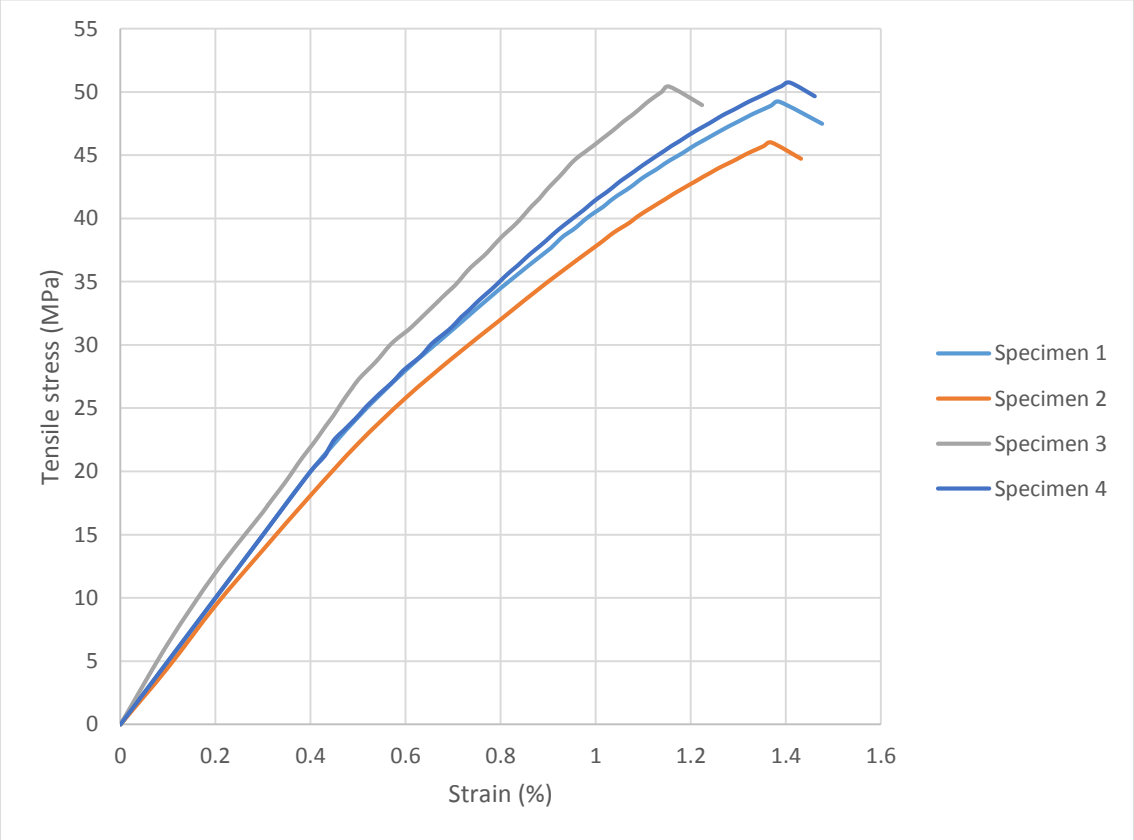

Figure 33. Experimental curves for the tensile bulk test of the adhesive AV138.

Figure 34 shows the experimental curves for the DP-8005 bulk specimens tested. Once again, due to the consistency of the results, only 4 of 8 specimens were necessary to obtain the required adhesive properties.

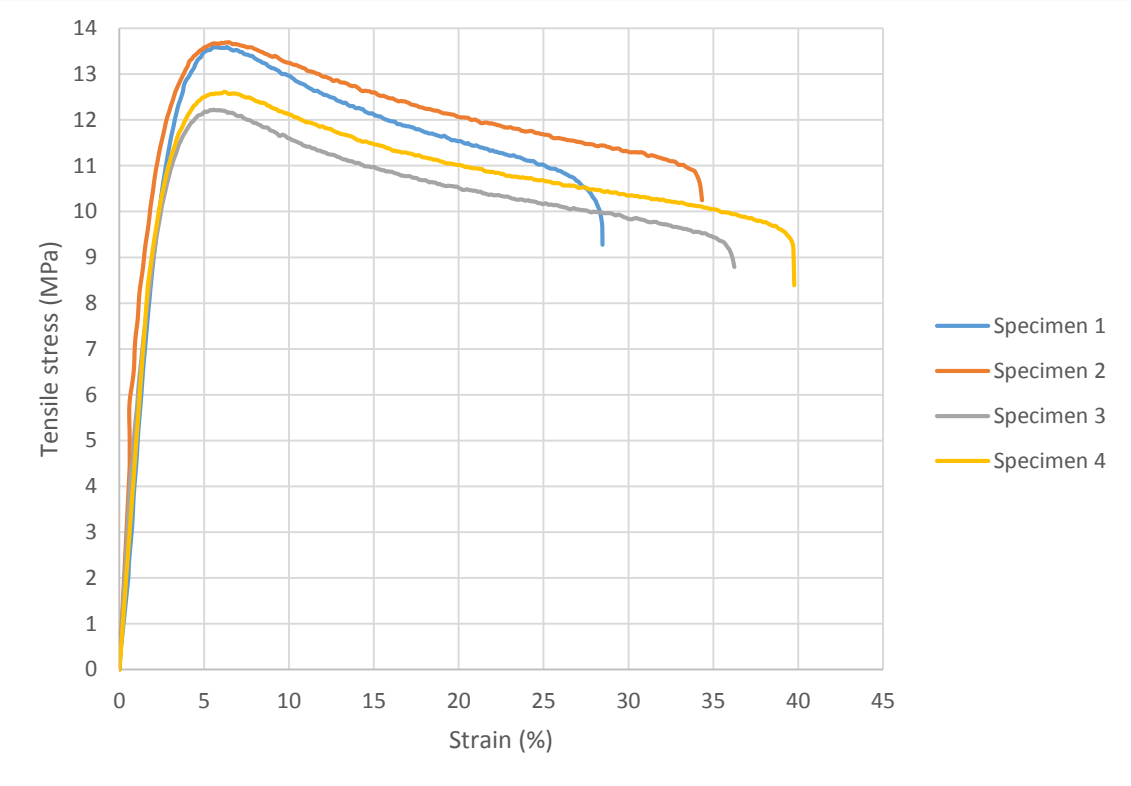

Figure 34. Experimental curves for the tensile bulk test of the adhesive DP-8005.

The results obtained from the tests for both adhesives are summarized in Table 5.

Table 5. Results obtained from AV138 and DP-8005 tensile bulk tests.

Adhesive	Maximum tensile stress (MPa)	Maximum strain (%)	Young's modulus (MPa)
AV138	49.09 ± 2.17	1.31 ± 0.11	4827.59 ± 341.95
DP-8005	13.03 ± 0.73	35.21 ± 3.49	525.08 ± 63.83

3.3 SLJ specimens manufacturing

The specimens manufactured for the tests consisted in single lap joints with two different overlaps, 25 mm and 50 mm, to represent as best as possible an adhesive joints used in automotive structures. These adhesive joints are relatively simple to manufacture but can provide reliable results regarding the strength of an adhesive substrate combination.

The defined overlaps were selected taking in consideration that, within the mixed adhesive technique, two different adhesives would be placed together separated by a physical spacer and a short overlap could result in a difficult manufacture process as the area for the ductile adhesive would be too small. Also, as proven by previous works found in literature, the mixed adhesive technique results better for longer overlaps as the improvement of joint strength is more susceptible.

In the first specimens produced, the material for the adherends was mild steel, but due to the adherends yielding in almost all of the SLJ configurations tested, the results did not reproduce the full potential of the adhesives used, with joints prematurely failing due to the high concentration of peeling forces, created thanks to the plasticization of the steel. Despite that, all of the predefined adhesive configurations manufactured with mild steel adherends were still tested in static conditions to compare the results and investigate the adherends influence. Furthermore, to ensure that the results obtained derived principally from the work of the adhesives in the joint, high strength steel was used in order to avoid the plasticization of the adherends, and consequently, premature failures.

The specimens geometry used is shown in Figure 35, representing the two overlap types manufactured, according with the ASTM D 1002 and ISO 4587 standards. For both geometries, both adherends were similar with a thickness of 2 mm and a width of 25 mm, varying only the length according to the type. The defined geometries are very similar to those used in other related research works and thus, a comparison with results from other works can be made if necessary.

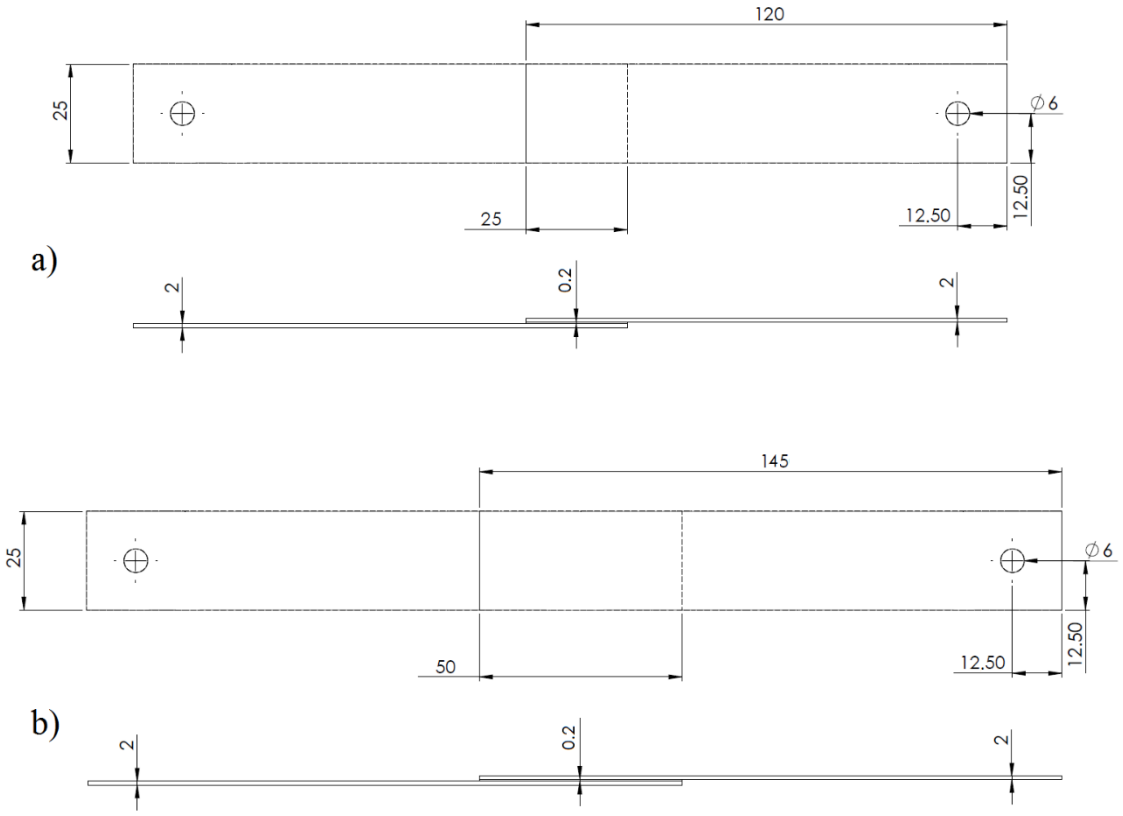

Figure 35. SLJ specimens geometry (dimensions in mm). (a) 25 mm overlap, (b) 50 mm overlap.

The bondline thickness was defined to be 0.2 mm as it is recommended by the adhesives manufacturers for a proper single lap joint, exhibiting good results. Also, as found in literature review, the optimum value of the adhesive thickness for an epoxy adhesive shall be between 0.1 and 0.2 mm, since for higher values the bending moment increases the peeling stresses and thus, compromising the joint strength. Moreover, Mata [40] has found in his works that under impact conditions, 0.4 mm bondline thickness single lap joints exhibited lower performances compared to 0.2 mm.

Although single lap joint specimens with two different overlaps were manufactured, only 25 mm overlap length specimens were tested at impact due to limitations in the specimens fixing and handling mechanism of the impact machine that will be discussed later. Still, both overlaps were tested at static conditions.

3.3.1 Joint configurations

The joint configurations were defined by forming combinations with the four adhesives attained to this work. The set was formed by two ductile adhesives and two brittle or with high Young's moduli. As the mixed adhesive concept consists in the use of an high modulus adhesive combined with a low modulus for stress reduction at the ends of the overlap, four combinations could be made using this technique with the available adhesives. Given that, a useful mixed adhesive joint requires the employ of a ductile adhesive at the ends of the overlap length providing joint flexibility and a brittle adhesive in the centre to give stiffness. A configuration like this is shown in the scheme represented in Figure 36.

The centre region of the overlap must be the section with the greatest bonding area, with small displacements, while the ends of the overlap should comprehend a smaller bonding area able to handle large displacements. This way, in order to achieve strength improvements by using this technique, the mixed joint should have high strength and low flexibility at the centre and low strength but high flexibility at the ends of the overlap.

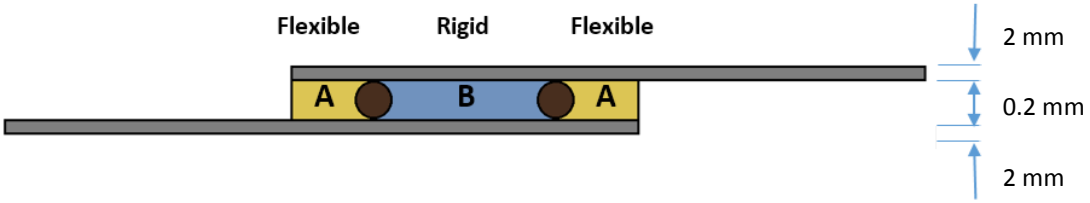

Figure 36. Scheme of the adhesives configuration studied.

Given that, the four working possible combinations are the following:

- RTV106 (edges) with AV138 (centre);
- DP-8005 (edges) with AV138 (centre);
- RTV106 (edges) with XNR6852E-2 (centre)
- DP-8005 (edges) with XNR6852E-2 (centre)

The remaining arrangements such as the combination of RTV106 with DP-8005 and AV138 with XNR6852E-2 were of small interest or impracticable. In the first case the result would be a very flexible mixed joint by combining two flexible adhesives and in

the second case the result would still be a very stiff mixed joint due to the high stiffness of the combined adhesives.

Also, the combination of RTV106 with XNR6852E-2 had not demonstrated great interest since the XNR6852E-2 adhesive has already some flexibility, and as the main objective of using the RTV106 is to provide flexibility to a stiff joint, this seemed to be unnecessary. In the other hand, the maximum strength of both adhesives is very different and an attempt to produce this joint configuration might result in lower strength than a joint with only the XNR6852E-2 adhesive along the whole overlap. Given this reasons and the limited time available to perform all the experimental work, this configuration was discarded from the main four configurations, reducing this number to only three.

Although the manufacturing of all of the main three combinations was attempted, some of them didn't go very well, resulting in problems in the manufacturing stage and or during the tests that will be approached and discussed later in this work. The possible manufactured combinations were then tested at static conditions and the results were analysed so that only the combinations with good results were tested at impact.

Also, single adhesive joints were manufactured with all of the adhesives proposed for this work. The specimens were tested both on static and impact conditions to serve as reference to compare the results and to explore possible improvements of joint strength.

3.3.2 Ratio of adhesive stiffness (E_{LM}/E_{HM})

As already discussed in the literature review, the ratio of adhesive stiffness (E_{LM}/E_{HM}) is an important feature of a mixed adhesive joint as it provides different results with small variations. Thus, a bad applied ratio can compromise the joint strength instead of resulting in an improvement.

In order to define the adhesive stiffness ratio to be used, the three lengths (L1, L2, and L3) from Figure 37 needed to be settled.

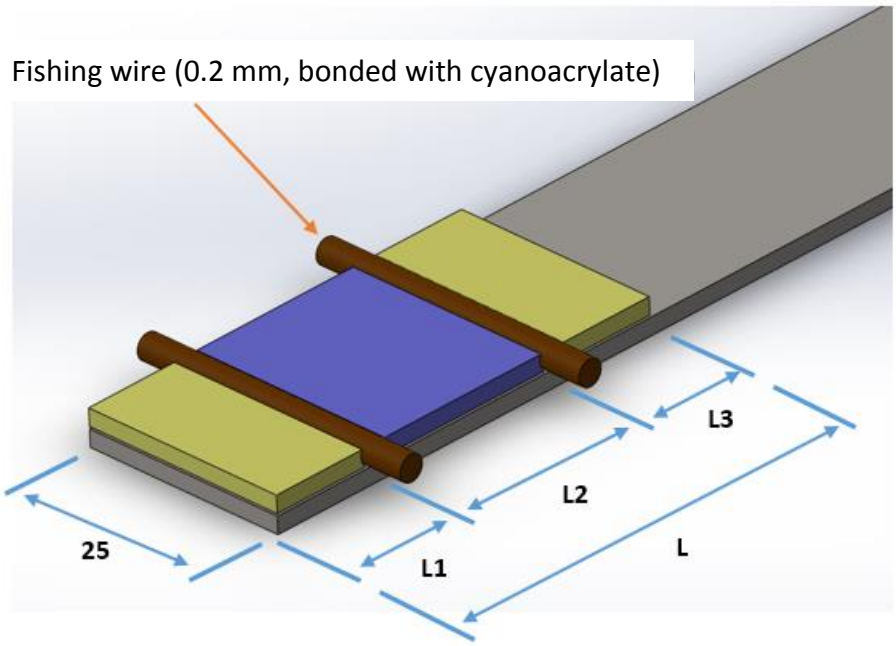

Figure 37. Scheme of the splitted overlap length.

For that, two proposals from literature review were analysed and studied. One of them was found in previous Marques works [41] where the overlap distribution was as shown in case A of Figure 38. With this distribution good results and good behaviour of the joints were found, as well as ease of manufacturing. The other proposal was found in Flaviani's works [31], where he developed an optimization model in Abaqus® for the ratio of stiffness distribution along the overlap but the results have not been tested experimentally yet. This proposal corresponds to the case B of Figure 38 where the values of percentage area of the overlap length are represented.

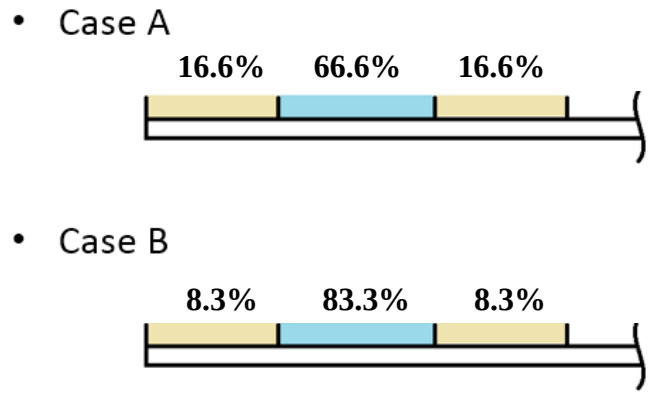

Figure 38. Overlap splitting case studies.

The selection of the best case was made taking in consideration the manufacturing difficulty. Although Flaviani has proved with an Abaqus® simulation that the ratio of case B is the configuration that offers best results in joint strength improvement, the manufacturing process with a ratio like this will result in small areas of adhesive application. As seen in Figure 39 where the partitioned length of the overlap is represented in millimetres for both cases, for the 50 mm overlap length it should not be a significant problem in any of the configurations, but looking at the 25 mm overlap, the ratio from case B will result in an approximately 2 mm part of the overlap for the application of the ductile adhesive, which seems to be impracticable to be manufactured in real situations.

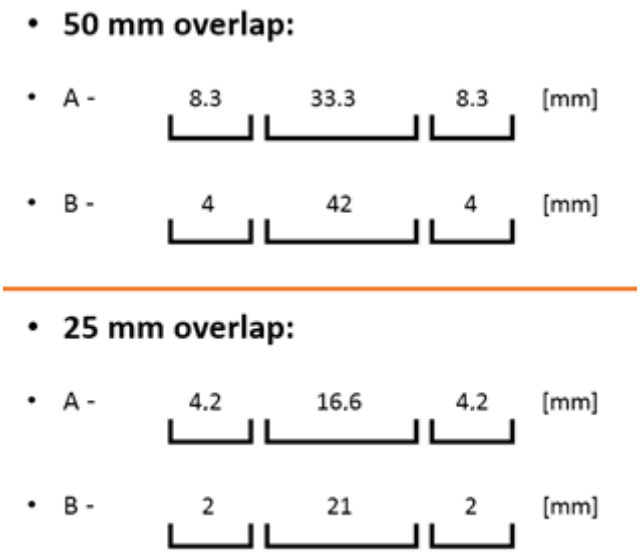

Figure 39. Divided parts of the overlap length according to both cases.

For this reasons and in order to ease the manufacturing process, the case A from Marques was selected to be used in both of the overlaps lengths during the course of this work.

3.3.3 Manufacturing process

For the manufacture process, 2 mm thick steel adherends were collected and sandblasted in the overlap area surface. The surface was then degreased with acetone to ensure a proper cleaning prior to the application of the adhesive.

As the mixed adhesive technique requires the use of at least two different adhesives in the same overlap, two different adhesives separation methods were studied by trial and error. Various attempts were made to avoid the mixing of the adhesives in the overlap during the manufacturing and curing stage. The analysed proposals involved the use of a physical separator such as an extra-thin silicone cut stripe with the same thickness as the bondline and the use of nylon fishing wire with 0.2 mm diameter. Both of separators were glued to the adherends with a cyanoacrylate based glue.

To select the best separation technique, two test specimens were produced with a mixed configuration of the silicone RTV106 with the epoxy AV138, one with the silicone rubber stripes as separator and the other with the fishing wire, as shown in Figure 40.

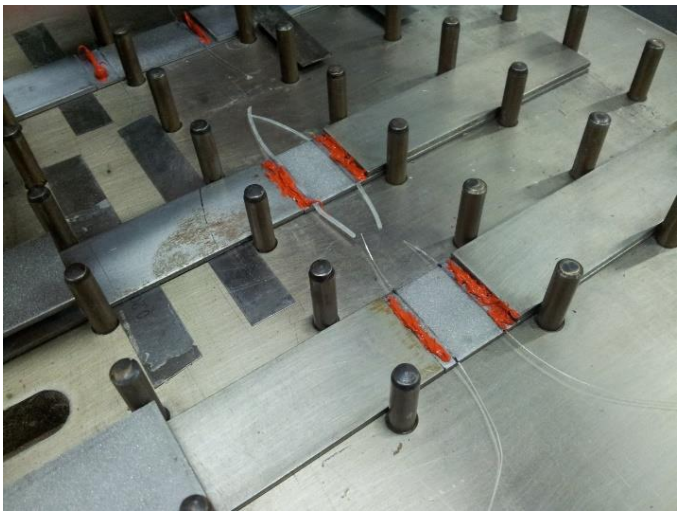

Figure 40. Testing of the separator technique.

After the curing stage with pressure and temperature, both specimens were tested in the tensile test machine in static conditions in order to examine the failure mode and evaluate the separation of the adhesives in the overlap. The tests have proved that the fishing wire technique functioned better than the silicone stripes, exhibiting better separation of the adhesives with almost no mixing and superior joint strength while the silicone stripes didn't adhere well to the adherends and allowed some degree of mixture of the adhesives. Also, even as thin as the stripes could be made, the silicone spacers still covered a larger area than the fishing wire, thus reducing the working area of the adhesives in the overlap, and that could be part of the explanation for the lower joint strength verified. As for the fishing wire, this problem was not encountered due to the reduced non-working area, which was significantly less.

After a proper surface preparation of the adherends, marks were drawn in the adherends with a permanent marker and a ruler to mark the location where the spacers should be placed. The location of the points were previously defined and explained and resulted in a ratio of 66.6% of the overlap area to be occupied with the centre adhesive and the rest of the overlap area (33.4%) to be occupied with the ductile adhesives divided in two parts, one for each end of the overlap. The splitting points of the overlap areas were shown previously in Figure 39.

After that, the fishing wire was glued to the adherends with a cyanoacrylate glue aligned to the marked points previously defined as shown in Figure 41.

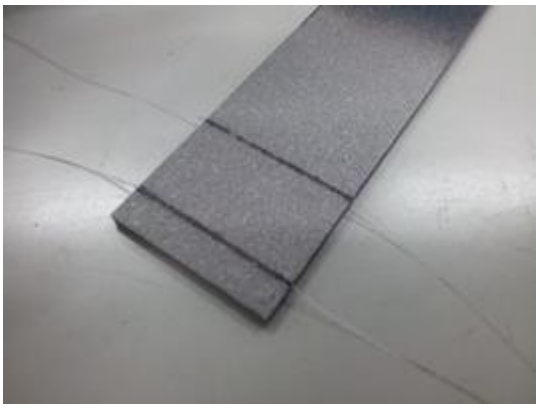

Figure 41. Final result of the fishing wire glued to the adherend.

With the help of SLJ specimens' mould, represented in a schematic view in Figure 42, the specimens can be correctly aligned as the curing process takes its time, providing uniform pressure distribution and temperature as well as control of the specimens' dimensions, while keeping them from moving. The mould was specially designed by the adhesives group members at FEUP to manufacture SLJ's specimens easily and with quality and accuracy. It allows the production of 6 specimens with 25 mm width at the same time.

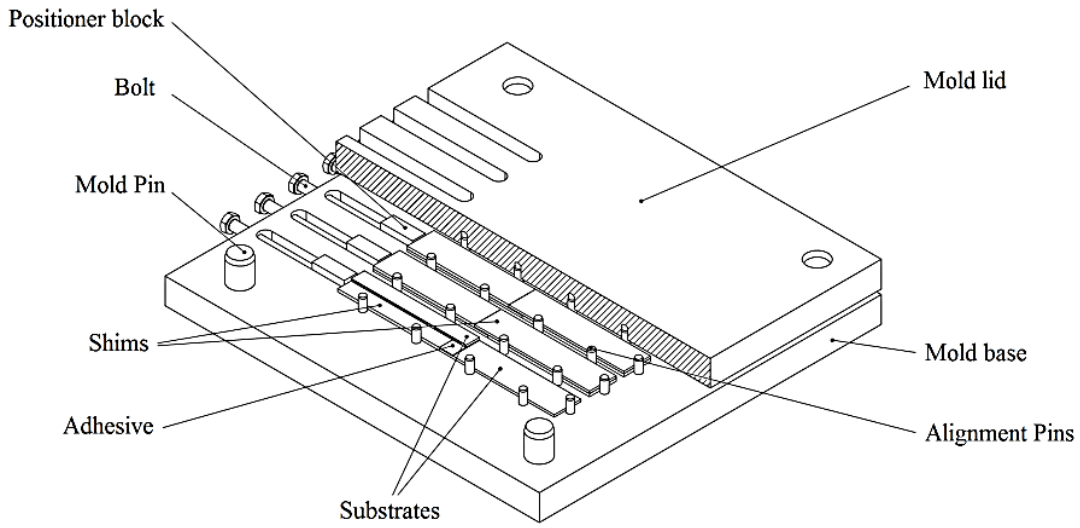

Figure 42. Scheme of the mould used to produce SLJ [38].

Prior to the specimens assembly, the mould needs to be cleaned with acetone to remove possible adhesive remains from previous fabrications and clean the surfaces. The whole surface was then covered with the release agent Frekote® 770-NC from Loctite® in order to allow a proper releasing of the specimens once the cure of the adhesives was complete and avoid the adhesives to stick to undesired surfaces. All packing shims, alignment pins and calibrated tape, when used, needed also to be covered with the mould release agent so that no adhesive stays stuck in a disassembling stage. The parts to be surface covered were heated to 80ºC in the furnace to speed up the cure reaction of the mould release agent and then three coats were applied with a brush with five minutes interval between them in order to allow a complete solvent evaporation. Security procedures needed to be employed to avoid health damage as this product can be toxic and carcinogenic to the human skin and airways.

3.3.4 Adhesives preparation

Among the available adhesives, the AV138 and DP-8005 are a two-part system adhesives that needed preparation before application. In the case of DP-8005, the adhesive is provided in a small two compartment recipient with an application tool and mixing nozzles. The mixing nozzles ensures a proper mixing of the two parts and eases the application of the adhesive but these accessories are a bit expensive and thus, there is an

interest in recycling them. As the working time of this adhesive is very tight (2.5 to 3 minutes, according to data sheet), normally the recycling of the nozzles would be a two man job, one needed to complete the specimens construction and close the mould before the adhesive gains toughness and the other to clean the remain unused adhesive from inside the nozzle at the same time with acetone and compressed air for example, right after the adhesive application.

The preparation of the AV138 consists in mixing the adhesive with an hardener (HV998) with a proportion of 4 grams of hardener to 10 grams of adhesive. The mixing of the two parts was done in a centrifugal mixing machine (SpeedMixer™, FlackTek Inc, Landrum, South Carolina) and the application of the adhesive was done with a spatula.

For the other two remaining adhesives, no special preparations were necessary as the adhesives are composed of just one part but for the XNR6852E-2, in order to simplify the application of the adhesive in the overlap area, a pre-heating in the oven at 50ºC for 2 to 5 minutes reduces the viscosity and improves the manageability. As for the RTV106, the adhesive was applied directly in the overlap from the container without pre-treatments nor mixing parts.

3.3.5 Bonding stage

The adherends and packing shims where then placed in respective positions into the mould for the adhesives application (see Figure 43).

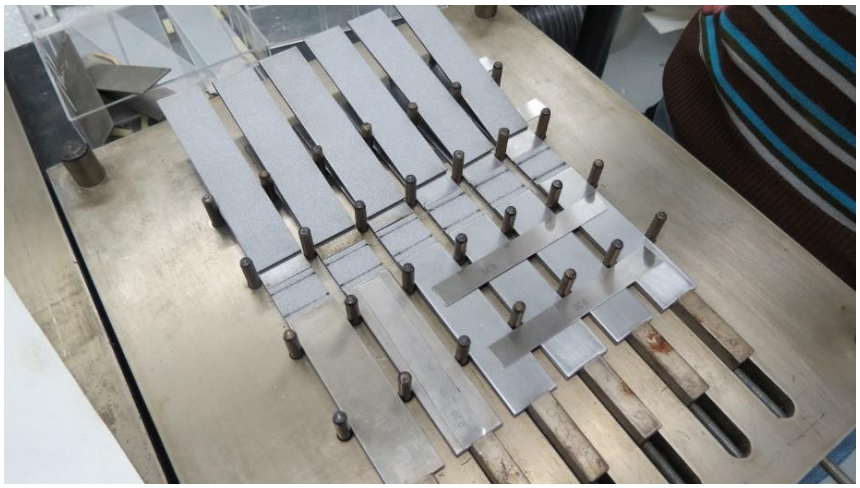

Figure 43. Adherends placed in mould ready for the adhesives to be applied.

After the preparation, the adhesives were then applied along the overlap with a spatula or with a mixing nozzle (in case of DP-8005) to spread it to the whole surface area. A careful spreading of the adhesive was very important in order to avoid entrapment of air bubbles and voids and ensure a sufficient filling of the gap when closing the mould. Also, as two adhesives were applied and no mixing was allowed, it was essential to ensure that the adhesives didn't cross the separator and spread to the other side. Figure 44 shows the step of adhesives application for 3 single lap joint mixed adhesive specimens with RTV106 and AV138 with 25 mm overlap.

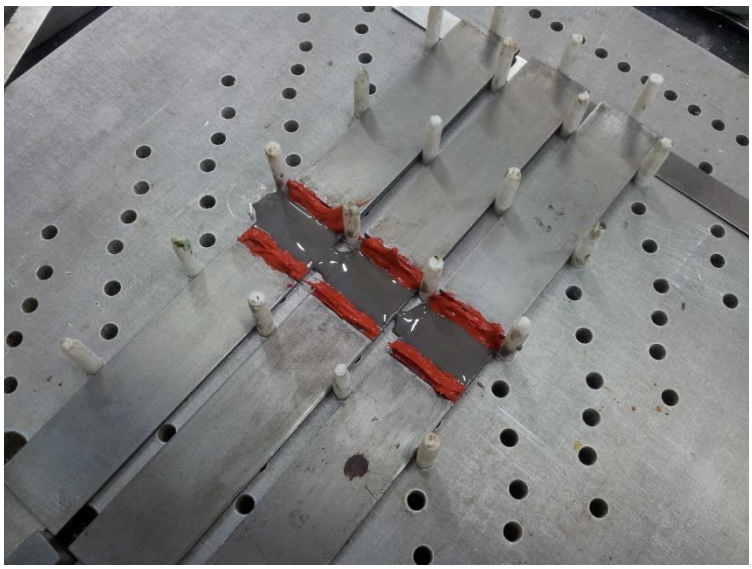

Figure 44. Mixed adhesive application with RTV106 and AV138.

The specimens were completed by applying the top adherends over the adhesive. Whenever possible, a small amount of adhesive was also applied on the top adherends to improve the adhesion and ensure sufficient gap filling. In the end, the mould was closed and left in an hydraulic hot plate press under 2 MPa pressure, with or without time and (or) temperature as needed by the adhesives curing requirements.

3.3.6 Curing schedules

The curing phase of the adhesives presented in this work shows a wide range of different requirements between all of them, from cures at room temperature to cures that require 150ºC to fully complete, which is the case of XNR6852E-2. The curing times also differ, varying from just a few minutes to days. In normal single adhesive applications specimens, this was not relevant and the curing process required by manufacturers could be applied normally without problems. But when at least two different adhesives are used in the same overlap, two different curing requirements needed to be combined, which sometimes results in manufacturing problems and impossible combinations.

According to datasheet of the adhesives, the curing requirements for each adhesive are shown in Table 2 in section 3.1. With the exception of the combination with DP-8005 and XNR6852E-2, the curing stage for all the other specimens went without problems. As the XNR6852E-2 adhesive requires a minimum temperature of 150ºC and 3 hours for a full cure and the DP-8005 adhesive cures at room temperature taking at least 8 hours, the mixed combination of these two adhesives required at least 3 hours at 150ºC and 5 more hours to complete the cure of the acrylic, at the same 150ºC in one of the attempts and at room temperature in the others. The time requirements for both adhesives were satisfied but the problem arose with the applied temperatures to DP-8005, as it started to deteriorate and yellowish marks appeared on the adhesive, similar to burn marks (see Figure 45).

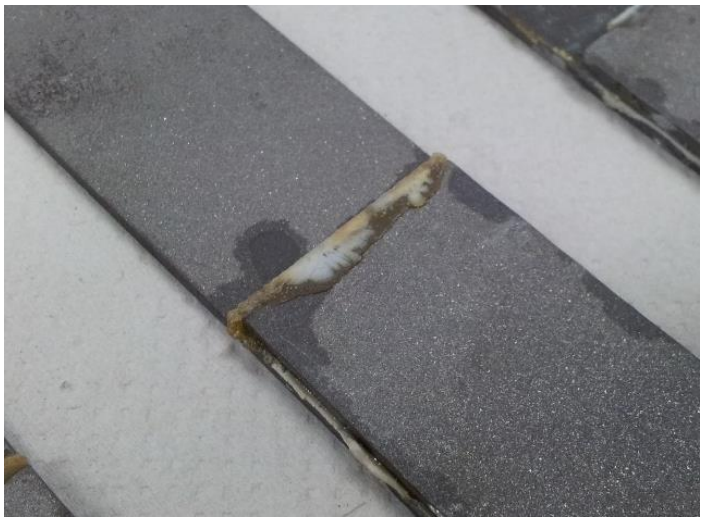

Figure 45. Burn marks encountered in the adhesive DP-8005 when 150ºC temperature curing's were performed.

Attempts were made to investigate the maximum handling temperature that the adhesive could sustain without deterioration, which demonstrated a maximum handling

temperature of around 110ºC. Given that, an attempt to cure a mixed joint with this adhesive plus the XNR6852E-2 was made at 110ºC but, as expected, the applied temperature wasn't the necessary to cure the second adhesive, proving that both adhesives can't be properly combined on the same overlap.

Due to this reasons, the main combinations for mixed joints with the available adhesives were reduced to only two: a combination of the AV138 with RTV106 and another with DP-8005.

3.3.7 Post-cure and rectifications

Once the curing process was completed, the specimens were withdrawn from the mould and any excess adhesive was removed with the help of the drilling machine with a millstone coupled to it.

The cure of the AV138 is very flexible and can be done at room temperature for 24 hours or in a few minutes with temperature, so no post-cure was needed, but for the joints containing the adhesives DP-8005 and RTV106, where the cure is based in the absorption of humidity from the air, a few more days were given at room temperature for a post-cure of the adhesive in order to ensure a complete and appropriate cure. For the XNR6852E-2, no complications where found when the required curing settings were satisfied.

Once all of these steps were concluded, the specimens were ready to be tested.

In addition, for reference and comparison purposes, SLJ specimens with 25 mm and 50 mm overlap with a single adhesive along the overlap were also manufactured for static and impact tests with all four adhesives. The manufacture process had exactly the same steps as the manufacture for mixed adhesive joints with the exception of applying the adhesives separator, as only one adhesive is used.

3.4 Test procedures

3.4.1 Static tests

For static tests, the manufactured specimens were tested in a universal test machine INSTRON® model 3367 (Norwood, Massachusetts, USA), equipped with a load cell with a max capacity of 30 kN. The test consisted on a load application to the specimen in a longitudinal direction until failure, with a constant displacement rate of 1 mm/min (quasi-static) and under room temperature conditions. The load and displacement values were recorded and processed electronically so as to draw the P-Delta curves, allowing the determination of various properties of the specimen such as the stiffness in the elastic zone and the maximum load and displacement at failure.

All of the manufactured combinations were tested, both 25 mm and 50 mm overlaps plus mixed and single adhesive joints. The results are shown in Chapter 5.

In the first tensile tests, the use of the original wedge-grips fixing mechanism to fix the specimens resulted in some slippage that was reflected in a variation of the slope in the elastic zone of the load-displacement curve and thus, producing wrong and misleading results. To avoid this problem, the fixing mechanism was replaced with bolt-on grips tightened with four screws and a supporter pin, for each side of the specimen.

Also, tabs were inserted in between to ensure a vertically alignment of the substrates and thus, a reduced possibility to create eccentric loads.

3.4.2 Impact tests

The impact tests were performed in a Rosand® Instrumented Falling weight impact tester, type 5 H.V. (Stourbridge, West Midlands, U.K.). The concept of the test is to drop a mass guided from a certain height that impacts on the lower fixing tool of the specimen, transferring energy to it in order to break the bond. The specifications for the tests were defined and implemented electronically. When setting the necessary energy and mass, the computer makes the calculations of the impact speed and initial height to obtain the impact load requested.

The fixing system necessary for the tested single lap joint specimens is shown in Figure 46. Two screws holds the specimen in place in the fixing tools with tabs inserted in

between to ensure a vertically alignment of the substrates and thus, a reduced possibility to create eccentric loads. The guide was properly adjusted to make sure that the load was accurately aligned and no accidents could occur.

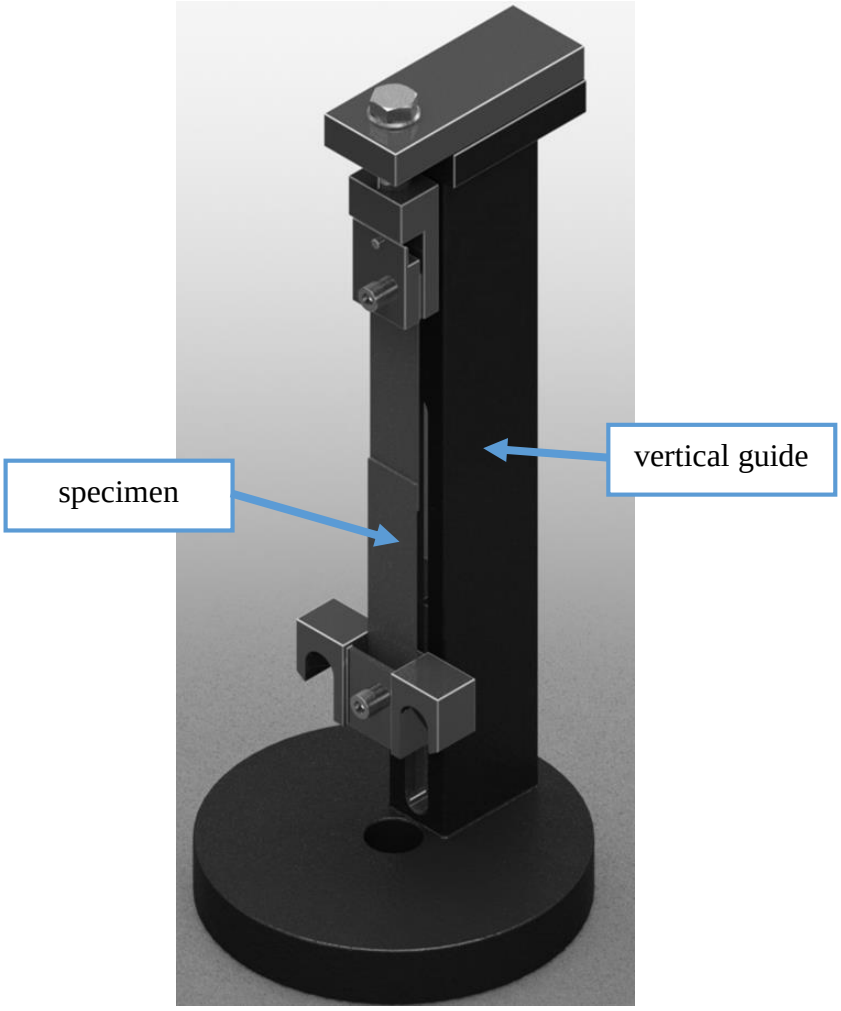

Figure 46. Specimens fixing tool for impact tests [42].

Then, an impactor slides down and hits the tool. A load cell placed at the top of the impactor was used to measure the loads that were processed in a computer and then load, velocity and energy curves were plotted.

For the performed tests, the machine was configured so that 40 J of energy were applied at impact. A 26 Kg mass was already set in the testing machine so the necessary height was obtained with the following equation:

$$E = m \cdot g \cdot h_0 \tag{15}$$

where E is the applied energy, m is the mass, g is the gravitational acceleration and h_0 is the initial height. Given that, for 40 J of energy and a mass of 26 Kg, the initial height necessary was approximately 15.7 centimetres.

The final speed at impact was obtained with the following equation:

$$E = \frac{1}{2} \cdot m \cdot v^2 \tag{16}$$

where v is the resulting velocity. The applied energy resulted in a speed of 1.75 m/s.

Due to limitations of the impact machine relating to the existing displacement of the impactor where values can be recorded, the specimens with 50 mm overlap didn't fitted to the machine's base for being too big and so, only 25 mm overlap specimens could be tested with the available configuration. For each joint combination, three specimens were tested within the same conditions.

4. Numerical simulation

4.1 Static

A finite element analysis was performed using the numerical simulation program Abaqus® (Dassault Systèmes, Suresnes, France) to obtain the load-displacement curves and get a prediction of the failure load. The adhesive properties applied in the model were the same as the properties showed in Table 1 and were converted to a cohesive triangular law, using quads damage for the traction separation. Only high strength steel was considered for the adherends, thus no deformation was taken in consideration in order to simplify the model. No plasticity properties were then included for the steel.

The numerical model for the simulation consisted in a standard explicit model computed in a general/static analysis and was created as a 2D deformable part, involving cohesive elements in the bondline.

The geometry of the modelled part corresponded to that of the 25 mm overlap single lap joint specimens, as well as the boundary conditions, in order to reproduce the experimental testing conditions and compare the results. Those are represented in the scheme of the Figure 47.

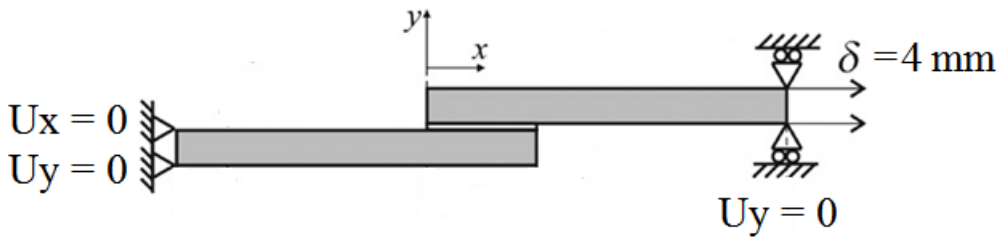

Figure 47. Boundary conditions applied for the static model.

Scalar stiffness degradation (SDEG) was requested in field outputs in order to observe the crack propagation as a degradation of the cohesive elements. Figure 48 shows an example of a visualization of the SDEG results.

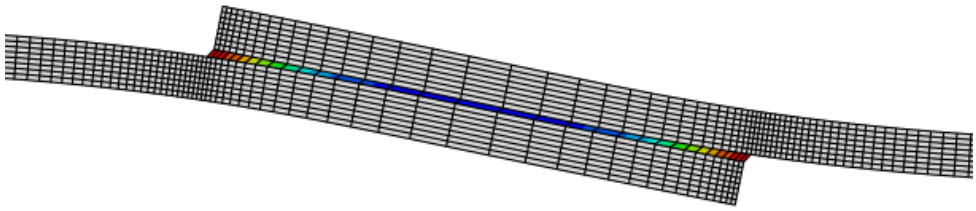

Figure 48. Visualization example of SDEG results.

For the adhesive bondline area, the mesh was defined automatically, requesting square cohesive finite elements with 0.2 mm edge. For the rest of the model, seeds were defined using biasing effects to refine the mesh in the zones where stress gradients are known to be greater such as the overlap ends and in the zones of modulus transition, in order to improve the accuracy of the calculations, as seen in Figure 49.

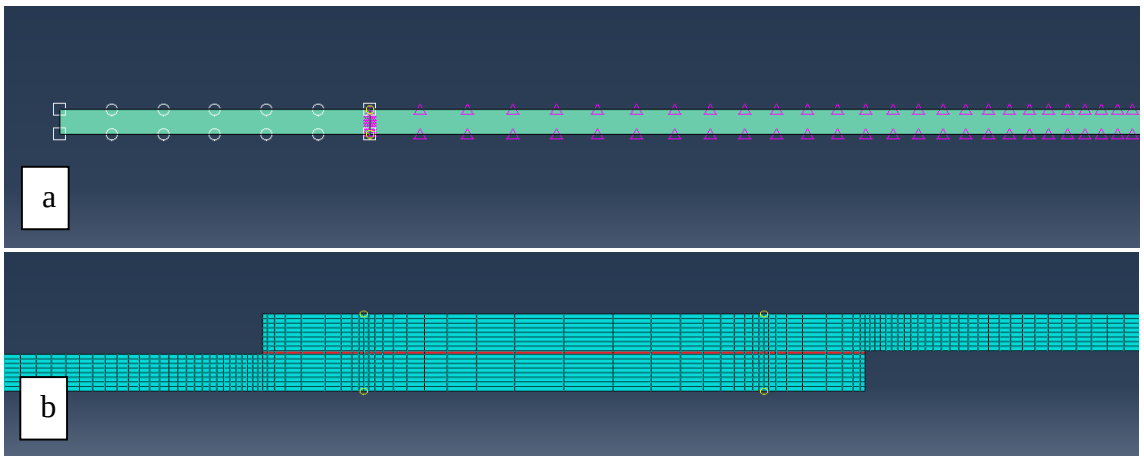

Figure 49. Model mesh definition. (a) applied seeds; (b) final mesh.

The element types for the bondline area were defined as a 4-node two-dimensional cohesive element (COH2D4) while for the substrates, a 4-node bilinear plane strain quadrilateral, reduced integration, hourglass control (CPE4R) elements were used.

As the main objective of the simulation tests is to get a comparison with the experimental results obtained in static and impact tests and only 25 mm overlap specimens were tested at impact, only 25 mm overlap was simulated, both for single and mixed adhesive joints.

4.2 Dynamic

For impact conditions, the model was the same used in static simulations consisting in a 2D deformable part, with a few modifications regarding to the boundary conditions and the analysis type.

The properties of the materials introduced for the impact simulation are presented in Table 6. Properties for XNR6852E-2 at high strain rate were determined in a parallel work during the course of this thesis. For the adhesives DP-8005 and AV138, bulk tests were performed at 100 mm/min and the tensile strength – t_n – was extrapolated by a logarithmic tendency function (see Equation 17) to impact velocity using the values from 1 mm/min and 100 mm/min tests, as seen in Figures 50, 51 and 52, using the same method found in [43]. The shear strength – t_s, – was predicted using the same relationship of proportionality found in tensile strength between the 1 mm/min and 100 mm/min tests. For the RTV106, this extrapolation was not performed. This is due to the adhesion problems encountered both in static and impact experimental tests. As the failure is always adhesive and, therefore, unpredictable, it does not make sense to introduce higher mechanical properties for the dynamic models. The adhesion properties were therefore considered to be independent from the strain rate. To avoid overestimation of failure loads the same properties of the 1 mm/min test were used for the impact simulation. For all materials studied, and to simplify the simulation, the Young's and shear modulus and the mode I and mode II fracture energy were considered not strain rate dependent, with no change in the properties from the low speed tests. However, it is expected a slight reduction in fracture energy properties with an increase of the strain rate, so this approximation may not be fully accurate.

$$\sigma = A \cdot ln(\dot{\varepsilon}) + B \tag{17}$$

with the coefficients A and B determined from the logarithmic tendency function.

The strain was calculated with the following equation:

$$\dot{\varepsilon} = \frac{v}{L_0} \tag{18}$$

where v is the velocity of the test and L_0 is the initial calibrated longitudinal deformation length of the specimen section where the strain is measured.

Table 6. Adhesive properties at different strain-rate speeds.

Adhesive	Speed (mm/min)	L_0 (mm)	Strain (s^{-1}) *	Tensile strength [MPa]	Shear strength [MPa]	Mode I fracture energy [N/mm^2]	Mode II fracture energy [N/mm^2]
DP-8005	1	60	2.78×10^{-4}	6.3	8.4	1.1	6
	100	25	6.67×10^{-2}	13	17.4	-	-
	105000	0.2	8750	27.5	36.7	1.1	6
AV138	1	60	2.78×10^{-4}	41	30.2	0.35	4.9
	100	50	3.33×10^{-2}	49.1	36.2	-	-
	105000	0.2	8750	70.2	51.7	0.35	4.9
XNR6852 E-2	1	28	5.95×10^{-4}	42.9	28.7	1.68	18
	100	25	6.67×10^{-2}	46	33.6	-	-
	105000	0.2	8750	53.7	45.8	1.68	18
RTV106	1	60	2.78×10^{-4}	2.3	1.97	2.73	5
	100	-	-	N/A	N/A	N/A	N/A
	105000	-	-	N/A	N/A	N/A	N/A

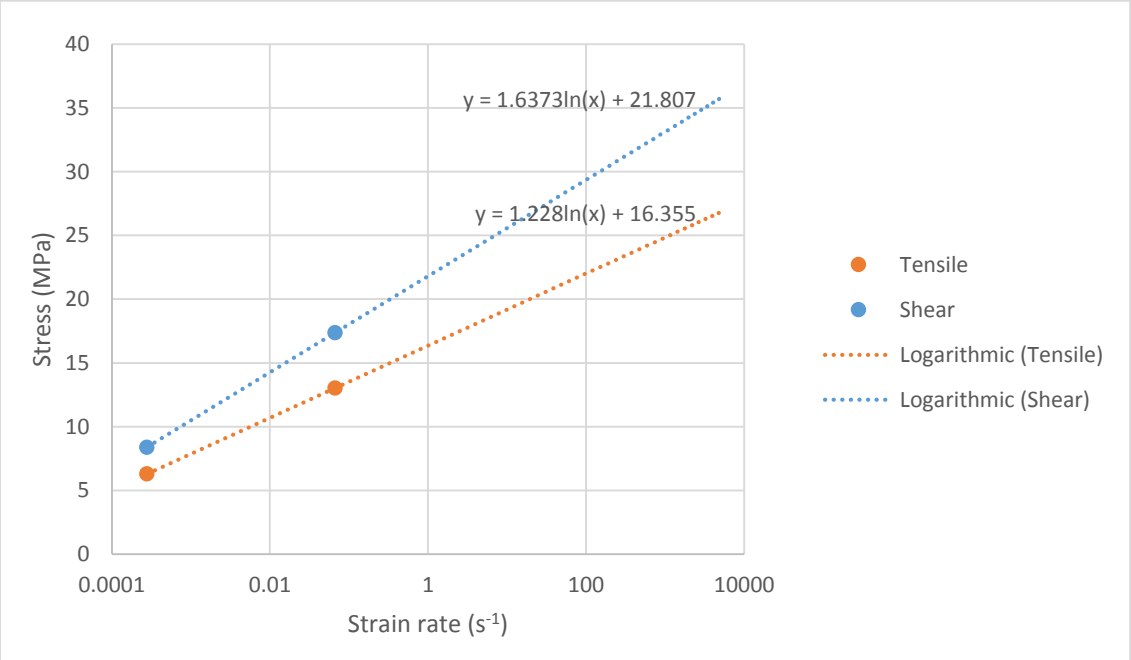

Figure 50. Extrapolation curves for DP-8005.

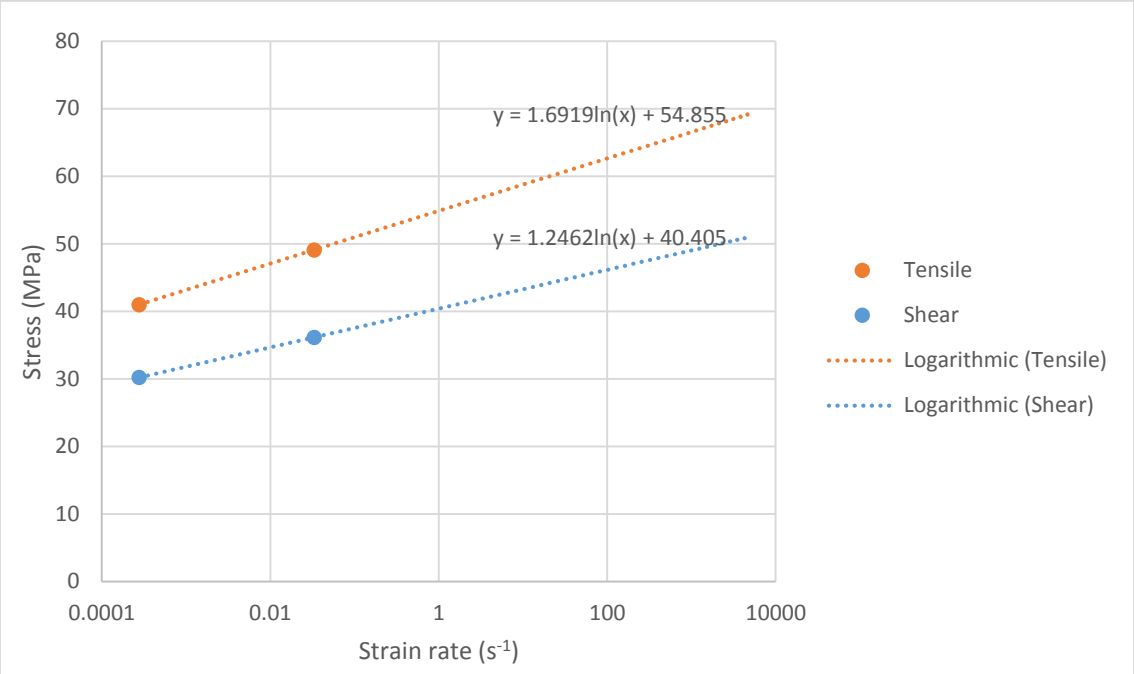

Figure 51. Extrapolation curves for AV138.

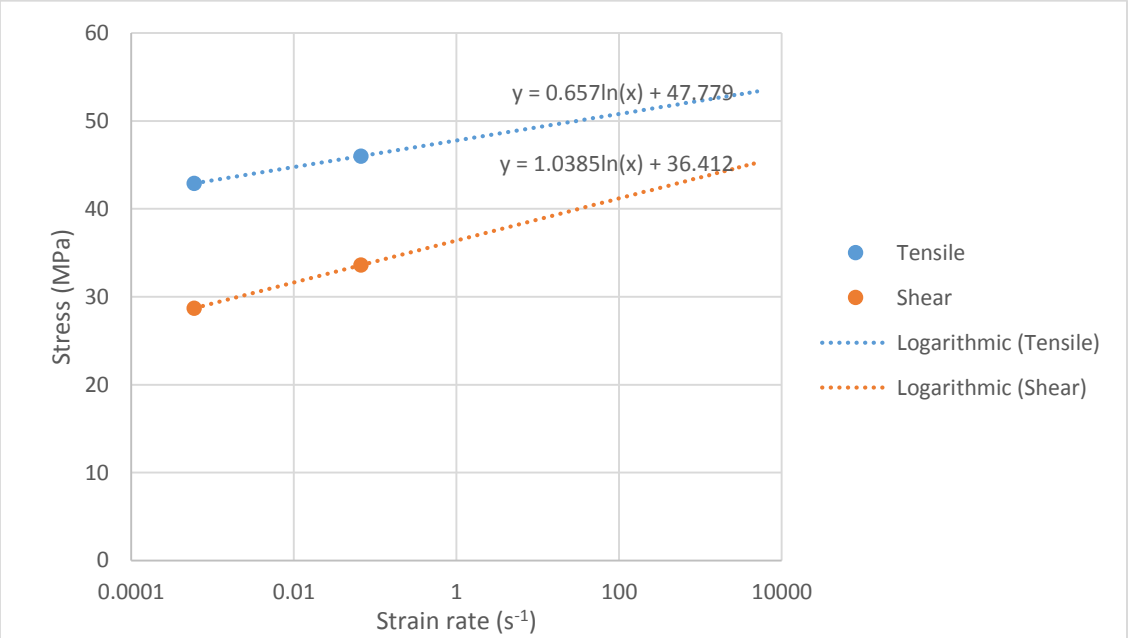

Figure 52. Extrapolation curves for XNR6852E-2.

The density of the adhesives and substrates was introduced according the Table 7.

Table 7. Density of the materials.

Material	Density
High strength steel	7.8
RTV106	1.07
DP-8005	1.06
AV138	1.7
XNR6852E-2	1.5

Material properties for a mass to simulate the impactor in the impact testing machine were also included. This mass block with 26 Kg (as in the impact machine) was introduced in the last 25 mm length of the free adherend, as shown in Figure 53, with an applied predefined field, substituting the boundary condition of the 4 mm horizontal displacement present in static simulation. Once again, this was made to replicate the boundary conditions and applied loads of the experimental test, shown in Figure 54.

Figure 53. Simulated mass block applied to the specimen.

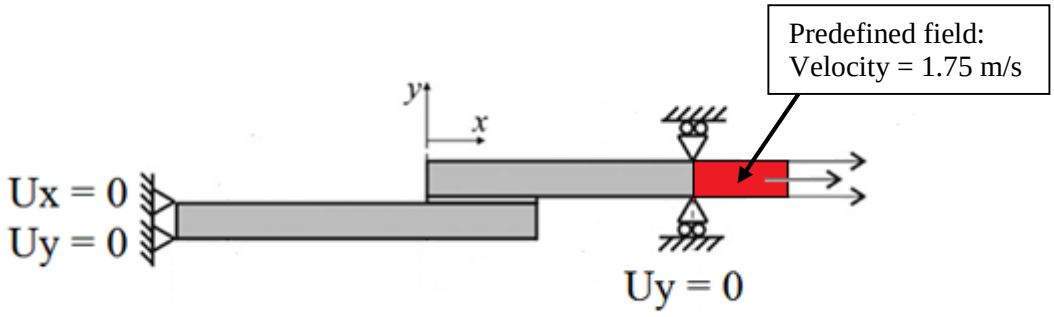

Figure 54. Boundary conditions applied for the dynamic model.

The volume of the block is 1250 mm^3 and to simulate an impact with 40 Joules of energy and a velocity of 1.75 m/s, the density was set to 2.08E+7 Kg/m^3.

For the analysis, the step was replaced with a dynamical explicit calculation with a time period of 0.005 seconds and non-linear geometry ON (nlgeom). A velocity type predefined field was applied to the initial step with a value of 1750 (mm/s) in the region corresponding to the block mass. In field outputs an SDEG was also requested as well as the reaction forces and displacements of selected nodes in order to draw the impact load-displacement curves. At last, the mesh element types were changed to explicit elements with the same controls as for the static simulation.

5. Results and discussion

In this chapter, the results obtained during testing of the specimens are shown and consideration are made regarding interesting values and behaviours. Additionally, pictures of the failure modes were taken and presented for analysis.

5.1 Experimental results

5.1.1 Static tensile test results

5.1.1.1 *Mild steel adherends*

Tensile tests were first performed with mild steel adherends in joints with single adhesive application containing AV138, DP-8005, RTV106 and XNR6852E-2 and mixed adhesive applications with RTV106 + AV138, DP-8005 + AV138 and DP-8005 + XNR6852E-2. The results of the tensile tests and the failure modes are shown below. Only 25 mm overlap length was used with mild steel adherends in order to investigate the influence in maximum strength of the joints.

Figure 55 shows the resulting P-Delta curves of the tensile tests performed with all of the combinations manufactured with mild steel adherends. The tested overlap was 25 mm.

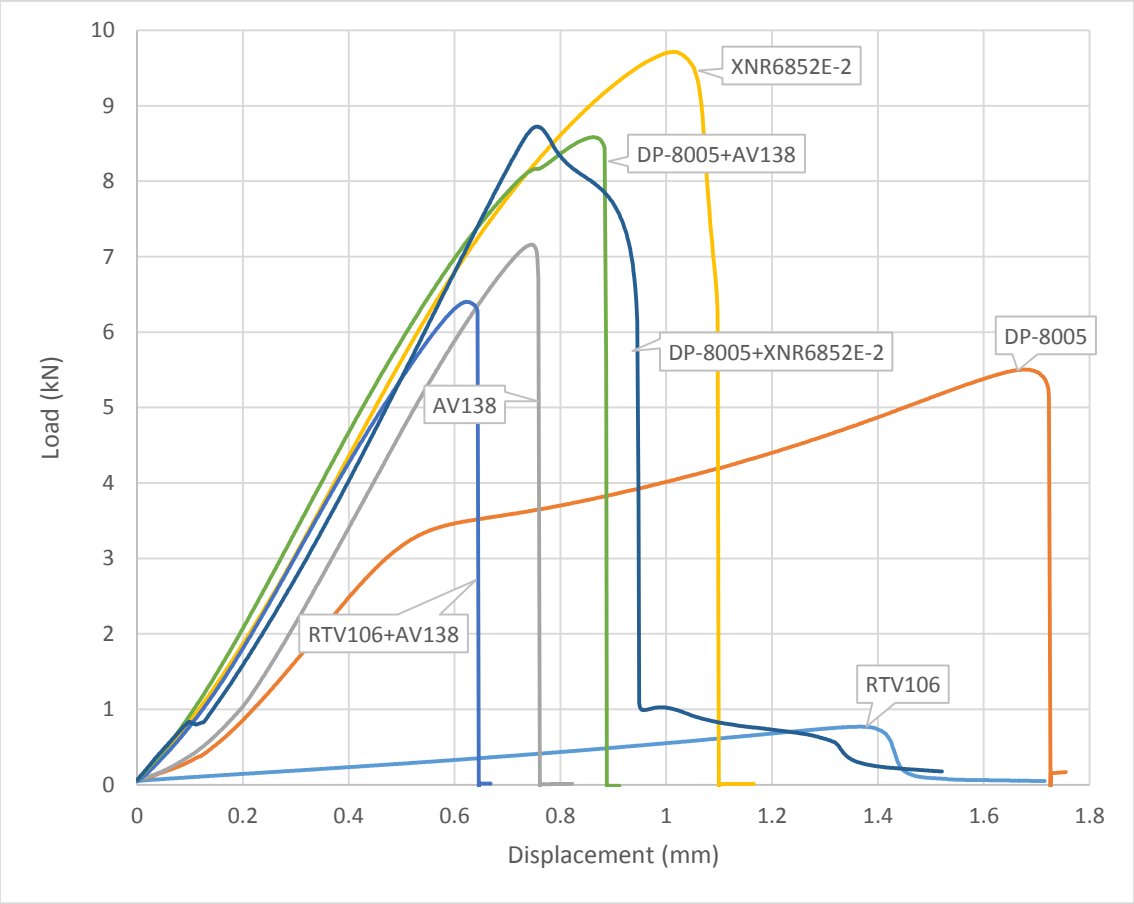

Figure 55. Typical P-Delta curves for all of the tested specimens with mild steel adherends.

Apart from the ductile adhesives when used alone on the overlap, all of the combinations resulted in similar slope of the elastic zone, but different strains at failure point were obtained.

Figure 56 represents a comparison between the average maximum loads and standard deviation obtained from the tensile tests for all joint combinations.

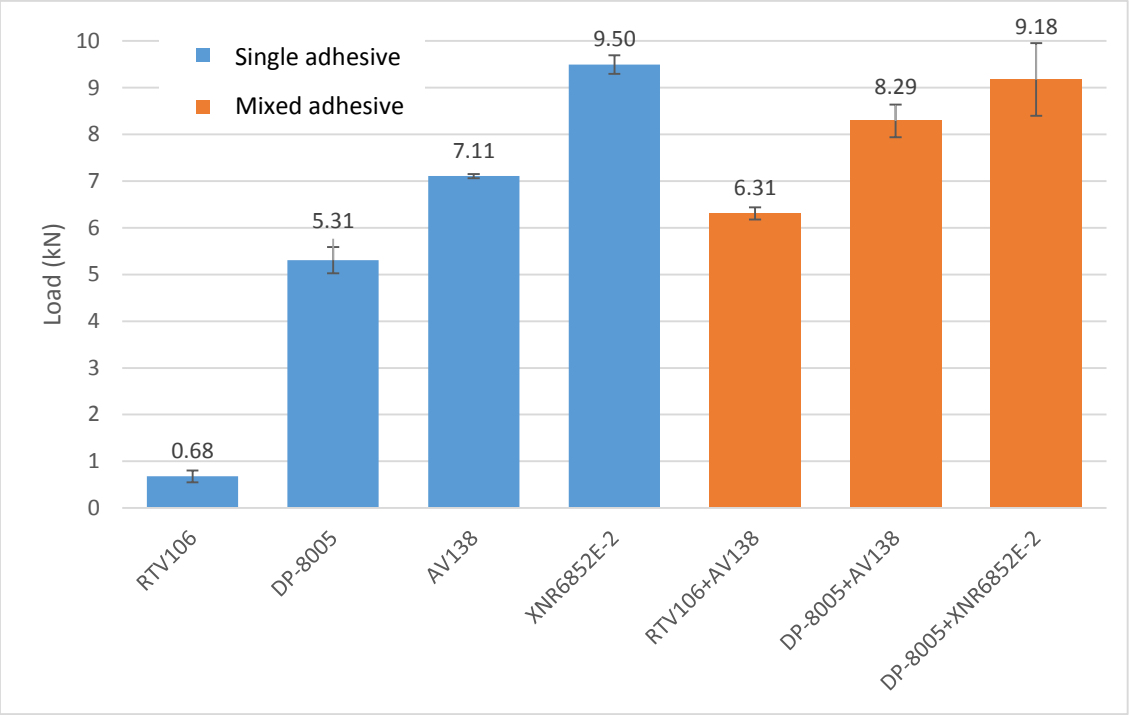

Figure 56. Average maximum load for the joint combinations tested.

The configuration exhibiting the highest maximum load was the single application of the adhesive XNR6852E-2 while the lowest maximum load was obtained from the configuration of a standalone application of RTV106, which resulted in very weak loads due to adhesive failure in almost all of the overlap. Several specimens with the adhesive RTV106 were tested, including mixed adhesive joints, resulting in bad adhesion using steel adherends, as shown in Figure 59.a) and e). Furthermore, the RTV106 is a sealant adhesive designed mainly for applications with temperature and not for joint strength, so low values were always expected. Within this problem, the maximum strength of the mixed adhesive joint configuration with RTV106 and AV138 was found to have a reduction of 11.3% when compared with AV138 only, as shown in Figure 57. Therefore, when mild steel adherends are used, this combination of mixed adhesive technique has demonstrated no improvement of the performance.

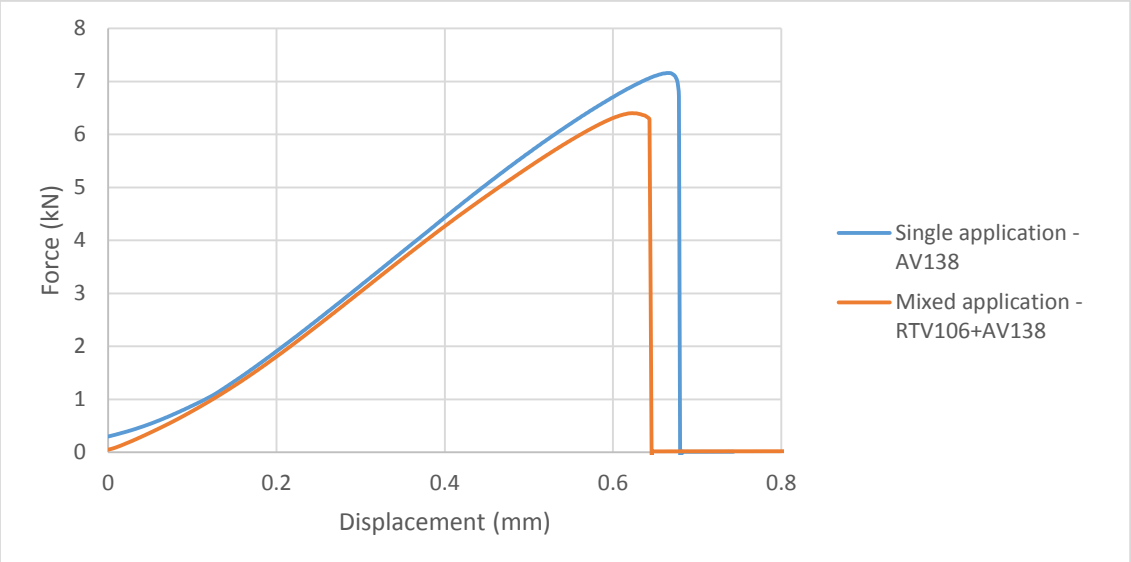

Figure 57. Comparison of single and mixed adhesive application for RTV106 and AV138 with mild steel adherends.

The combination containing the adhesives DP-8005 and AV138 has shown better results when compared with configurations of both adhesives used alone. The improvement of combining this ductile adhesive in the same overlap with the epoxy is around 17%, compared to a configuration where only AV138 is used, as shown in Figure 58.

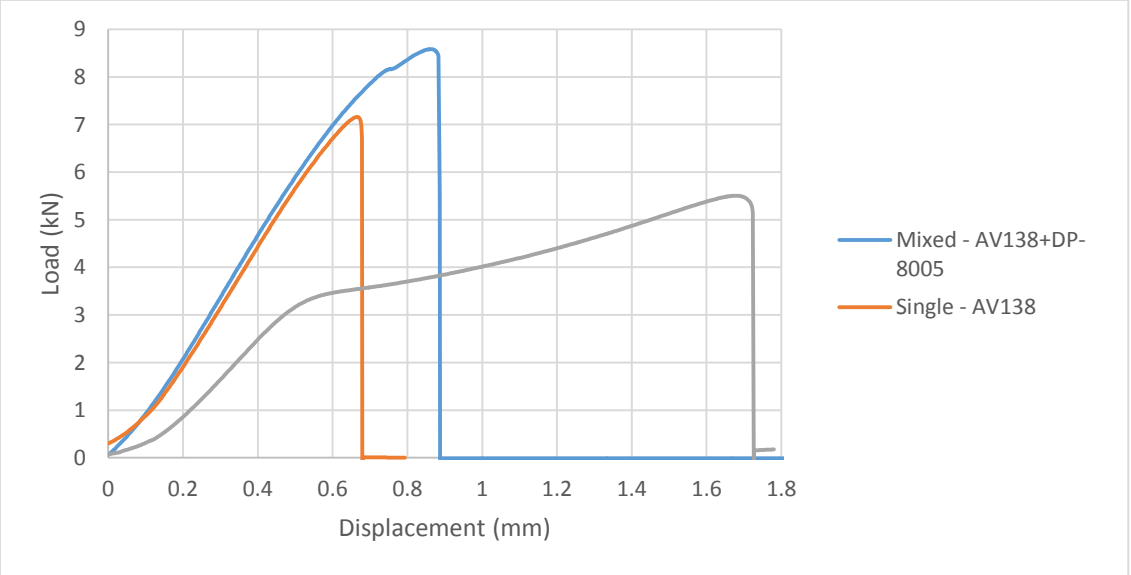

Figure 58. Comparison of single and mixed adhesive applications for DP-8005 and AV138 with mild steel adherends.

With this results, it is proved that the use of a ductile adhesive in the ends of the overlap combined with a brittle adhesive can improve the maximum strength of the joint for certain adhesive configurations, like in this case. Not only the maximum strength was improved but also the extension at failure, resulting in a more flexible joint and allowing for more energy absorption without failure, which could be a good characteristic for impact conditions. The use of the adhesive DP-8005 combined with AV138 instead of the adhesive RTV106 has improved the maximum strength of the joints by 31.4%, which proves the importance of the adhesives selection when using the mixed adhesive technique.

Another configuration that could be interesting is the combination of DP-8005 with XNR6852E-2, but due to the problems with curing schedules and temperatures explained in the section of specimens manufacturing, the joint suffered a reduction in maximum strength and no improvements were able to be found. Even so, the results of the mixed configuration were similar to the results of a single application of XNR6852E-2, as these were found to be inside the standard deviation of the first ones. The main cause for failure for both of these combinations was the yielding of the adherends, which was found to be very high compared to the other combinations. The joints with the ductile adhesives didn't exhibit plastic deformation of the adherends after failure, the combination of RTV106 with AV138 showed a bit of plasticization and the other combinations were those that revealed higher effects. Also, the higher values of extension were found for DP-8005 and RTV106 due to its flexibility, followed by the hybrid epoxy adhesive XNR6852E-2.

Figure 59 shows the pictures taken to the overlap surface to analyse the failure mode of the different adhesive configurations.

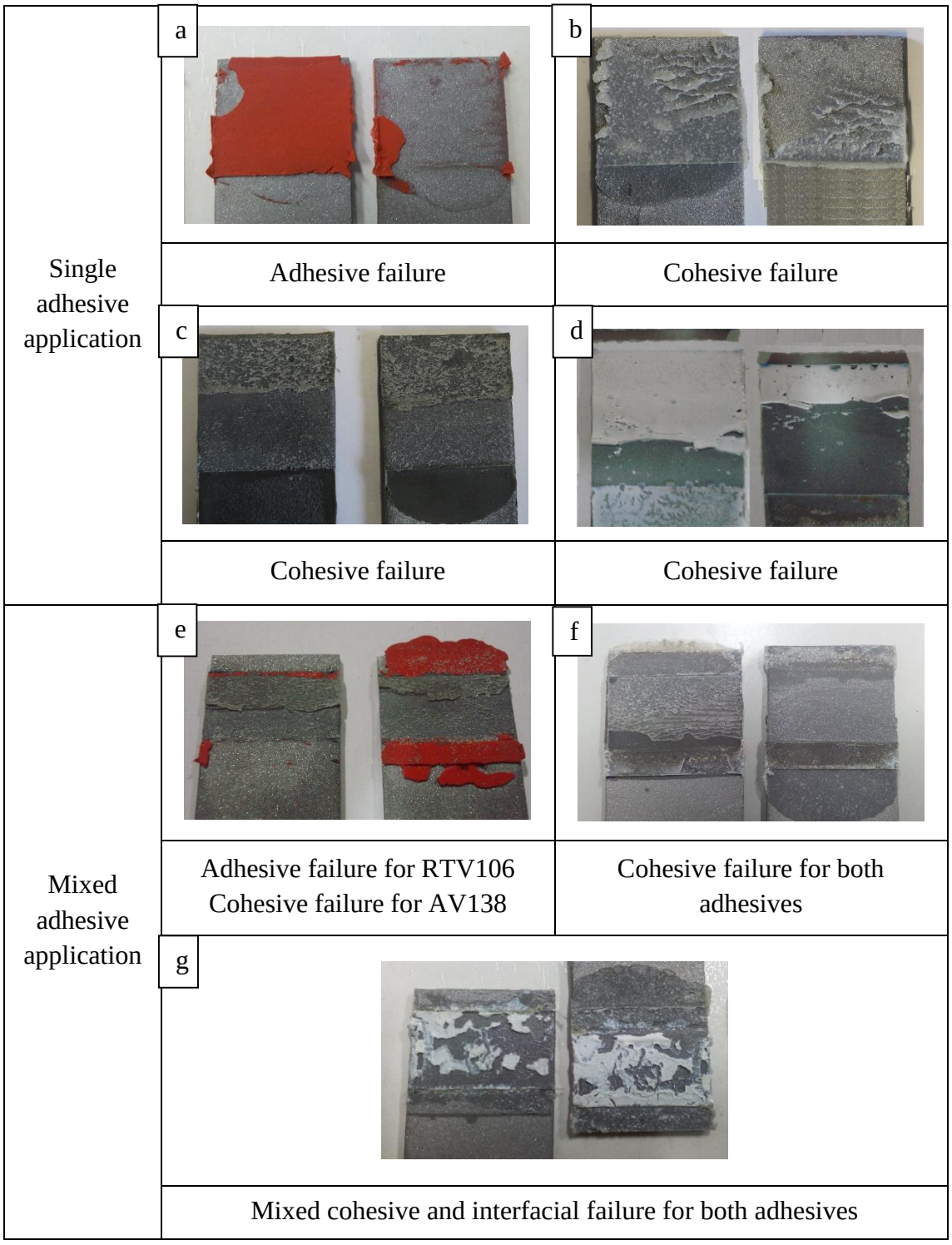

Figure 59. Failure modes for all of the tested joint configurations with mild steel adherends.

The failure mode was cohesive in all specimens with exception for the combinations with RTV106. These joints exhibited an adhesive failure in the adhesive and a mixed adhesive and cohesive failures for the mixed joints with AV138. A justification for this result is that in practice the use of RTV106 results in very weak joint strength when using thin adhesive layers due to its extremely low modulus of elasticity. As for the mixed adhesive joint with DP-8005 and XNR6852E-2, the overlap region showed a strange failure mode with bad adhesion and adhesive degradation. The combination of both adhesives somehow created a chemical reaction on the adhesives and, combined with the long and high temperature curing schedules from the manufacturing stage, the adhesive layer became powdery and crumbled to pieces. Because of that, the strength of this joint configuration was lower than the use of only the adhesive XNR6852E-2, so there's no interest in combining these two adhesives on the same overlap.

Lastly, for all the tested joints there was good adhesive separation.

5.1.1.2 *High strength steel adherends*

In order to avoid the plasticization of the adherends and consequently premature failures of the joints by concentration of peeling forces, specimens with high strength steel adherends were tested to analyse the full potential of the adhesives used in pure shear strength. The same joint configurations were tested and Figure 60 shows the resulting P-Delta curves of the tensile tests performed with high strength steel as the substrates. In this case, the tested overlap was again 25 mm.

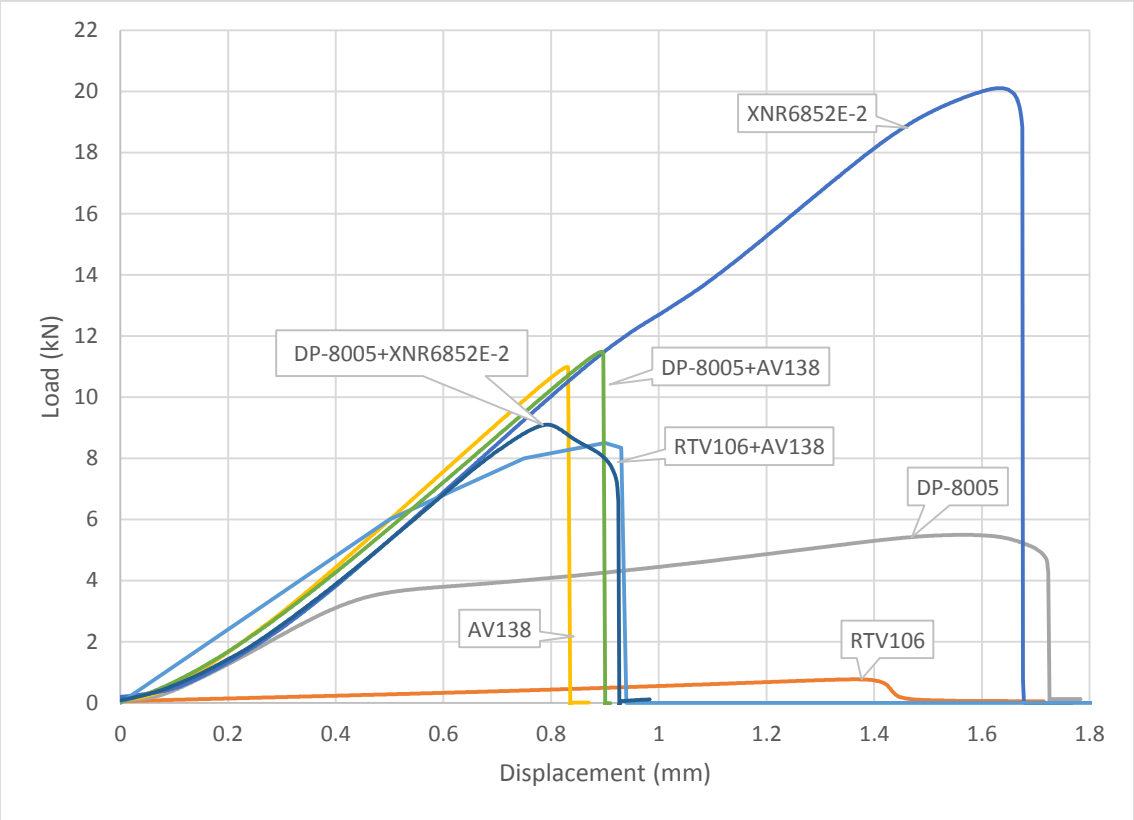

Figure 60. Typical P-Delta curves for all of the tested specimens with high strength steel adherends, 25 mm overlap.

The same test was performed for specimens with 50 mm overlap to investigate the influence in maximum strength of the joints. The influence of the mixed adhesive technique is expected to be most evident when larger overlaps are used. The results are shown in Figure 61. In this case, the mixed adhesive configuration of the adhesives DP-8005 with XNR6852E-2 was not performed due to the problems encountered in previous tests as well as the configurations containing the adhesive RTV106 due to the already described bad adhesion problems and consequent reduction of the joint strength when combined with AV138.

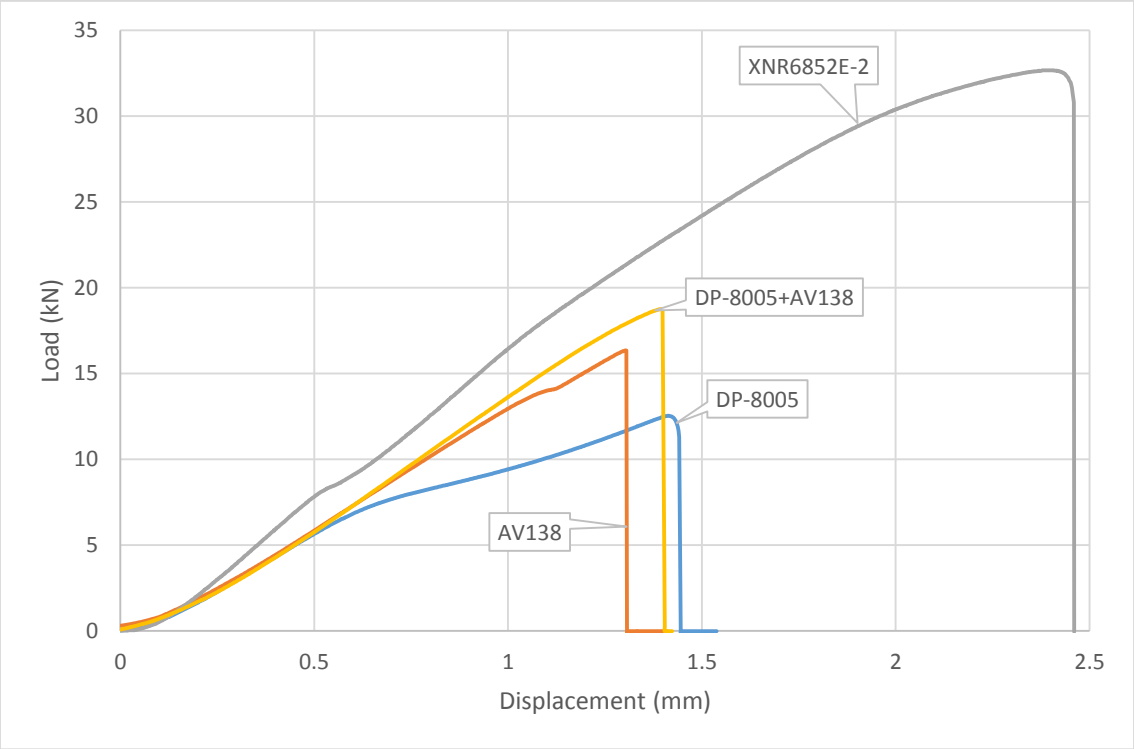

Figure 61. Typical P-Delta curves for all of the tested specimens with high strength steel adherends, 50 mm overlap.

Figure 62 represents a comparison between the average maximum loads and standard deviation obtained from the tensile tests for all joint combinations with high strength steel as the substrates for both 25 mm and 50 mm overlap lengths.

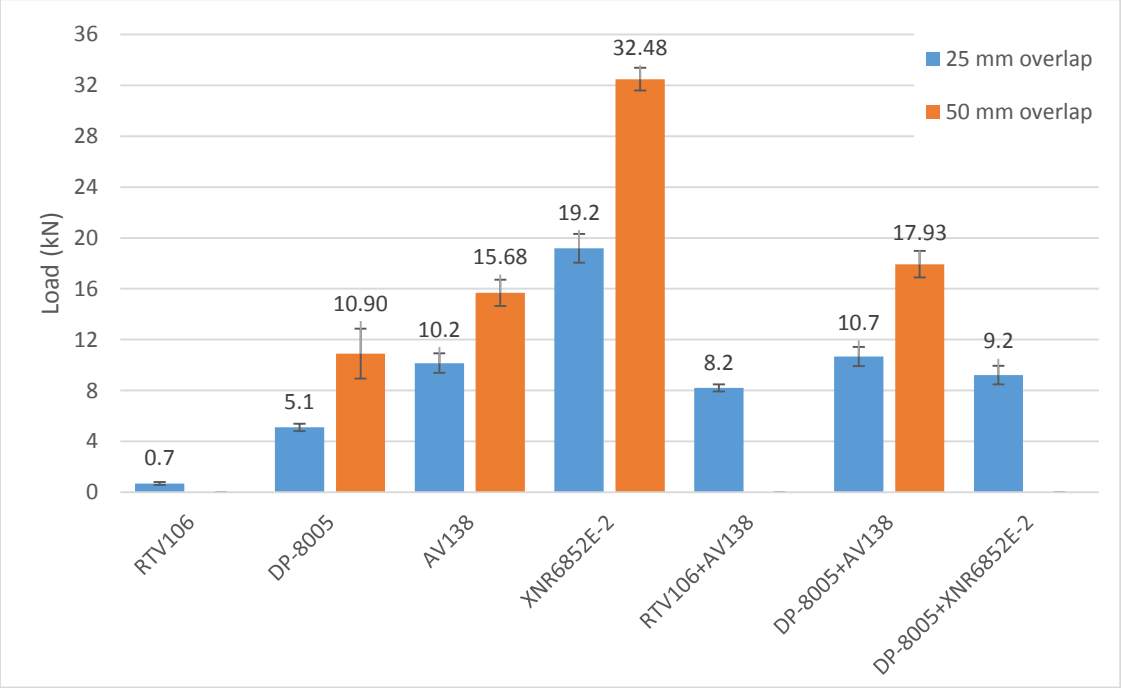

Figure 62. Average maximum load for the joint combinations tested. 25 mm versus 50 mm.

For the specimens using high strength steel, the results were about the same as the specimens with mild steel adherends in respect of the joint configurations with maximum and minimum strength, but the values were slightly different. The maximum strength was once again obtained by using a single application of the XNR6852E-2 adhesive, achieving a maximum load of around 19 kN average. The same result occurred for a configuration with RTV106 and AV138, which exhibited a maximum strength reduction when combined together. In this case with around 20% lower results than using only AV138. Also, an improvement of joint strength by placing the adhesive DP-8005 on the same overlap of AV138 was exhibited, but in this case the improvement was less significant, as seen in Figure 63. Furthermore, the mixed combination of DP-8005 and XNR6852E-2 revealed once again bad results and no differences between the types of steel used. Due to the same problems encountered with mild steel adherends, in this case it was proven that the joint strength of this combination was significantly affected, revealing a reduction of around 50% of the joint strength of a single application of XNR6852E-2.

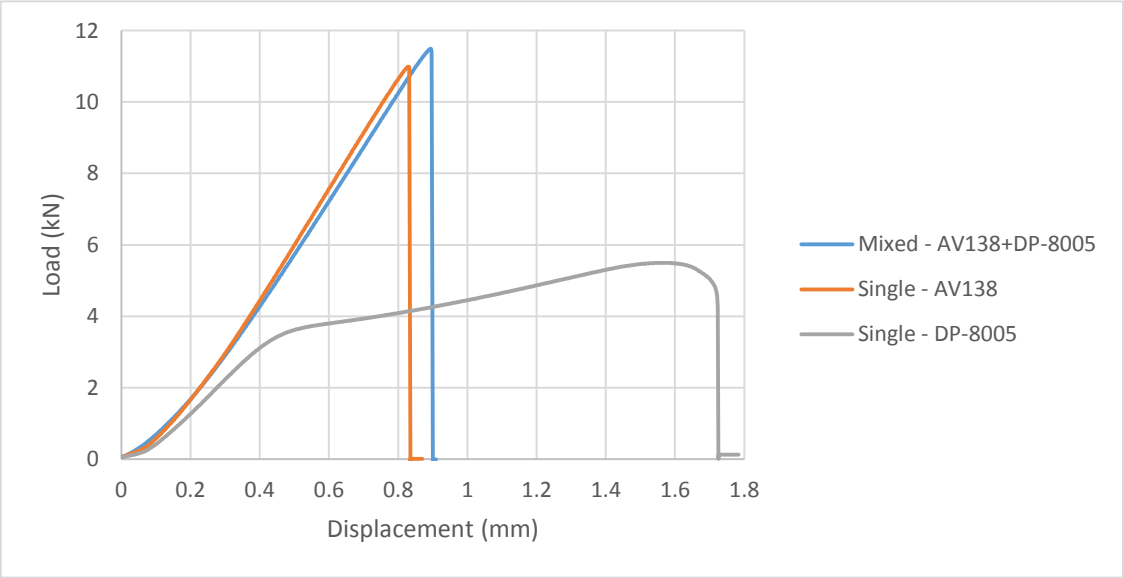

Figure 63. Comparison of single and mixed adhesive applications for DP-8005 and AV138 with high strength steel adherends and 25 mm overlap.

Figure 64 shows the failure load in function with the overlap length for the tested configurations, both for 25 mm and 50 mm overlap.

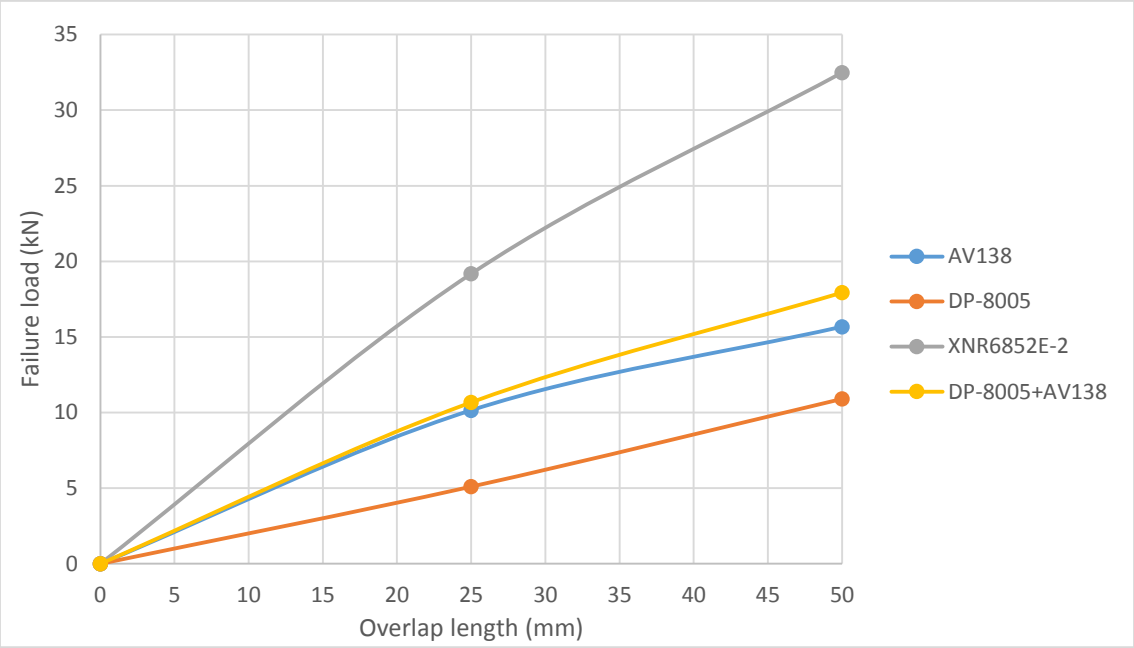

Figure 64. Failure load as a function of the overlap length.

As seen in Figure 64, the variation of the overlap resulted in double joint strength for specimens with only DP-8005, which, as it is a ductile adhesive, the joint strength was almost proportional to the overlap length. The adhesive deformed plastically and as the load increases it redistributed the stresses. On the other hand, an increase of only around 54% was found when doubling the overlap of AV138. In this case, the joint strength was not proportional to the overlap length and a justification for this is that the stress concentrates at the ends of the overlap and increasing its length does not vary the stress distribution. The same occurred to the XNR6852E-2 but the increase in joint strength was around 69%, a value due to the fact that the adhesive has some flexibility. This specimen was tested in another universal test machine present in LET (Laboratório de ensaios tecnológicos) at FEUP with a load cell with higher capacity. As for the mixed adhesive joint with DP-8005 and AV138, doubling the overlap area resulted in a joint strength increasing around 68%, which is a value encountered between the general 50% increasing of a pure brittle adhesive and a 100% increasing for a ductile adhesive. Also, the mixed combination produced an improvement of 15% in joint strength compared to a joint with only AV138 for a 50 mm overlap, while the same comparison with 25 mm overlap resulted in an improvement of only 5%. With this, it is concluded that the mixed adhesive technique increases the influence of the overlap variation, especially when a ductile adhesive is combined with a very stiff one.

Figure 65 shows the pictures taken of the 25 mm overlap surface with high strength steel adherends to analyse the failure mode of the different adhesive configurations.

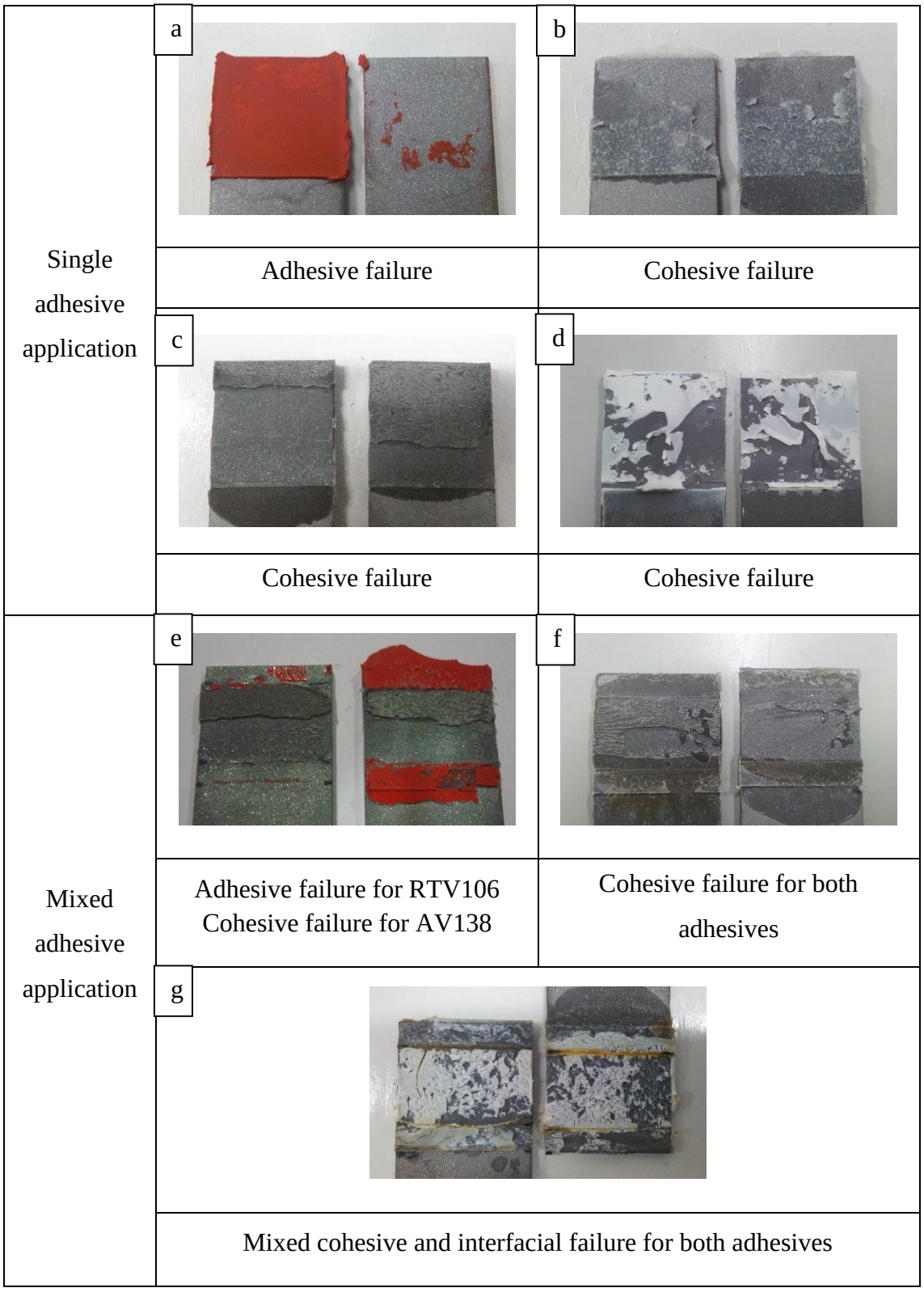

Figure 65. Failure modes for all of the tested joint configurations with high strength steel, 25 mm overlap.

Figure 66 shows the pictures taken of the 50 mm overlap surface with high strength steel adherends to analyse the failure mode of the different adhesive configurations.

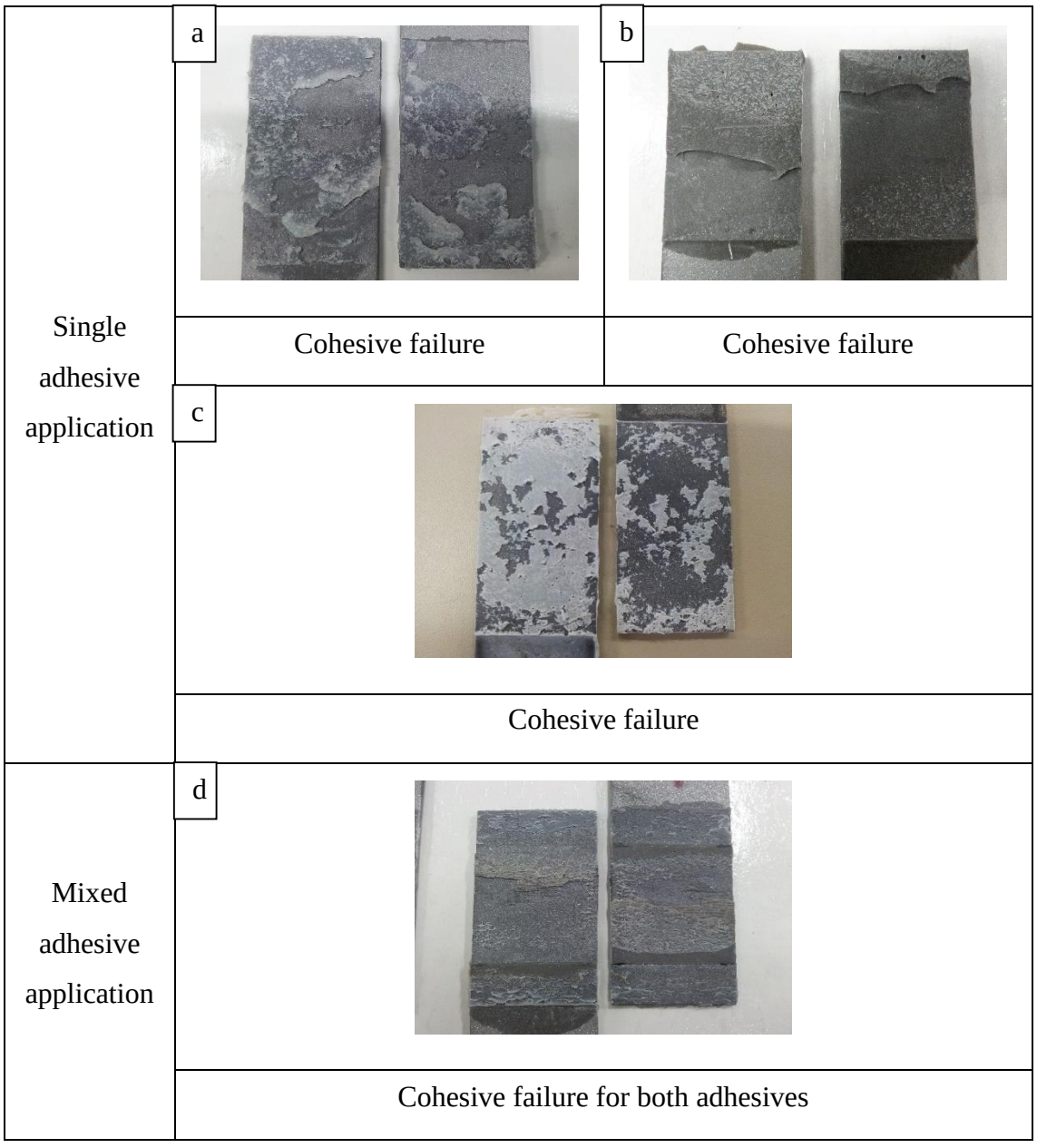

Figure 66. Failure modes for all of the tested joint configurations with high strength steel, 50 mm overlap.

For high strength steel adherends, the failure mode was very similar to that which occurred with mild steel adherends. Also, the overlap variation didn't make a significant influence, and the same trend can be observed for both situations. For both overlap lengths, cohesive failure was verified for joints containing AV138, DP-8005 and XNR6852E-2. As for the RTV106, the same adhesion problems were found as well for

the mixed adhesive configuration of DP-8005 with XNR6852E-2, exhibiting once again a failure surface with mixed cohesive and interfacial failure for both adhesives.

Also, no plastic deformation was verified on the adherends for both 25 mm and 50 mm overlap, which was expected given the high strength steel used.

5.1.1.3 *Mild steel vs. High strength steel*

Figure 67 shows a comparison of the results between the type of adherends used and the influence taken by each configuration.

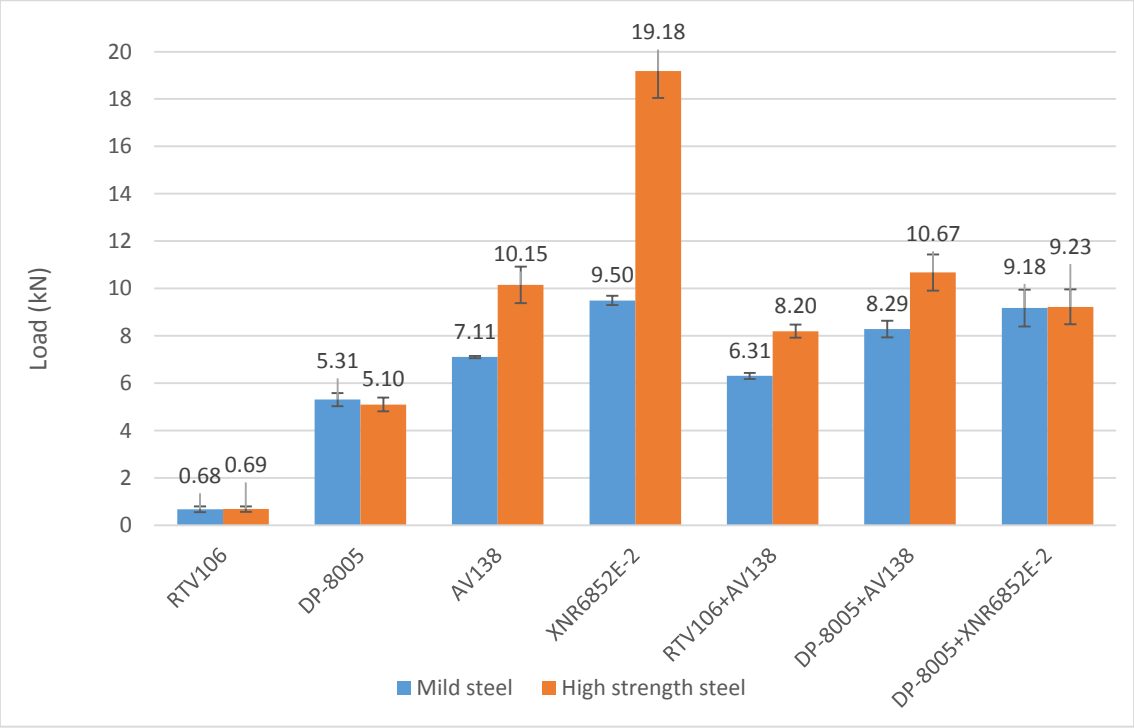

Figure 67. Comparison of mild steel and high strength steel adherends in maximum strength of the joint.

For the adhesive RTV106, due to its low modulus and bad adhesion encountered, no influence was noticed from the adherends material. The load at failure was very far from the necessary load where mild steel starts to yield. The same conclusion was observed for DP-8005, where the necessary load for break the bond was beyond the yield strength of the mild steel. Furthermore, due to its flexibility, the stress distributions was more uniform instead of being concentrated at the ends of the overlap, which also contributed

for the accommodation of higher loads without the yielding of the adherends. In the other hand, for high moduli adhesives like the AV138 and XNR6852E-2, the influence of the adherends was clear, especially for the second one where the adherends exhibited high plastic deformation and settled the main cause for joint failure. The use of mild steel adherends with AV138 resulted in 42% joint strength decline due to the significant concentration of peel stresses caused by the eccentric loads from the bending moments that led to a premature failure. Likewise, in comparison with the previous results with mild steel adherends, the maximum joint strength of the XNR6852E-2 had improved by around 100%, showing high influence of the adherends.

Also, for mixed adhesive joints, the results for the combination of RTV106 and AV138 did not allowed a clear conclusion because of the problems encountered but the influence of the adherends was mainly because of the adhesive AV138, with around 30% joint strength improvement with high strength steel adherends. A lower improvement compared to the configuration of only AV138, but no perceptible conclusions could be taken. For the configuration with DP-8005 and AV138, the influence of the adherends was less significant, even with maximum load values higher than only AV138. This showed that the application of a ductile adhesive along with a brittle one not only improved the joint strength but also reduced the plastic deformation of mild steel substrates, resulting in less influence of the adherends. A justification for this occurrence could be because of the lower peel stress concentration at the ends of the overlap, thanks to the more uniformed stress distribution sustained by the ductile adhesive. Lastly, the combination of DP-8005 with XNR6852E-2 exhibited similar results both with mild steel and high strength steel adherends, but no improvements were verified due to the problems faced with this joint configuration so no conclusions can be made by this comparison. However, when mild steel adherends were used, high plastic deformation was noticed so it is expected a considerable influence on the results with high strength steel adherends, similar to the influence of the XNR6852E-2 when used alone.

5.1.2 Impact test results

Impact tests were performed using joint specimens with only high strength steel adherends and in configurations with 25 mm overlap. All of the four adhesives in study were tested in a standalone application for reference purposes but only the two main configurations of mixed adhesive joints in study were tested due to the previously explained problems encountered during the manufacturing and static testing stages. Results of the failure load, energy absorbed, elongation and failure modes are represented.

Figure 68 shows the resulting P-Delta curves of the tensile tests performed with all of the combinations manufactured for impact tests. A cut-off frequency of 3000 Hz was applied to softening the curves to allow a clear comparison with all of them.

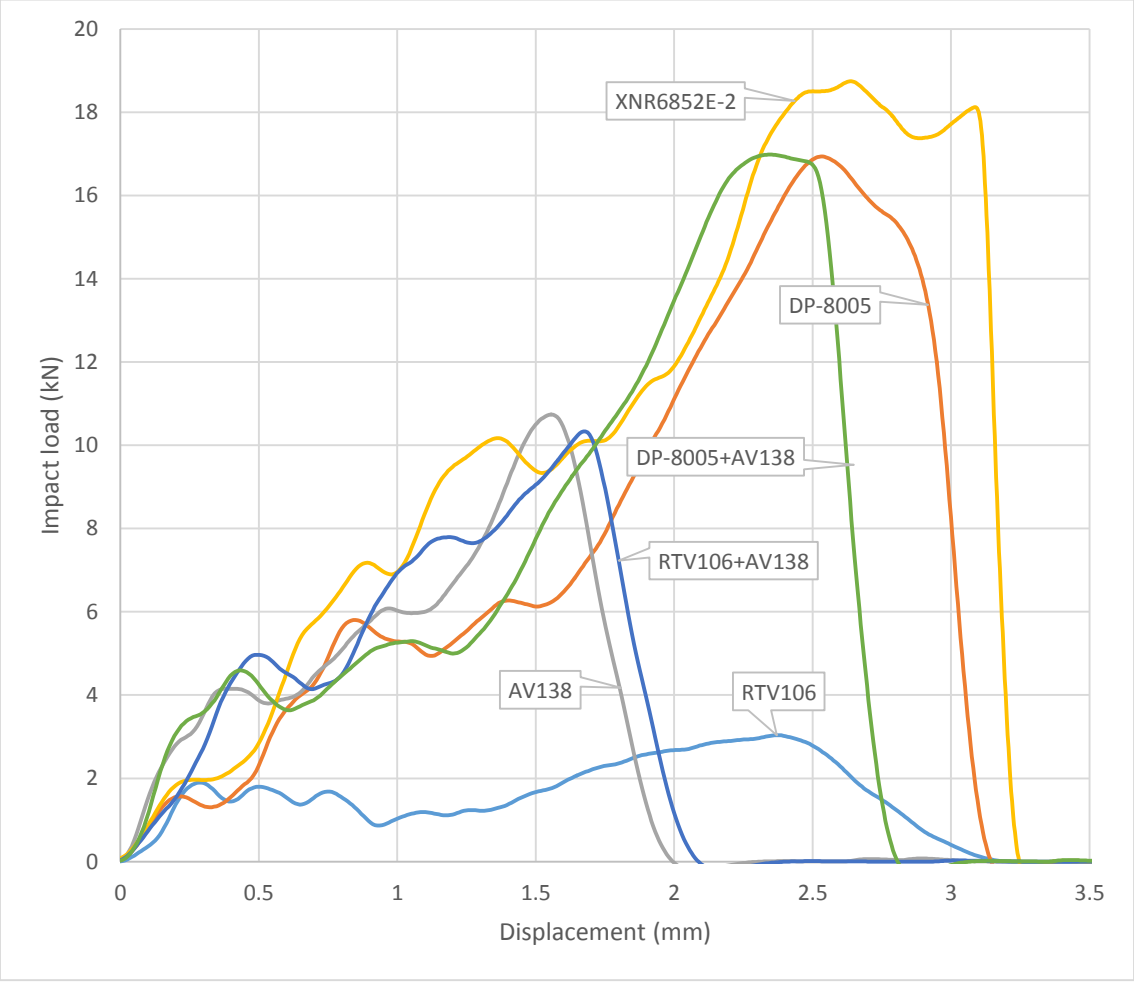

Figure 68. Typical P-Delta curves for all impact tests.

The curves of the impact tests exhibit a low displacement at failure for the configurations with AV138 due to its high stiffness, which was expected. In fact, the use of the RTV106 silicone in the same overlap allowed the joint to reveal a slightly higher displacement before

failing. The adhesives with some flexibility such as the DP-8005, RTV106 and XNR6852E-2 demonstrated the highest values for displacement.

Figure 69 represents a comparison between the average maximum loads and standard deviation obtained from the impact tests for all joint combinations tested. The typical curves of the energy absorbed by the specimens until failure is represented in Figure 70, automatically calculated by the software of the impact machine by the area bellow the P-Delta curves.

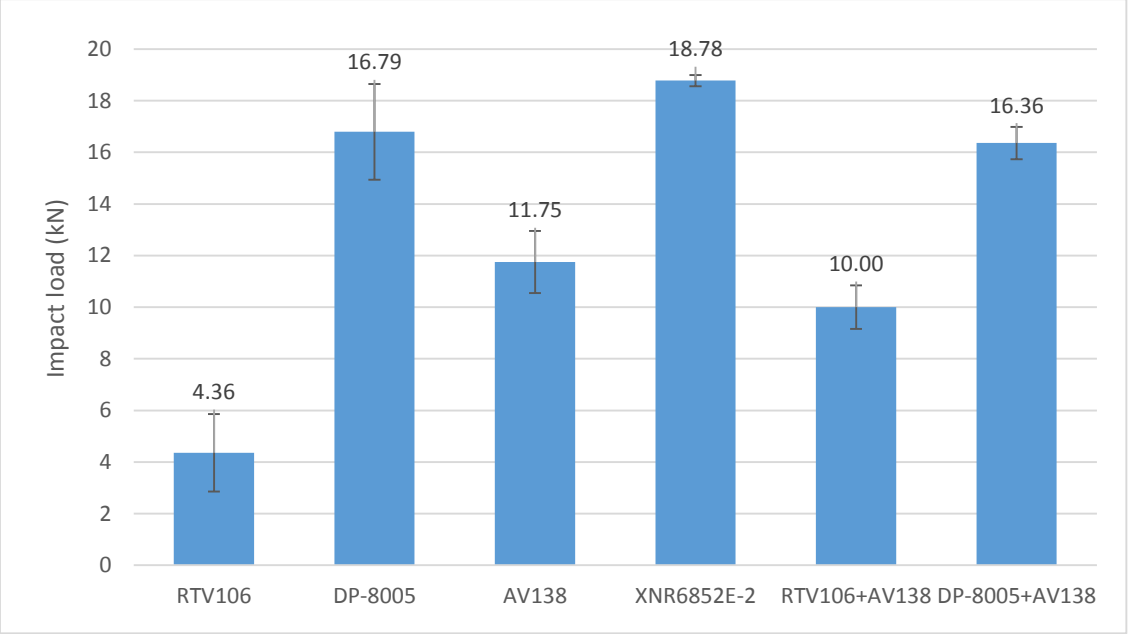

Figure 69. Average maximum load for the joint combinations tested at impact.

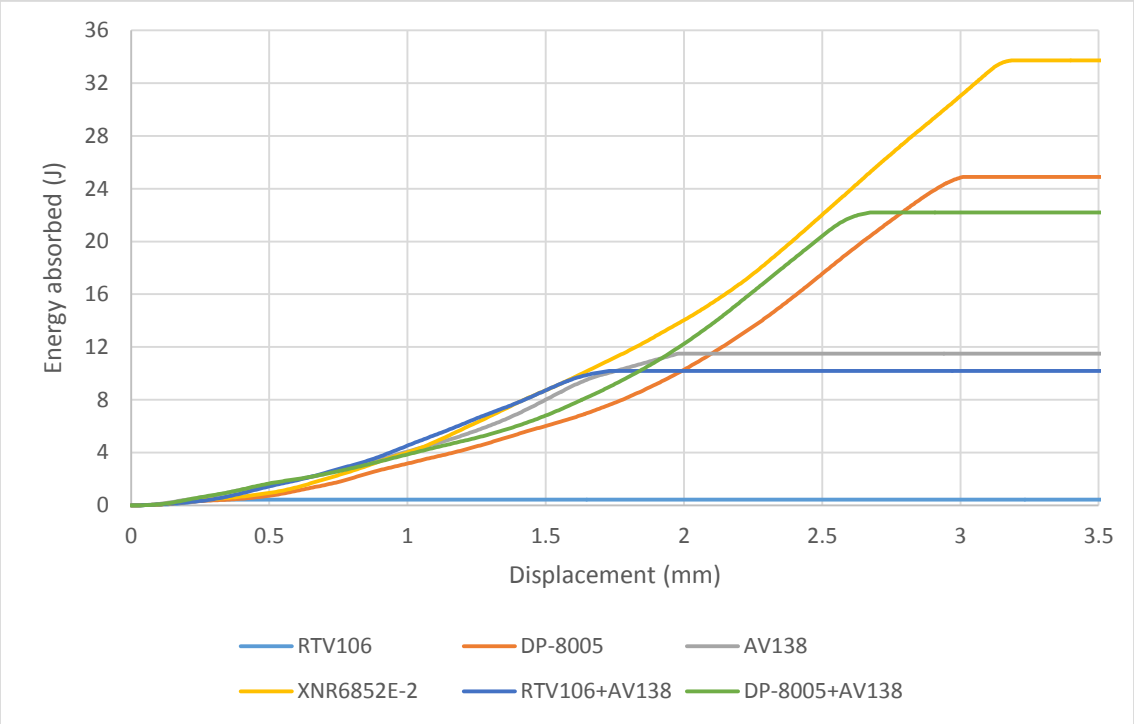

Figure 70. Typical curves of energy absorbed.

A comparison of the energy absorbed for different configurations with standard deviation is shown in Figure 71.

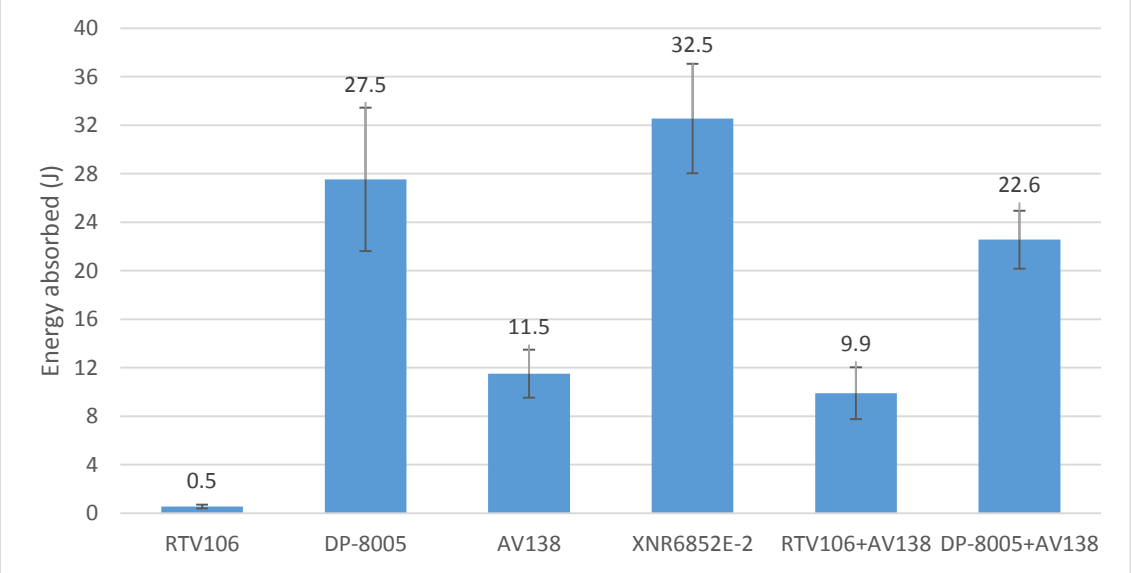

Figure 71. Comparison of the absorbed energy for the tested specimens.

Comparing the average maximum load of all of the configurations, it is clear that, apart from the configuration of only RTV106, the joints that revealed the highest values are

those containing mainly ductile adhesives or brittle ones combined with ductile adhesives in mixed adhesive layers, which is the case of the combination of DP-8005 with AV138. For RTV106, the problems of bad adhesion continued to influence the results, even at impact conditions, revealed once again the lowest maximum load and very low energy absorption. Furthermore, when combined with the stiff adhesive AV138, the joint strength was also reduced as in static tests, proving once again no improvements at impact conditions too. A very considerable strength improvement was provided by the combination of DP-8005 with AV138, where the impact strength was improved by almost 40%, which turned a very brittle joint into a good candidate for impact operations, exhibiting good behaviour and great values of energy absorption, and all of these achievements just by filling 33% of the overlap area with a ductile adhesive.

As for the XNR6852E-2, like in static tests, it once again exhibited the highest maximum load, making it a good adhesive for both conditions, without significant strain-rate dependency due to a bit of flexibility that it offers. The energy absorption was also the highest with this configuration. However, due to imposed limitations on the specimens fixing mechanism of the impact machine, this configuration was not possible to be properly tested as the fixing screws securing the specimen in place always broke at the impact moment. Given that, the previously shown results for this configuration refers to the load and energy necessary to break the screw, and not for breaking the adhesive bond. The conclusion can be drawn that at least 18 kN can be handled by the adhesive in impact conditions for a single lap joint with an overlap of 25 mm without failure and an energy of at least 32 J can be absorbed. In order to obtain an estimate of the actual failure load of this joint, three 12.5 mm overlap specimens were produced and tested under the same conditions. For this case the applied energy was able to break the smaller overlap joint, so the typical P-Delta and energy absorption curves of the tests are shown in Figure 72 and Figure 73, respectively.

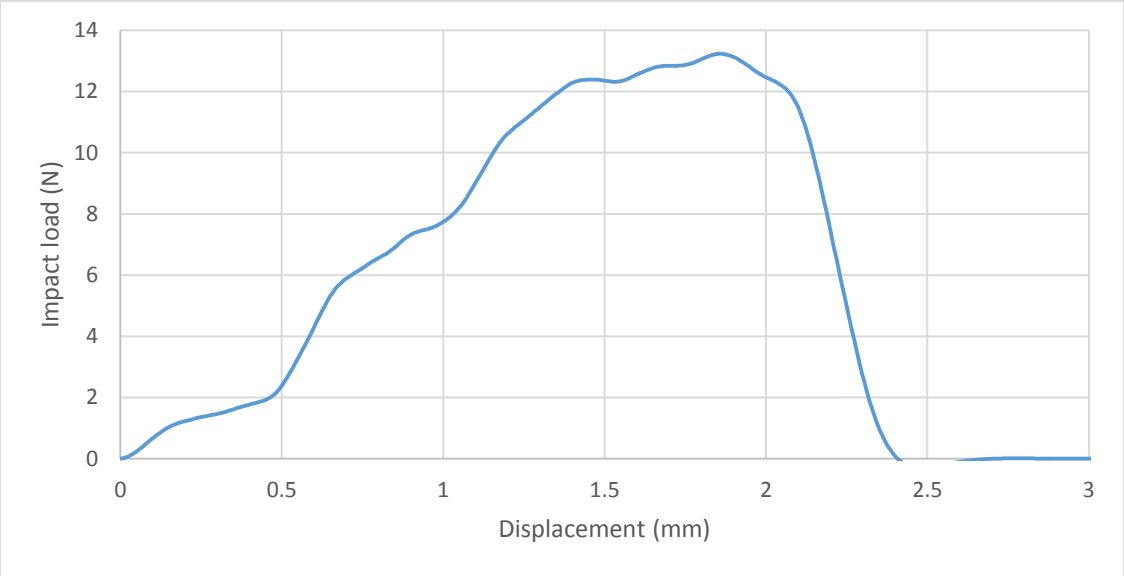

Figure 72. Typical P-Delta curve of the impact test performed to a 12.5 mm overlap XNR6852E-2 specimen.

The tested specimens exhibited an average maximum load of 14.27 kN with a standard deviation of 0.82 kN.

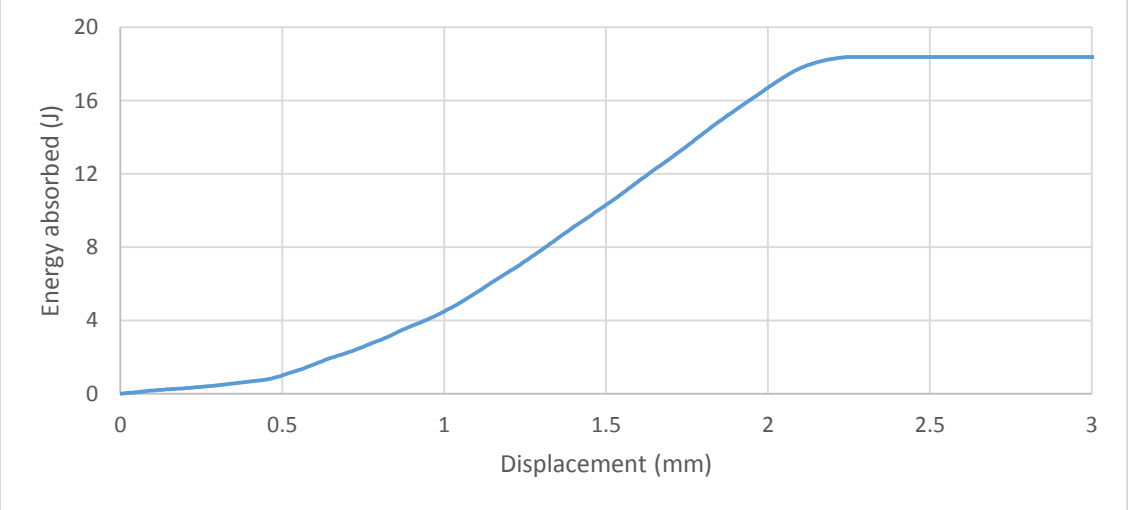

Figure 73. Typical energy absorption curve of the impact test performed to a 12.5 mm overlap XNR6852E-2 specimen.

The average energy absorption of the specimens was revealed to be 19.5 J with a standard deviation of 4.3 J.

Given this, a simple prediction of the maximum impact load for a 25 mm overlap can be done considering the overlap influence results approached in the quasi-static tests. For this purpose, a minor strain-rate dependency needs also to be considered, which cannot

be completely true, but it is only intended to represent a small comparison, so as a simple estimation it is sufficient. Thus, in quasi-static tests, by doubling the overlap from 25 mm to 50 mm, the joint strength was increased by 70% so, using the same proportionality, a joint of this kind with 25 mm overlap under impact conditions should handle around 24 kN for the maximum load and absorb an energy of 36 J.

A suitable comparison of the average maximum loads can now be made with the corrected values for the XNR6852E-2 (see Figure 74).

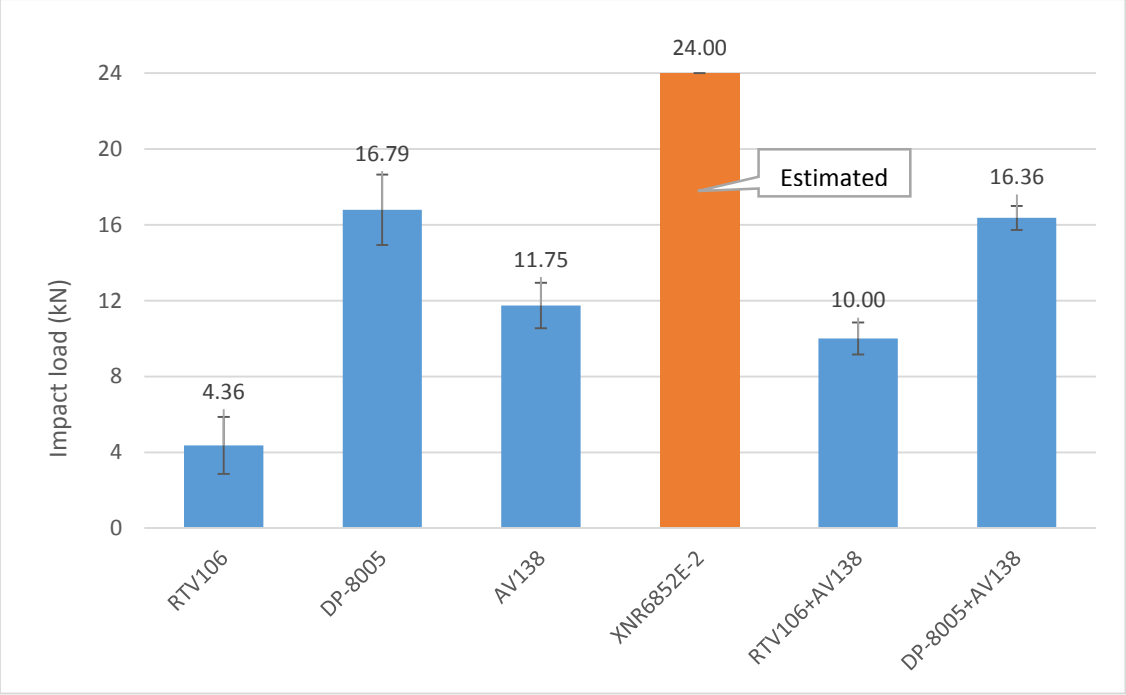

Figure 74. Average maximum load for the joint combinations tested at impact, with an estimated correction for the XNR6852E-2.

Figure 75 shows a comparison of the energy absorption in function with the average failure load, for all of the configurations tested at impact. The values for the adhesive XNR6852E-2 corresponds to the predictions explained above for the 25 mm overlap joint.

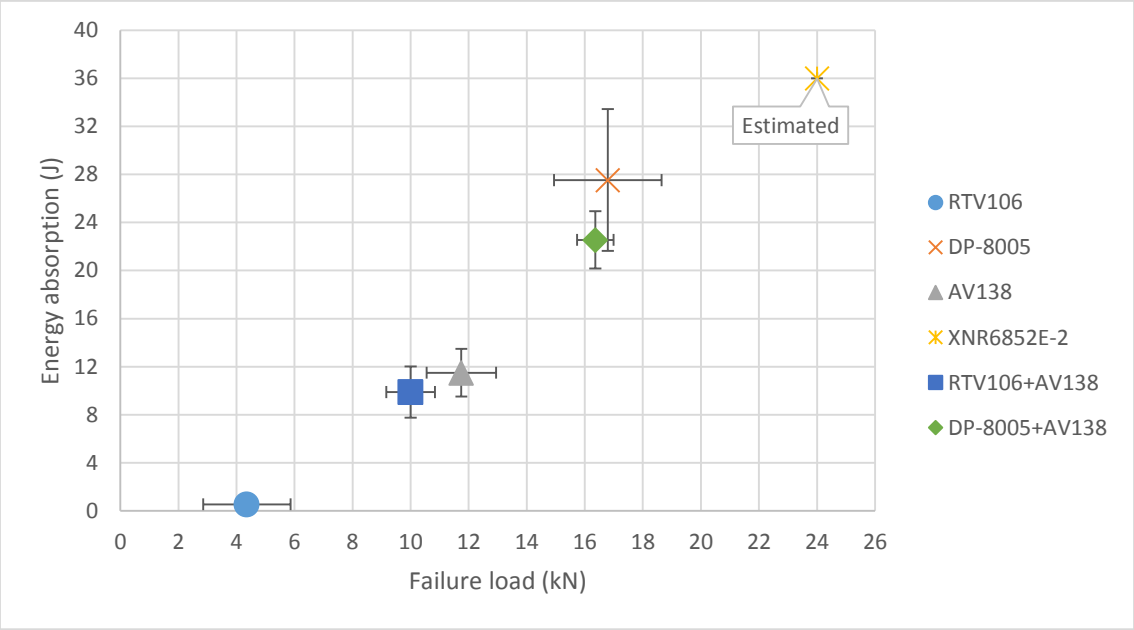

Figure 75. Energy absorption in function with the average failure load.

The same trend with the maximum impact loads exhibited by all of the combinations was noticed for the energy absorption, where the higher values were verified for higher maximum loads and the lower ones for lower maximum loads. It is verified the joint strength decline of the mixed adhesive of RTV106 with AV138, showing lower values both for energy and failure load in comparison with a joint with only AV138, but a great improvement was found by the combination of DP-8005 with AV138, showing around 100% increase in energy absorption compared to the energy absorbed by a configuration of only AV138 and placing a mainly brittle joint into a similar place of a mainly flexible joint such as the configuration of DP-8005, both for energy and strength. This proves the great improvement capabilities of the mixed adhesive technique in impact situations.

The mode of failure for all tested combinations can be observed in Figure 76.

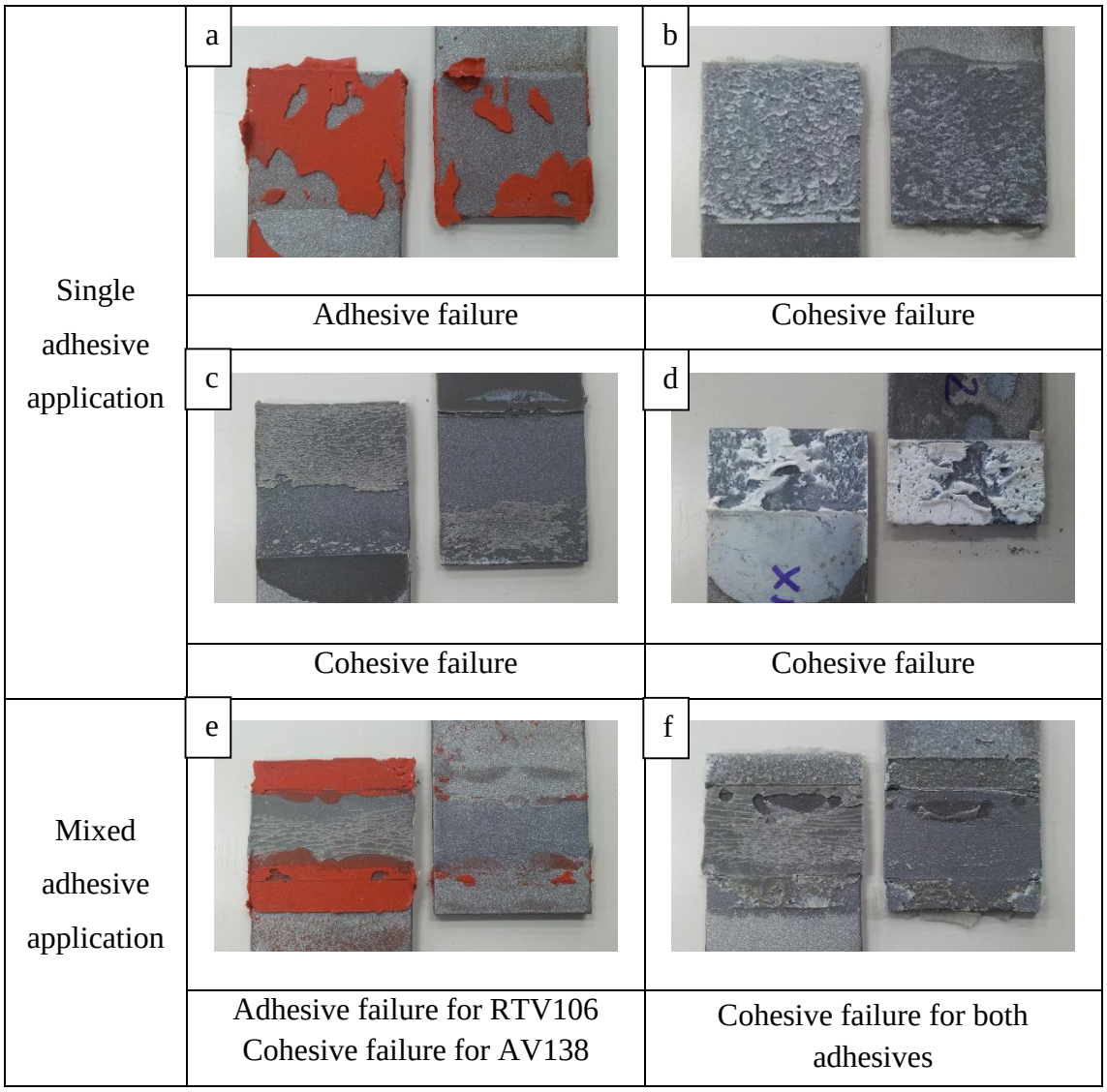

Figure 76. Failure modes for all of the tested joint configurations with high strength steel, 50 mm overlap.

For impact tests, the failure mode revealed almost no differences from the ones found in static tests. Cohesive failure was verified for joints containing AV138, DP-8005 and XNR6852E-2. For the RTV106, the same adhesion problems were found also in impact but the picture for the configuration of only RTV106 shows a greater adhesion in comparison with the failure mode from static tests. It's still a poor adhesion but the failure was sligtly better. Also, like in static conditions with high strength steel, no plastic deformation of the adherends was verified.

5.1.3 Static vs. Impact

Figure 77 shows a comparison between the average maximum load for static and impact tests for all tested configurations.

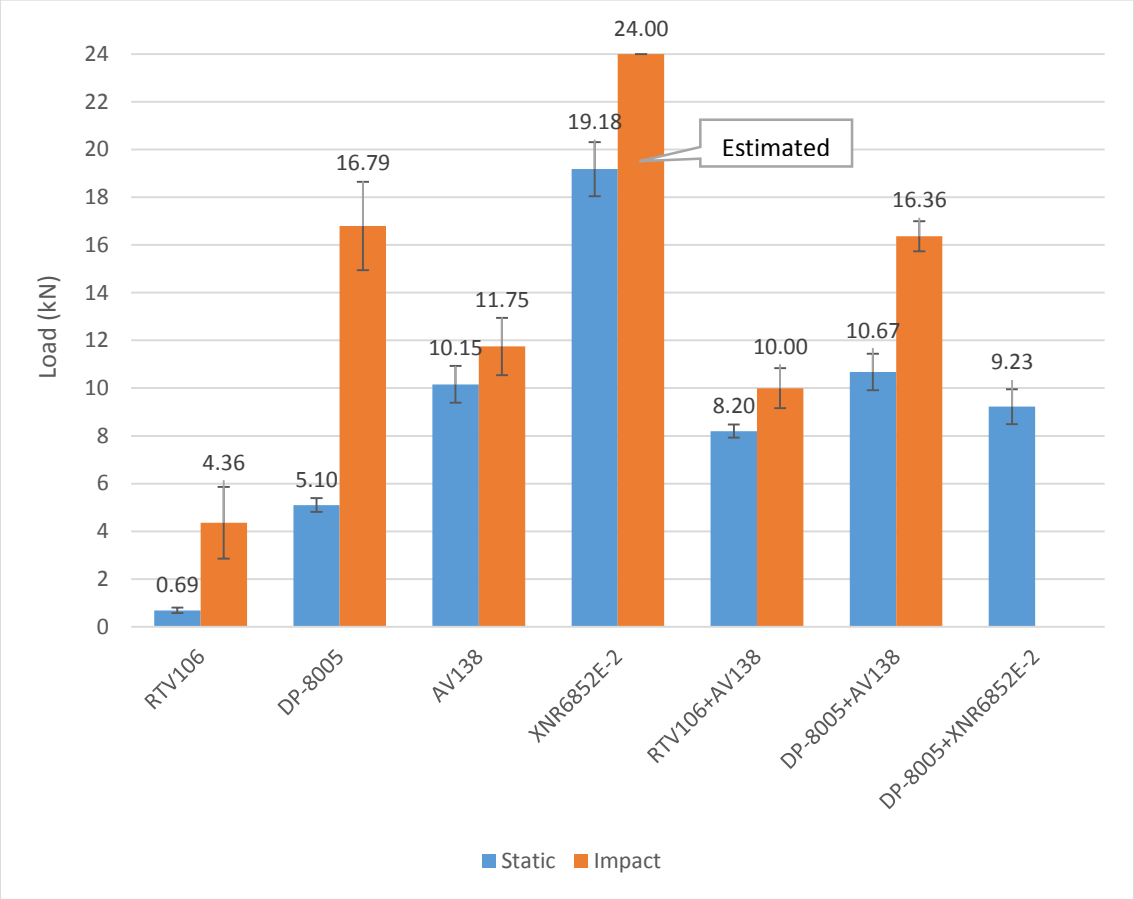

Figure 77. Average maximum load comparison between static and impact conditions.

In overall, the ductile joint configurations were the ones that exhibited greater variation between both testing conditions, proving that the flexibility of the adhesives is a good characteristic for impact conditions. In case of the RTV106, the impact load was six times higher than the load necessary to break the bond in static conditions, even with confronted adhesion problems. The adhesive DP-8005 revealed also a high strain-rate dependency due to some viscoelasticity, generating almost 17 kN in impact conditions from a joint that revealed only 5 kN in static tests for the maximum accepted load to fail and the main reason for such results was due to its high flexibility and energy absorption capabilities. In the other hand, the brittle adhesive AV138 exhibited 16% higher values than in static tests, which was expected due to its high stiffness behaviour, thus making it a poor choice

for impact operations when used alone. Still, even with the silicone applied on the same overlap, the joint didn't showed great variation compared to the static results, as the work was still mainly being done by the stiff adhesive. Even so, a small gain was evidenced when combining both adhesives, but it was very slight. However, the configuration of DP-8005 with AV138 had proved once again good results. By comparing the results from both test conditions, it is noticed that the use of the acrylic helped the joint in getting flexibility, reaching a variation in joint strength at impact of around 50% more compared to the static conditions.

Given this, although the best joint configuration for both static and impact conditions was proved to be the single application of the crash resistance adhesive XNR6852E-2, an interesting conclusion could be made relating to the mixed configuration of DP-8005 and AV138. By combining both adhesives, not only the joint strength in static conditions was improved compared to the adhesives used alone, but also an even higher improvement in joint strength of this configuration was accomplished for impact conditions. Also, within the same joint configuration and knowing that a suitable adhesive joint for a vehicle should bear good rigidity and strength for the normal operating conditions, but also resistance to impact in case of an accident to grant its integrity, this makes it a good applicant for the automotive industry. When looking at a normal adhesive joint with only one adhesive, the AV138 provides good joint strength in static conditions but poor behaviour under impact while the DP-8005 behaves in an opposite way, with good results for impact but low strength in normal conditions. By combining them together on the same joint, both joint strength and energy absorption are satisfied with good results, plus even some improvements to these could be revealed.

It can be concluded that the mixed adhesive technique has improved capabilities in joint strength for adhesive joints subject to impact loadings, especially when the technique is applied to a brittle adhesive. The flexibility of the joint is increased, resulting in better energy absorption capacity without failing, which is a fundamental characteristic for good behaviour under impact conditions.

5.2 Numerical results

5.2.1 Static tensile test results

Figure 78 shows a comparison of the numerical results with the experimental for the maximum failure load. In overall, the numerical model exhibited higher results compared to the experimental. The deviation can be justified by the mechanical properties applied to the model and also by manufacture problems of the experimental specimens, which can comprehend defects that causes strength degradation of the joints. Apart from the XNR6852E-2 adhesive that was very hard to simulate, the model seems to be adequate for validation of the experimental failure loads for some adhesive configurations, considering the justifications given above. However, for the other configurations the model was not sufficiently accurate to predict the failure load, as it is explained in the resulting curves shown below.

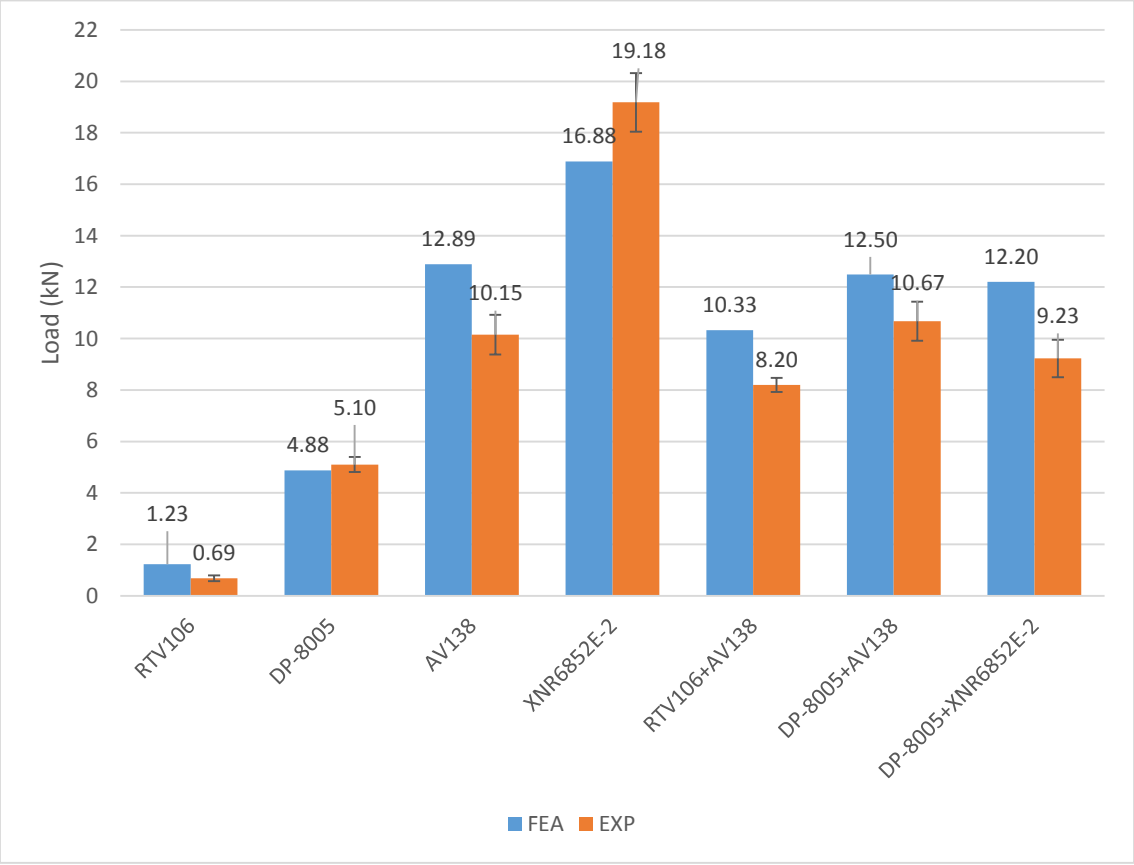

Figure 78. Maximum failure load results comparison between numerical and experimental.

Figures 79 to 85 represent the load displacement curves for the specimens in study for both experimental and numerical simulations.

For RTV106 (Figure 79), the numerical model exhibited an higher deviation from the experimental results, but this can be justified by the adhesion problems that were encountered and already discussed, so no proper comparison can be made for this model. The adhesive stiffness properties seems to be adequate, with a slope in the elastic zone very similar to the experimental one.

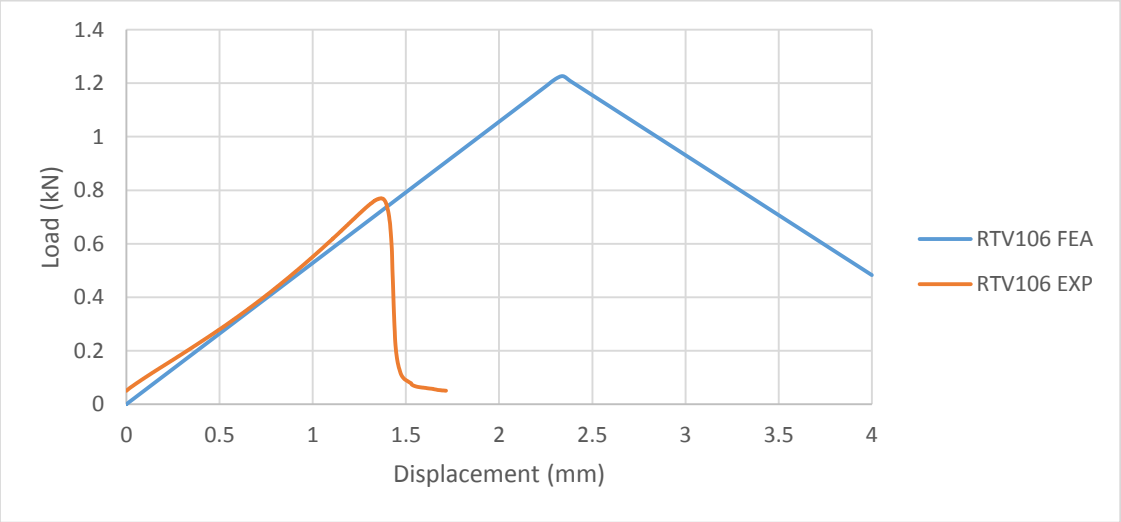

Figure 79. Numerical and experimental P-delta curves for RTV106.

The model with DP-8005 (Figure 80) exhibited good prediction for the maximum failure load, however, the stiffness of the adhesive didn't correspond to the experimental results. This variation can be mainly justified by the rigidity of the testing machine as no extensometer was used to measure the displacement of the joint during the test. Also, as this adhesive is very ductile, the triangular cohesive law was not especially adequate and resulted in a different behaviour of the curve. A trapezoidal cohesive law would be more adequate to simulate this ductile adhesive and could result in a behaviour closer to the experimental results. Still, an adequate strength prediction can be made.

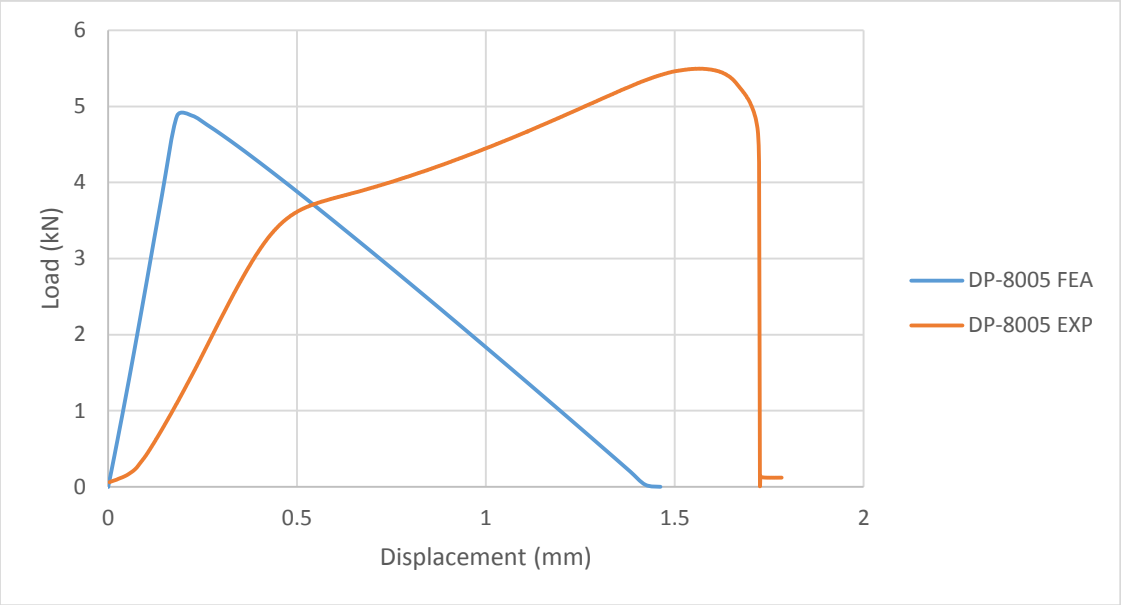

Figure 80. Numerical and experimental P-delta curves for DP-8005.

The resulting curve for the model with AV138 (Figure 81) exhibited also the wrong slope for the stiffness due to the testing machine characteristics, but the maximum predicted load seems to be adequate, with only a small deviation. The triangular cohesive law suited very well this brittle adhesive, with a very similar behaviour of both curves.

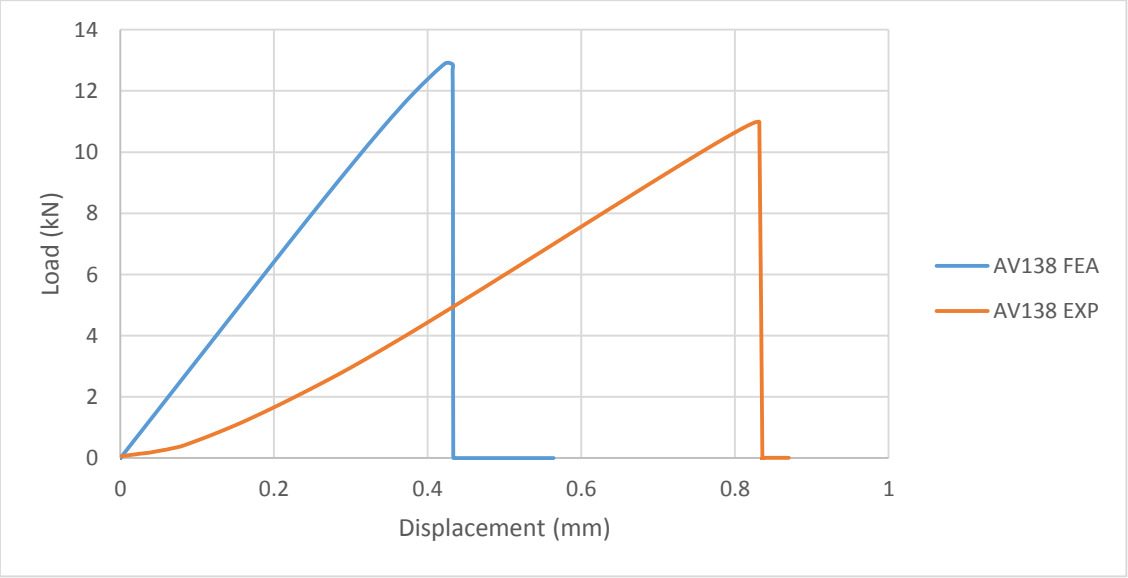

Figure 81. Numerical and experimental P-delta curves for AV138.

The numerical model for the XNR6852E-2 adhesive (Figure 82) didn't exhibit acceptable results, revealing lower mechanical properties than the ones found in experimental results. Despite the determination of the adhesive properties at high strain rates with different tests, these properties didn't provide an accurate prediction for the failure load. Given this, the joint behaviour was very hard to simulate dynamically so an accurate prediction cannot be done with this model.

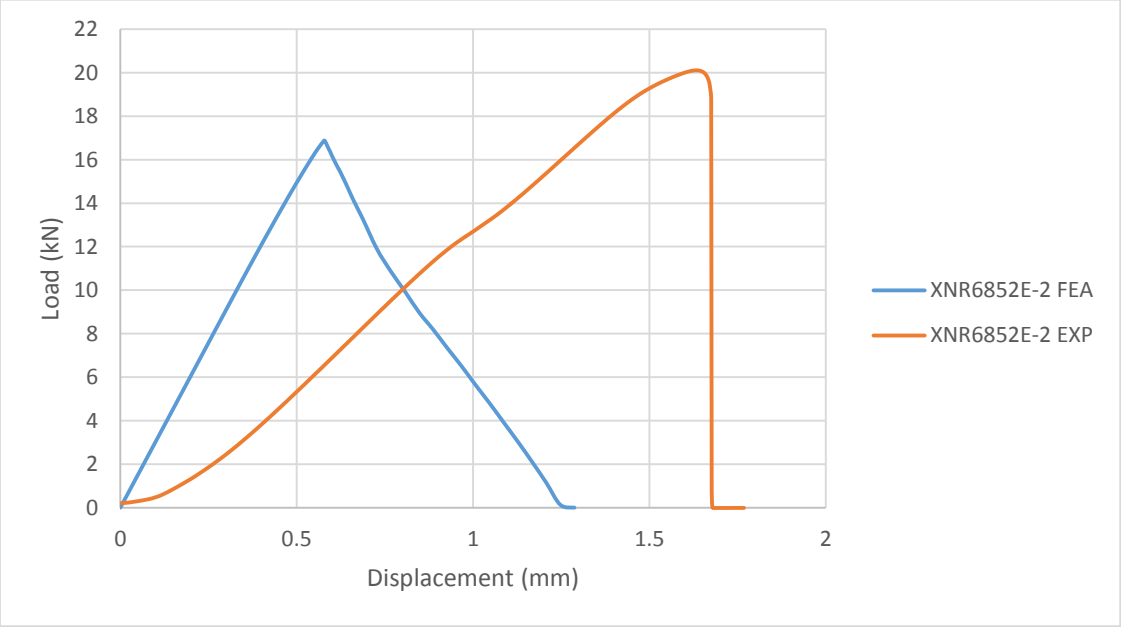

Figure 82. Numerical and experimental P-delta curves for XNR6852E-2.

The failure load prediction for the model of RTV106 with AV138 (Figure 83) exhibited lower joint strength compared to the model with only AV138, proving the same conclusions obtained in experimental tests. For this case, it is again noticed the variation slope of the curves in elastic zone due to the testing machine. The failure load prediction shows a small deviation but adhesion problems were encountered in the experimental specimens, so this model cannot be fully comparable in order to validate the results.

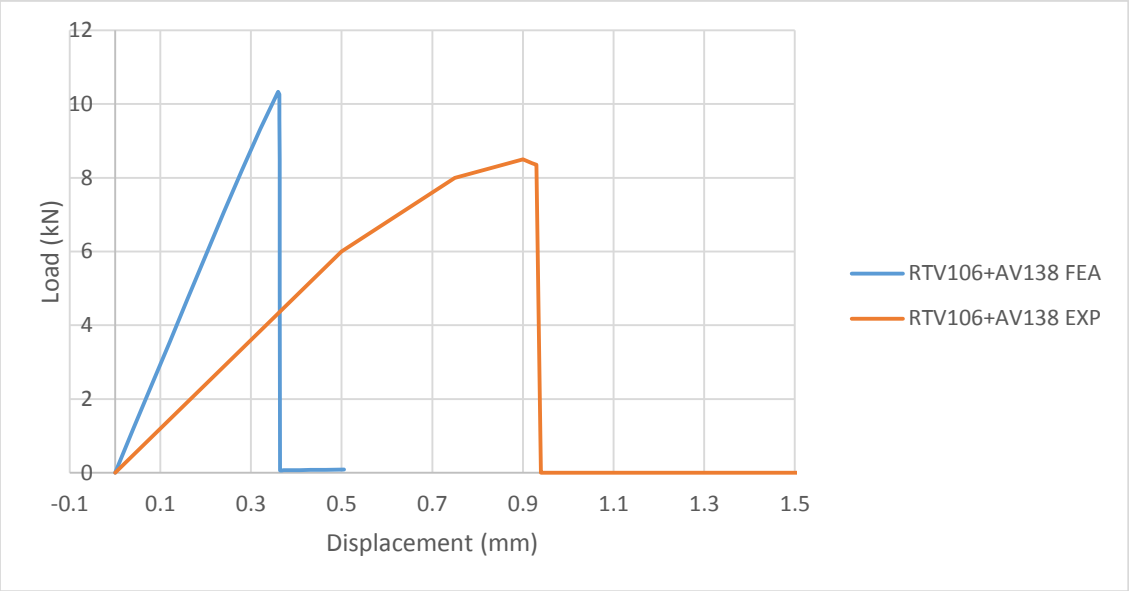

Figure 83. Numerical and experimental P-delta curves for RTV106+AV138.

Apart from the slope variation that were also found in this case, the model of the mixed adhesive joint containing DP-8005 and AV138 (Figure 84) exhibited a good prediction of the failure load, showing results similar to the experimental curve. However, the prediction failure load was very similar to the model with only AV138, which reveals no improvement in joint strength when using this combination. Compared to the experimental results, it is concluded that this model could not provide very accurate predictions. According to experimental results, joint strength improvement was expected and was not obtained.

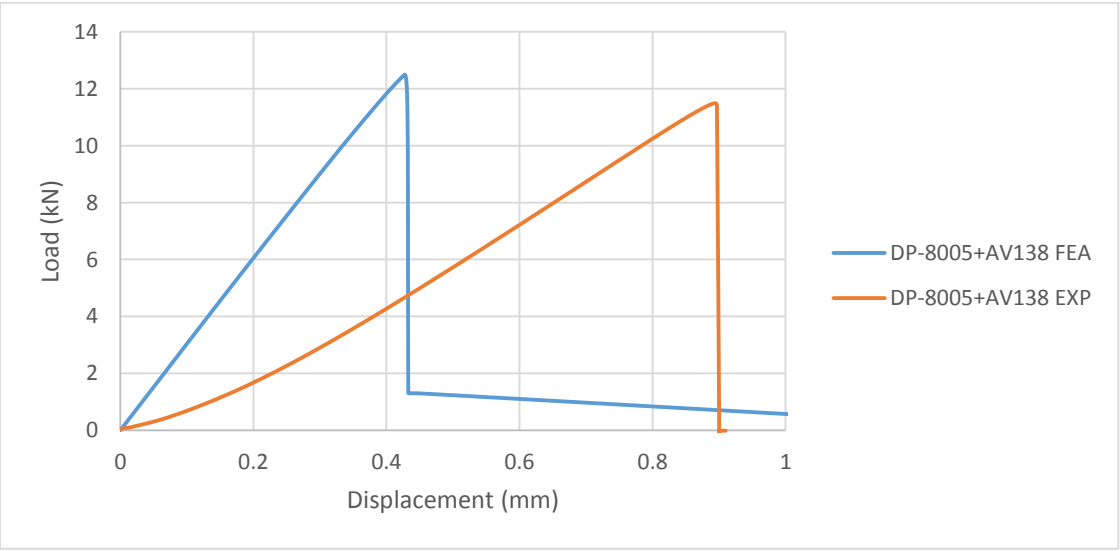

Figure 84. Numerical and experimental P-delta curves for DP-8005+AV138.

The mixed adhesive configuration model of DP-8005 with XNR6852E-2 (Figure 85) exhibited a very different behaviour from the experimental curves but, as manufacturing and testing problems were found with this combination, a proper validation of the results could not be done. Still, as expected, the prediction of the maximum failure load is higher than the experimental values but lower than the single application of the XNR6852E-2 adhesive, so it can be concluded that the combination of these two adhesives in this configurations for static conditions has small interest as it results in degradation of the joint strength.

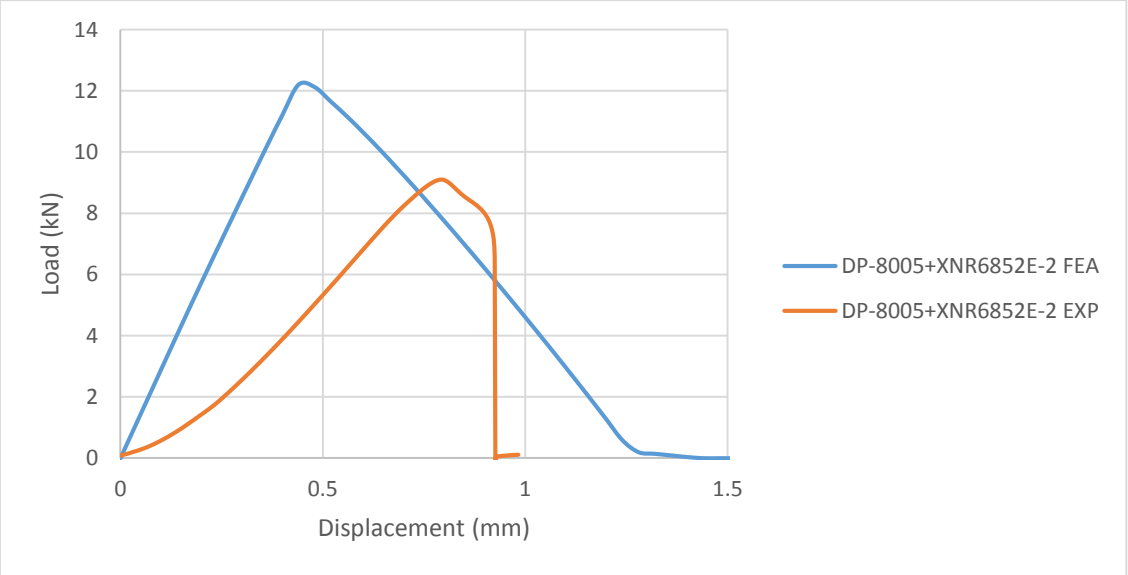

Figure 85. Numerical and experimental P-delta curves for DP-8005+XNR6852E-2.

5.2.2 Impact test results

Figure 86 shows a comparison of the numerical results with the experimental for the maximum impact load. In this case, the overall behaviour for the numerical model exhibited again higher results compared to the experimental. The deviation can also be justified by the mechanical properties applied to the model and by manufacture problems of the experimental specimens, which can comprehend defects that causes strength degradation of the joints. The dynamic effects of the impact testing machine can also be an important factor to justify the variation in the numerical results as it is very difficult to simulate with good precision all of the intrinsic variables and conditions of the experimental tests. In addition, the fracture energy properties were considered to be not variable with the strain rate. If a reduction of these properties was considered in the dynamic models, the maximum failure load would be almost certainly lower. However, there was not sufficient time to perform experimental measurements for the characterization of the fracture properties under high strain rates, so some differences are to be expected between experimental and numerical dynamic tests.

While the RTV106 adhesive specimens were simulated with non-strain dependent data and this caused large discrepancies between experimental and numerical data, the models seems to be adequate for the validation of the experimental failure loads for some adhesive configurations such as DP-8005, AV138 and RTV106+AV138. For the rest of the combinations, the deviation was more significant, resulting in less accurate failure load predictions. Still, taking in consideration the extrinsic error factors, a prediction can be made with the numerical models.

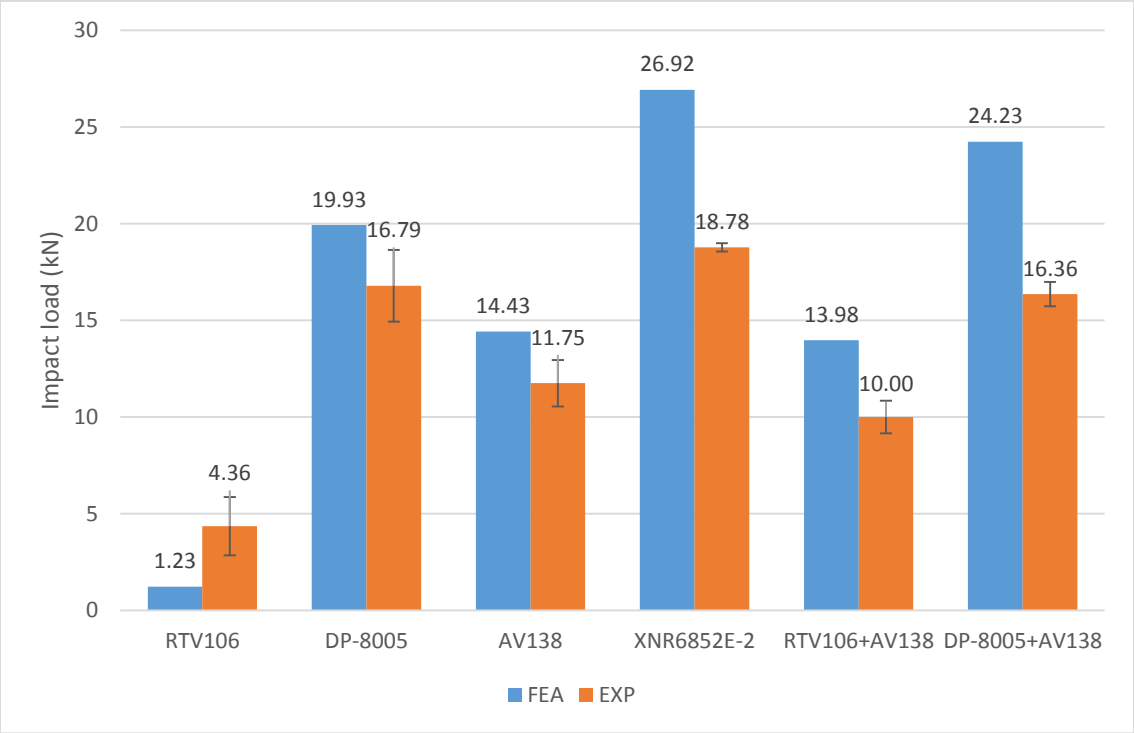

Figure 86. Maximum impact failure load results comparison between numerical and experimental.

Figures 87 to 92 represent the impact load and displacement curves for the specimens in study for both experimental and numerical simulations. A cut-off frequency of 10000 Hz was applied to soften the curves to allow a clear comparison with all of them. As the simulated displacement of the numerical model was not the same of the displacement exhibited from the impact machine, all of the numerical P-delta curves exhibit a significant variation of the displacement compared to the experimental curves. The main objective for these comparisons relies on the validation of the maximum impact failure load and a comparison between displacements has no interest.

For the model with the DP-8005 adhesive (Figure 87) the prediction failure load was in good agreement with experimental results. The deviation encountered can be justified by an overestimation of the adhesive properties obtained by the extrapolation function previously explained in numerical simulation procedure chapter. In addition, manufacturing problems can explain the variation in the maximum failure load, as this adhesive was one of the adhesives whose curing procedure is not easily controlled.

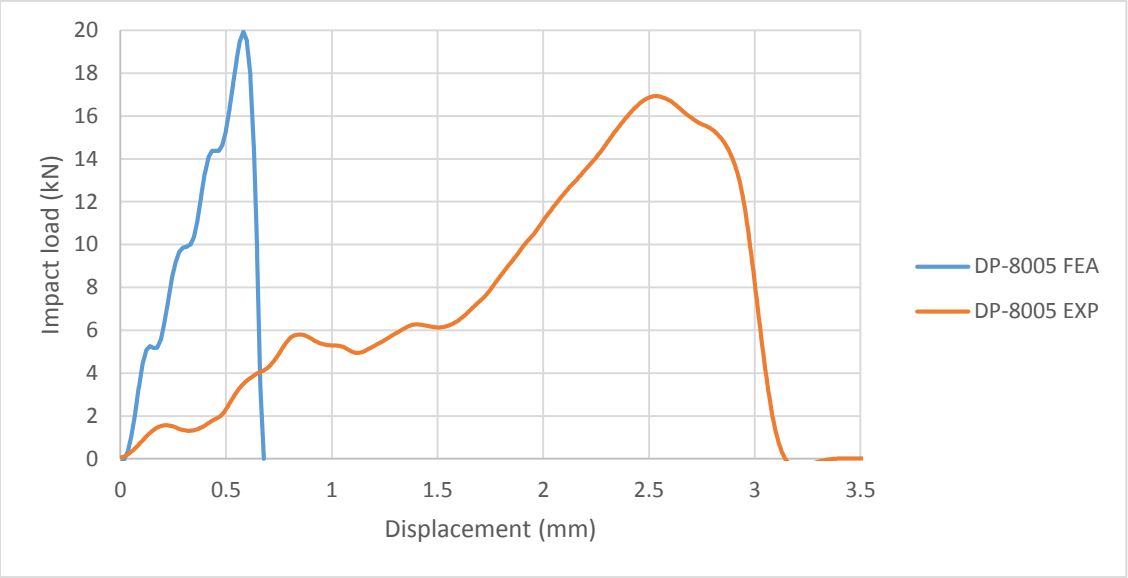

Figure 87. Numerical and experimental P-delta curves with impact conditions for DP-8005.

The numerical model with AV138 (Figure 88) exhibited similar justifications from the previous model, with failure load prediction close enough for this purpose. Manufacturing problems and joint defects can again be the main cause for the observed deviation.

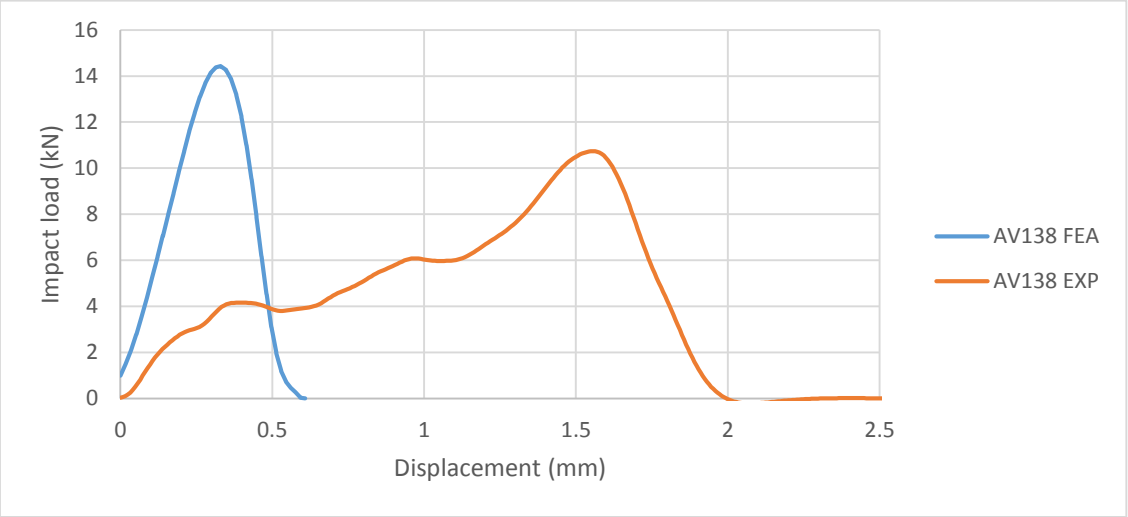

Figure 88. Numerical and experimental P-delta curves with impact conditions for AV138.

For the model with RTV106 (Figure 89), the joint behave significantly different from the experimental results as expected. Non-strain dependency of the adhesive for the simulation purpose due to the lack of characterization properties at high strain rate was considered. As adhesion problems were found in all experimental tests, limited consideration was given to this model because it would not be possible to make an

acceptable validation of the experimental results, even with the correct properties applied to the model. Additionally, the problem of the cohesive law shape persists, with the triangular law being insufficient to correctly model this extremely flexible adhesive. Still, for reference purposes, the curves are shown to analyse the behaviour of the model.

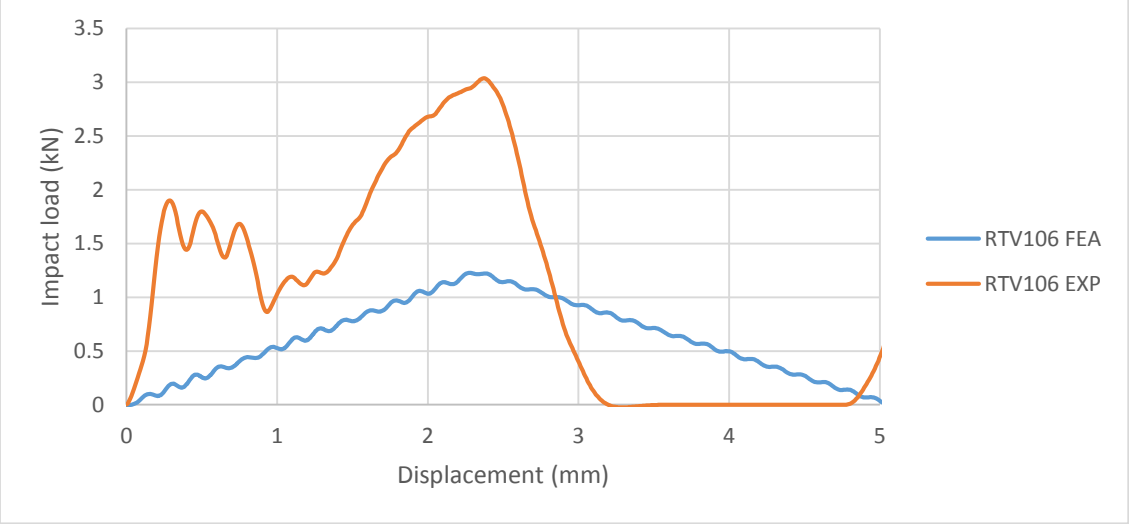

Figure 89. Numerical and experimental P-delta curves with impact conditions for RTV106.

The model with XNR6852E-2 (Figure 90) exhibited a significant deviation in the failure load, which results in less accurate load predictions. A justification for the higher deviation could be due to the overestimation of the values obtained from the extrapolation criteria. Similar to the static simulation, the adhesive was very hard to simulate and the error was more significant on the impact model.

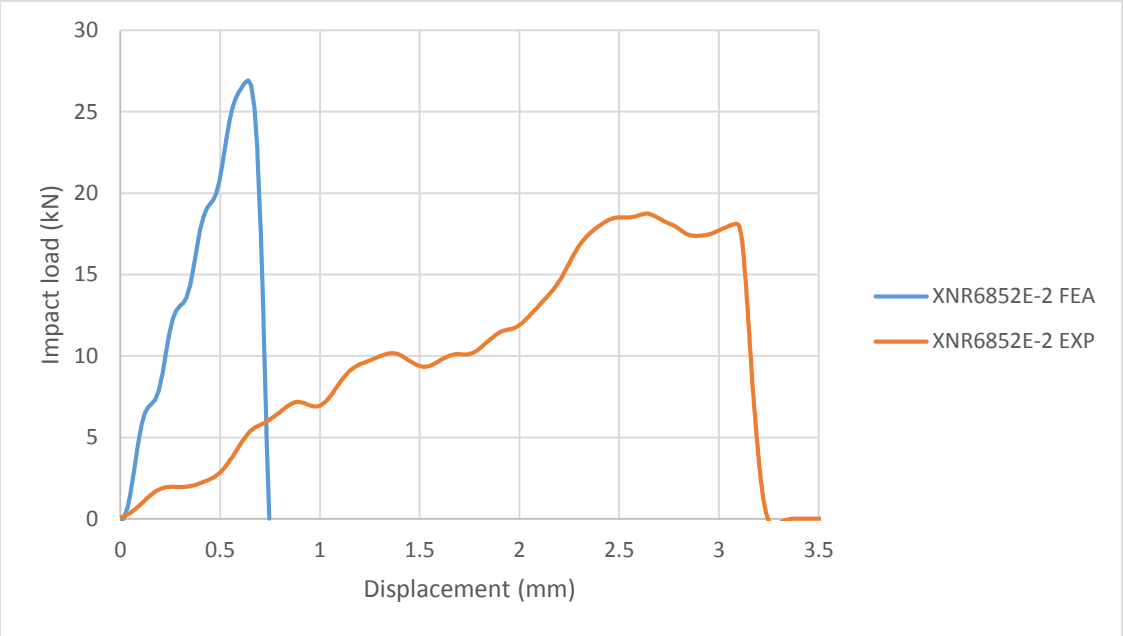

Figure 90. Numerical and experimental P-delta curves with impact conditions for XNR6852E-2.

For the mixed adhesive model with RTV106 and AV138 (Figure 91), the simulation results revealed a small decrease in joint strength which is in agreement with the same conclusion found in experimental results. As adhesion problems were found in experimental tests for the RTV106 adhesive, the deviation found for the maximum failure load could be a result of this, along with possible manufacture problems regarding the separation of the adhesives.

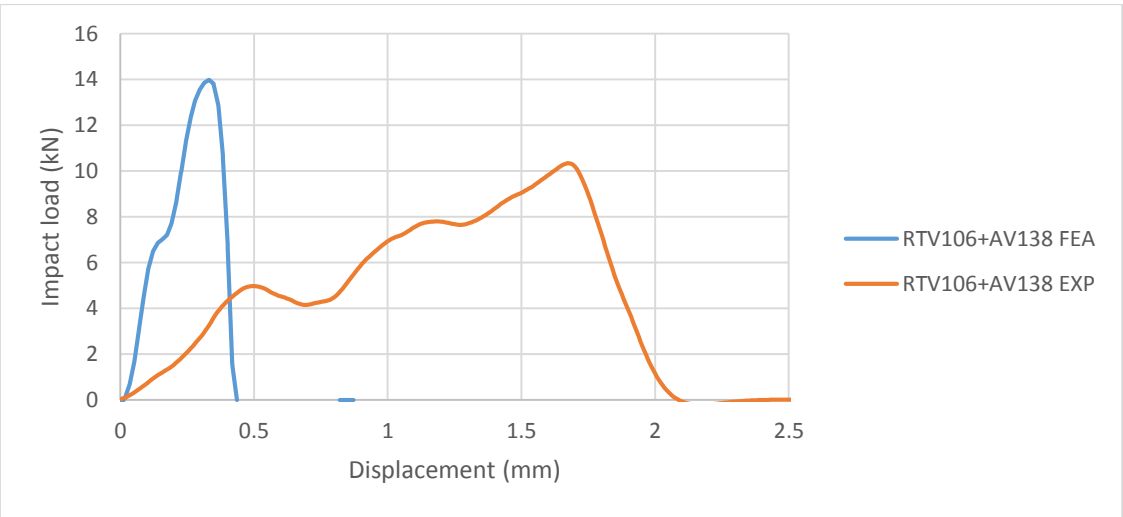

Figure 91. Numerical and experimental P-delta curves with impact conditions for RTV106+AV138.

Lastly, the model with DP-8005 and AV138 (Figure 92) exhibited also a significant deviation for the maximum failure load. The results revealed a joint strength increase by combining the adhesive DP-8005 with AV138, which validates the same conclusion found in experimental tests but also revealed a higher maximum load compared to the application of only DP-8005, something which was not verified in the experimental part. The mechanical properties applied for this mixed adhesive model may not be well determined and thus resulting in higher relative errors. Otherwise, the manufacture quality of the mixed adhesive joint specimen may not be as good as believed and a higher improvement of the combination of these adhesives could be expected. Due to this reasons, this model cannot be used to validate the experimental results with acceptable accuracy.

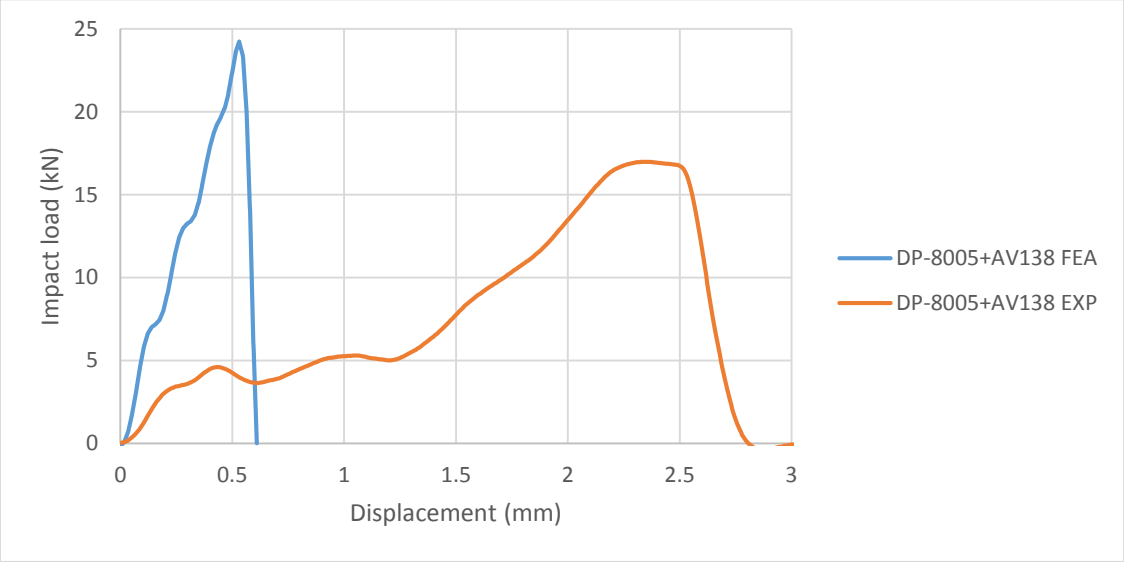

Figure 92. Numerical and experimental P-delta curves with impact conditions for DP-8005+AV138.

6. Conclusions

In this chapter the conclusions obtained during the course of this work are summarized, showing the highlights of this investigation. The main conclusions are:

- A new experimental technique was developed to manufacture single lap joints with mixed adhesive layers with a minimum amount of defects.
- The effectivity of the mixed adhesive technique increases with the use of longer overlaps, especially when a ductile adhesive is combined with a very stiff one. The technique results better in higher overlaps as the improvement of joint strength is more evident. Also, the application of a ductile adhesive along with a brittle one reduced the plastic deformation of mild steel substrates, resulting in an overall less influence of the adherends.
- Adhesion problems have been found using the adhesive RTV106 with steel as the substrate, so no improvements could be verified when applying RTV106 in mixed adhesive joints.
- Problems arose when applying high temperatures to DP-8005, causing it to start to deteriorate and burn. The maximum handling temperature for this adhesive was found to be around 110ºC.
- The overlap region of the configuration with DP-8005 and XNR6852E-2 showed a failure mode with bad adhesion and adhesive degradation. The adhesive layer became powdery and crumbled to pieces, rendering this configuration useless.
- The use of a ductile adhesive at the ends of the overlap combined with a brittle adhesive such as the combination of DP-8005 and AV138, improves the maximum strength of the joints. Not only was the maximum strength improved but also the extension at failure.
- The mixed configuration of DP-8005 and AV138 not only improved the joint strength in static conditions compared to the adhesives used alone, but also an even higher improvement in joint strength of this configuration was obtained for impact conditions. Although the maximum impact load was higher using DP-8005 alone than combined with AV138, the mixed adhesive combination revealed a close failure load and showed a 100% increase in energy absorption compared to the energy absorbed by a configuration of only AV138, proving the great

improvement capabilities of the mixed adhesive technique in impact situations, especially when it is applied with brittle adhesives.

- The use of mild steel adherends with AV138 resulted in 42% joint strength decline compared to the use of high strength steel adherends, mainly because of the significant concentration of peel stresses. Likewise, the maximum joint strength of the XNR6852E-2 had improved by around 100% for the same comparison, showing high influence of the adherends.
- The joint configurations with ductile adhesives were the ones that exhibited greater variation between static and impact testing conditions, reinforcing the idea that the flexibility of the adhesives is a good characteristic for impact conditions.
- The adhesive DP-8005 revealed an unexpected high strain-rate dependency, generating almost 17 kN in impact conditions from a joint that revealed only 5 kN in static tests for the maximum accepted load to fail.
- The best joint configuration for both static and impact conditions was proved to be the single application of the crash resistance adhesive XNR6852E-2.
- The mixed adhesive technique has improving capabilities in joint strength for adhesive joints subject to impact loadings, especially when the technique is applied to a brittle adhesive. The flexibility of the joint is increased, resulting in better energy absorption capacity, which is a fundamental characteristic for good behaviour under impact conditions.
- Two dimensional finite element models were created for all the joints experimentally tested in this work. These models considered static and dynamic conditions and made use of cohesive element modelling to simulate the failure process.
- There was generally a good agreement between the experimental and the numerically predicted failure load for the static finite element models. There was however a large discrepancy in stiffness, mainly due to the fact that the experimental displacement was obtained from crosshead displacement and not from an extensometer. Additionally, the flexible adhesives couldn´t be correctly modelled using the triangular traction separation laws.
- To enable the creation of the dynamic models, the strain rate dependence of the AV138 and DP-8005 adhesive was studied by doing tensile tests at two different

tests speeds and extrapolating those results to impact speed. Significant strain rate dependence was found for both adhesives studied.

- The experimental and numerical results for the dynamical tests had generally a good agreement in failure load. However, the difference in values between the experimental and numerical tests was higher than the difference found for the static cases. This can be explained by errors in the process of extrapolating the mechanical properties under impact. The stiffness and maximum displacement was also very different between the experimental and numerical cases, because it is difficult to accurately simulate the testing conditions under impact.

7. Future works

Due to the wide range of possibilities available to study the influence of the mixed adhesive technique in impact conditions, some ideas are listed here to improve the results obtained and allow to draw more conclusions:

- Perform the same tests with variations of temperature and humidity to investigate the influence of these parameters on the technique.
- Explore a way to increase the joint strength of the XNR6852E-2 with the mixed adhesive technique, to obtain an even better joint.
- Analyse the technique with composites such as carbon fibre.
- Improve the dynamical finite element model in order to obtain better agreement between experimental and numerical behaviour.
- Perform a numerical finite element analysis for optimization of the technique.
- Perform impact tests on different type impact machines to compare the results.
- Try to optimize the fixing tool of the drop-weight impact machine currently present in the laboratory to bear with higher loads without creating load concentrations in the screws.
- Test a new technique combining more than two adhesives on the same overlap, consisting in one stiff, one ductile and one with intermediate properties.
- Test and compare the technique of graded adhesive joints.

References

[1] Green V., Obtained from Via Green - Sustainable Logistics: http://www.viagreen.com.br/ecofreight_sustentabilidade.php (2013)

[2] da Silva L.F.M., Öchsner A., Adams R.D.: Handbook of Adhesion Technology, 1st ed., Springer, Berlin (2011)

[3] da Silva, L.F.M., das Neves, P.J.C., Adams, R.D., Spelt, J. K.: Analytical models of adhesively bonded joints-Part I: Literature survey. Int J Adhes Adhes; 29(3): 319-330 (2009)

[4] Adams R.D., Comyn J., and Wake W.C.: Structural adhesive joints in engineering, 2nd ed. London: Chapman & Hall (1997)

[5] Karachalios E.F., Adams R.D., da Silva L.F.M.: Single lap joints loaded in tension with ductile steel adherends. Int J Adhes Adhes; 43: 96–108 (2013)

[6] Grant L.D.R., Adams R.D. da Silva L.F.M.: Experimental and numerical analisys of single-lap joints for the automotive industry. Int J Adhes Adhes; 29(4): 405-413 (2009)

[7] da Silva L.F.M., das Neves P.J.C., Adams R.D., Wang A., Spelt J.K.: Analytical models of adhesively bonded joints—Part II: Comparative study. Int J Adhes Adhes; 29(3): 331-341 (2009)

[8] da Silva L.F.M., Pirondi A., Öchsner A.: Hybrid Adhesive Joints, Springer, Berlin (2011)

[9] Breto R., Chiminelli A., Duvivier E., Lizaranzu M., Jiménez M.A.: Functionally graded bond-lines for metal/composite joints. European Conference on Composite Materials, Seville, Spain (2014)

[10] Raphael C.: Variable adhesive bonded joints. App Polym Symp; 3: 99-108 (1966)

[11] Hart-Smith L.J.: Adhesive-Bonded Double Lap Joints, Nasa Contract Report, CR-112235 (1973)

[12] Fitton M.D., Broughton J.G.: Variable modulus adhesives: an approach to optimized joint performance. Int J Adhes Adhes; 25(4): 329-336 (2005)

[13] da Silva L.F.M., Adams R.D.: Adhesive joints at high and low temperatures using similar and dissimilar adherends and dual adhesives. Int J Adhes Adhes; 27(3): 216-226 (2007)

[14] da Silva L.F.M., Lopes M.J.C.Q.: Joint strength optimization by the mixed adhesive technique. Int J Adhes Adhes; 29(5): 509-514 (2009)

[15] Fitton M.D.: Multi-modulus adhesive bonding of advanced composite materials, Ph.D. Thesis, Oxford Brookles University, UK (2004)

[16] Gordon T.L., Fakley M.E.: The influence of elastic modulus on adhesion to thermoplastics and thermoset materials. Int J Adhes Adhes; 23(2): 95-100 (2003)

[17] Srinivas S.: Analysis of bonded joints, NASA TN D-7855 (1975)

[18] Pires I., Quintino L., Durodola J.F., Beevers A.: Performance of bi-adhesive bonded aluminium lap joints. Int J Adhes Adhes; 23(3): 215-223 (2003)

[19] Marques E.A.S., da Silva L.F.M.: Joint strength optimization of adhesively bonded patches. J Adhesion; 84(11): 915-934 (2008)

[20] Zgoul M., Crocombe A.D.: Numerical modelling of lap joints bonded with a rate-dependent adhesive. Int J Adhes Adhes; 24(4): 355-366 (2004)
[21] Adams R.D.: Adhesive Bonding, Science, Technology and Applications. Woodhead Publishing Limited, Cambridge England (2005)
[22] Saldanha D.F.S., Canto C.M.S., da Silva L.F.M., Carbas R.J.C., Chaves F.J.P., Nomura K., Ueda T.: Mechanical characterization of a high elongation and high toughness epoxy adhesive. Int J Adhes Adhes; 47: 91–98 (2013)
[23] Adams R.D., Harris J.A.: An assessment of the impact performance of bonded joints for use in high energy absorbing structures. J Mech Eng Sci; 199(2): 121-131 (1985)
[24] Goglio L., Rossetto M.: Impact rupture of structural adhesive joints under different stress combinations. Int J Impact Eng; 35(7): 635-643 (2008)
[25] Kadioglu F., Adams R.D.: Flexible adhesives for automotive application under impact loading. Int J Adhes Adhes; 56: 73-78 (2015)
[26] Bezemer A.A., Guyt C.B., Vlot A.: New impact specimen for adhesives: optimization of high-speed-loaded adhesive joints. Int J Adhes Adhes; 18(4): 255-260 (1998)
[27] Avalle M., Peroni L., Peroni M., Scattina A.: Bi-material joining for car body structures: experimental and numerical analysis. J Adhesion; 86(5-6): 539-560 (2010)
[28] da Silva L.F.M., Öchsner A.: Modeling of Adhesive Bonded Joints. Springer, Berlin (2008)
[29] Gozluklu B.; Delamination analysis by using cohesive interface elements in laminated composites. Ph.D. Thesis (2009)
[30] De Xie A., Waas M.: Discrete cohesive zone model for mixed-mode fracture using finite element analysis. Eng Fract Mech; 73(13): 1783–1796 (2006)
[31] Flaviani M.: Testing and simulation of mixed adhesive joints for aerospace applications. Master Thesis, Faculdade de Engenharia da Universidade do Porto (2013)
[32] Banea M.D.: High temperature adhesives for aerospace applications. Ph.D. Thesis, Faculdade de Engenharia da Universidade do Porto (2001)
[33] da Silva L.F.M., Campilho R.D.S.G.: Advances in Numerical Modelling of Adhesive Joints, Springer, (2012)
[34] Marques E.A.S., Banea M.D., da Silva L.F.M., Carbas R.J.C., Sato C.: Effect of low temperature on tensile strength and mode I fracture energy of a room temperature vulcanizing silicone adhesive. J Test Eval; DOI: 10.1520/JTE20140208 (2016)
[35] da Silva L.F.M, da Silva R.A.M., Chousal J.A.G. and Pinto A.M.G.: Alternative Methods to Measure the Adhesive Shear Displacement in the Thick Adherend Shear Test. J Adhes Sci Technol; 22(1): 15-29 (2008)
[36] Pinto A.M.G., Magalhães A.G., Campilho R.D.S.G., de Moura M.F.S.F. and Baptista A.P.M.: Single-Lap Joints of Similar and Dissimilar
Adherends Bonded with an Acrylic Adhesive. J Adhesion; 85(6): 351-376 (2009)
[37] da Silva L.F.M., de Magalhães F.A.C.R.G., Chaves F.J. P. and de Moura M.F.S.F.: Mode II Fracture Toughness of a Brittle and a Ductile Adhesive as a Function of the Adhesive Thickness. J Adhesion; 86(9): 891-905 (2010)

[38] Canto C.M.S.: Strength and fracture energy of adhesives for the automotive industry. Master Thesis, Faculdade de Engenharia da Universidade do Porto (2013)
[39] da Silva L.F.M., Dillard D.A., Blackman B.R.K., Adams R.D.: Testing Adhesive Joints, Best practices. WILEI-VCH (2012)
[40] Mata R.A.: Impact of adhesive joints for the automotive industry at low and high temperatures. Master Thesis, Faculdade de Engenharia da Universidade do Porto (2014)
[41] Marques E.A.S., Magalhães D.N.M., da Silva L.F.M.: Experimental study of silicone-epoxy dual adhesive joints for high temperature aerospace applications. Mat.-wiss. u. Werkstofftech; 42(5): 471-477 (2011)
[42] Mata R.A.; Impact of adhesive joints for the automotive industry at low and high temperatures. Conference poster, Faculdade de Engenharia da Universidade do Porto (2014)
[43] Carlberger T., Biel A. and Stigh U.: Influence of temperature and strain rate on cohesive properties of a structural epoxy adhesive. Int J Fracture; 155(2): 155-166 (2009)